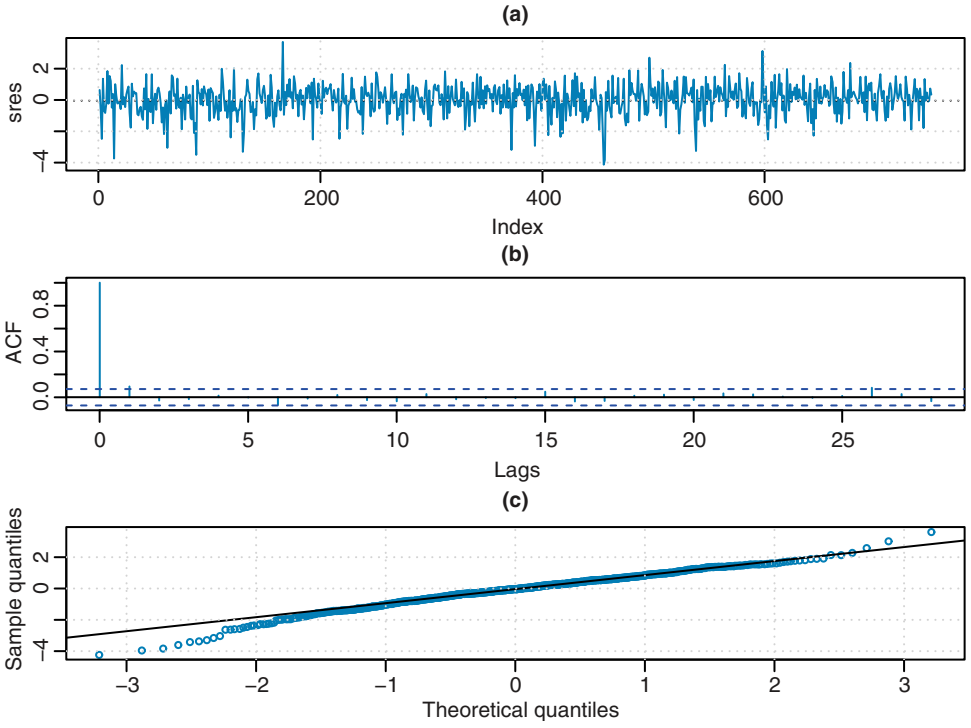

FIGURE 10.3 Model diagnostics for the GARCH(1, 1) model fitted to the S&P 500 weekly log returns: (a) standardized residuals, (b) autocorrelation function of the squared standardized residuals, and (c) a normal Q–Q plot of the standardized residuals.

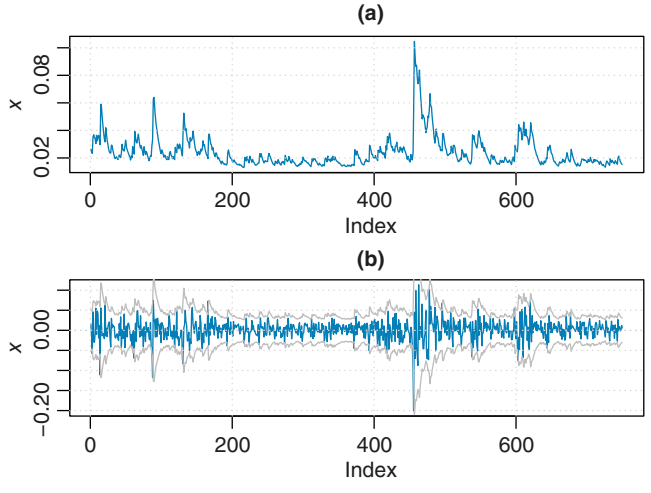

FIGURE 10.4 Conditional standard deviations for the S&P 500 weekly log returns (a) and the weekly log returns with two standard deviation limits imposed (b).

Exponential GARCH Models. The earliest model that allows for an asymmetric response due to leverage effects is the exponential GARCH, or EGARCH, model introduced by Nelson (1991). The EGARCH(1, 1) model is defined as $a_t = \sigma_t e_t$, where

$$\ln(\sigma_t^2) = \alpha_0 + g(e_{t-1}) + \beta_1 \ln(\sigma_{t-1}^2)$$

The function $g(e_{t-1})$ determines the asymmetry and is defined as the weighted innovation

$$g(e_{t-1}) = \alpha_1 e_{t-1} + \gamma_1[|e_{t-1}| - E(|e_{t-1}|)]$$

where α_1 and γ_1 are real constants. The model then becomes

$$\ln(\sigma_t^2) = \alpha_0 + \alpha_1 e_{t-1} + \gamma_1 |e_{t-1}| - \gamma_1 E(|e_{t-1}|) + \beta_1 \ln(\sigma_{t-1}^2)$$

From here it is easy to see that a positive shock has the effect $(\alpha_1 + \gamma_1)e_{t-1}$ while a negative shock has the effect $(\alpha_1 - \gamma_1)e_{t-1}$. The use of $g(e_{t-1})$ thus allows the model to respond asymmetrically to ''good news'' and ''bad news.'' Since bad news typically has a larger impact on volatility than good news, the value of α_1 is expected to be negative when leverage effects are present. Note that since the EGARCH model describes the relation between the logarithm of the conditional variance σ_t^2 and past information, the model does not require any restrictions on the parameters to ensure that σ_t^2 is nonnegative. The general EGARCH(s, r) model has the form

$$\ln(\sigma_t^2) = \alpha_0 + \sum_{i=1}^{s} g_i(e_{t-i}) + \sum_{j=1}^{r} \beta_j \ln(\sigma_{t-j}^2)$$

with

$$g_i(e_{t-i}) = \alpha_i e_{t-i} + \gamma_i(|e_{t-i}| - E(|e_{t-i}|)$$

However, as in the GARCH case, the first-order model is the most popular in practice.

Nelson (1991) specified the likelihood function assuming that the errors follow a generalized error distribution that includes the normal distribution as a special case. Properties of the QML estimator based on the normality assumption for the EGARCH(1, 1) model were studied by Straumann and Mikosch (2006) who verified the conditions for consistency of this estimator. Further properties and details related to the model building process can be found in Tsay (2010) and Teräsvirta et al. (2010), for example.

The GJR and Threshold GARCH Models. The so-called GJR-GARCH model of Glosten, Jagannathan, and Runkle (1993) and the threshold GARCH model of Zakoïan (1994) provide an alternative way to allow for asymmetric effects of positive and negative volatility shocks. Starting from the GARCH(1, 1) model, the GJR model assumes that the parameter associated with a_{t-1}^2 depends on the sign of the shock so that

$$\sigma_t^2 = \alpha_0 + (\alpha_1 + \gamma_1 I_{t-1})a_{t-1}^2 + \beta_1 \sigma_{t-1}^2$$

where the indicator variable I_{t-1} assumes the value 1 if a_{t-1} is negative and zero if it is positive. The constraints on the parameters needed to ensure that the conditional variance σ_t^2 is nonnegative are readily derived from those of the GARCH(1, 1) process. Using this formulation, the noise term a_{t-1} has a coefficient $\alpha_1 + \gamma_1$ when it is negative, and α_1 when it is positive. This allows negative shocks to have a larger impact on the volatility. The

GJR model is relatively simple and empirical studies have shown that the model performs well in practice. For general GARCH(s, r), the model generalizes to

$$\sigma_t^2 = \alpha_0 + \sum_{i=1}^{s}(\alpha_i + \gamma_i I_{t-i})a_{t-i}^2 + \sum_{j=1}^{r}\beta_j\sigma_{t-j}^2$$

although applications with r and s greater than 1 seem to be very rare. Zakoïan (1994) introduced a model with the same functional form as the GJR model, but instead of modeling the conditional variance, Zakoïan models the conditional standard deviation. Since the coefficient associated with a_{t-1} changes its value as a_{t-1} crosses the *threshold* zero, Zakoïan referred to this model as a threshold GARCH, or TGARCH, model.

Nonlinear Smooth Transition Models. For the threshold model described above, the impact of past shocks changes abruptly as a_{t-i} crosses the zero threshold. Attempts have been made in the literature to develop nonlinear extensions of ARCH and GARCH models that allow for more flexibility and a smoother transition as a lagged value a_{t-i} crosses a specified threshold. These extensions include the logistic smooth transition GARCH model proposed by Hagerud (1997), and a similar model proposed independently by González-Rivera (1998). This model assumes that the model parameters α_i in the ARCH or GARCH model are not constant but functions of the lagged a_{t-i} so that $\alpha_i = \alpha_{1i} + \alpha_{2i}F(a_{t-i})$, $i = 1, \ldots, s$, where $F(\cdot)$ is a transition function. Hagerud considered two transition functions, the logistic and the exponential. The GARCH(s, r) model with a logistic transition function has the form

$$\sigma_t^2 = \alpha_0 + \sum_{i=1}^{s}[\alpha_{1i} + \alpha_{2i}F(a_{t-i})]a_{t-i}^2 + \sum_{j=1}^{r}\beta_j\sigma_{t-j}^2$$

where

$$F(a_{t-i}) = \frac{1}{1 + \exp(-\theta a_{t-i})} - \frac{1}{2}$$

with $\theta > 0$. In contrast to the GJR model that follows one process when the innovations are positive and another process when the innovations are negative, the transition between the two states is smooth in the present model. Hagerud provided conditions for stationarity and nonnegativity of the conditional variances.

Lanne and Saikkonen (2005) proposed a smooth transition GARCH process that uses the lagged conditional variance σ_{t-1}^2 as the transition variable, and is suitable for describing high persistence in the conditional variance. The first-order version of this model can be written as

$$\sigma_t^2 = \alpha_0 + \alpha_1 a_{t-1}^2 + \delta_1 G_1(\theta; \sigma_{t-1}^2) + \beta_1\sigma_{t-1}^2$$

where the transition function $G_1(\theta; \sigma_{t-1}^2)$ is a continuous, monotonically increasing bounded function of σ_{t-1}^2. Lanne and Saikkonen used the cumulative distribution function of the gamma distribution as the transition function. The original purpose for introducing this model was to remedy a tendency of GARCH models to exaggerate the persistence in volatility as evidenced by $\Sigma(\alpha_i + \beta_i)$ often being very close to one. Using empirical examples involving exchange rates, the authors showed that this formulation alleviates the problem

of exaggerated persistence. For further discussion of these and related models, see, for example, Mills and Markellos (2008) and Teräsvirta (2009).

GARCH-M Models. Many theories in finance postulate a direct relationship between the expected return on an investment and its risk. To account for this, the GARCH-in-mean, or GARCH-M, model, allows the conditional mean of a GARCH process to depend on the conditional variance σ_t^2. This model originates from the ARCH-M model proposed by Engle et al. (1987). The mean value function is specified as

$$\mu_t = \beta_0 + \beta_1 g(\sigma_t^2)$$

where $g(\sigma_t^2)$ is a positive-valued function and β_1 is a positive constant called the risk premium parameter. An increase or decrease in the conditional mean is here associated with the sign of the partial derivative of the function $g(\sigma_t^2)$ with respect to σ_t^2. In many applications, $g(\sigma_t^2)$ is taken to be the identity function or the square root function so that $g(\sigma_t^2) = \sigma_t^2$ or $g(\sigma_t^2) = \sigma_t$. The parameters of the GARCH-M model can be estimated using the maximum likelihood method. However, because of the dependence of the conditional mean on the conditional variance, the information matrix is no longer block diagonal with respect to the conditional mean and variance parameters. This makes joint maximization of the likelihood function with respect to the two sets of parameters necessary. Also, consistent estimation of the parameters in the GARCH-M models requires the full model be correctly specified. Applications of the GARCH-M model to stock returns, exchange rates, and interest rates were discussed by Bollerslev et al. (1992).

IGARCH and FIGARCH Models. As noted earlier, the GARCH(1, 1) model is weakly stationary assuming that $(\alpha_1 + \beta_1) < 1$. When the GARCH model is applied to high-frequency financial data, it is often found that $\alpha_1 + \beta_1$ is close to or equal to1. Engle and Bollerslev (1986) refer to a model with $\alpha_1 + \beta_1 = 1$ as an integrated GARCH, or IGARCH, model. The motivation is that this implies a unit root in the autoregressive part of the ARMA(1, 1) representation of the GARCH(1, 1) model for a_t^2 in (10.2.11). With $\alpha_1 + \beta_1 = 1$, the model becomes $(1 - B)a_t^2 = \alpha_0 + \nu_t - \beta_1 \nu_{t-1}$. Similar to a random walk process, this process is not mean reverting since the unconditional variance of the process is not finite. Also, the impact of a large shock on the forecasts of future values will not diminish for increasing lead times. But while the GARCH(1,1) process is not weakly stationary, Nelson (1990) showed that the process has time-invariant probability distributions and is thus strictly stationary. A necessary condition for strict stationarity is $E[ln(\alpha_1 a_{t-1}^2 + \beta_1)] < 0$. For further discussion of this model, see, for example, Teräsvirta (2009).

Fractionally integrated GARCH, or FIGARCH, models have also been proposed in the literature. These differ from the IGARCH model in that the degree of differencing d is allowed to be a fraction rather than a constant. The FIGARCH(1, 1) model, in particular, is of the form $(1 - B)^d a_t^2 = \alpha_0 + \nu_t - \beta_1 \nu_{t-1}$, where d is a constant such that $0 < d < 0.5$. For the FIGARCH model, the empirical autocorrelations of a_t^2 need not be very large but they decay very slowly as the lag k increases. This is indicative of so-called *long memory* behavior in the series. Models involving fractional differencing will be discussed further in Section 10.4 in relation to long-range dependence in the conditional mean μ_t.

Other Models. Numerous other models have been proposed to account for conditional heteroscedasticity. For example, a natural extension of the ARCH(s) model specified in

(10.2.1) is to let $\sigma_t^2 = \alpha_0 + \boldsymbol{a}_{t-1}'\boldsymbol{\Omega}\boldsymbol{a}_{t-1}$, where $\boldsymbol{a}_{t-1} = (a_{t-1}, \ldots, a_{t-s})'$ and $\boldsymbol{\Omega}$ is a $s \times s$ nonnegative definite matrix. The ARCH(s) model is then a special case that requires that $\boldsymbol{\Omega}$ be diagonal. One way that the above form can arise is through the conditional heteroscedastic ARMA (CHARMA) model specification discussed by Tsay (1987). Other approaches to volatility modeling include the random coefficient autoregressive model of Nicholls and Quinn (1982) and the stochastic volatility models of Melino and Turnbull (1990), Jacquier et al. (1994), and Harvey et al. (1994). A brief description of the stochastic volatility models is provided below.

10.2.6 Stochastic Volatility Models

Stochastic volatility models are similar to GARCH models but introduce a stochastic innovation term to the equation that describes the evolution of the conditional variance σ_t^2. To ensure positiveness of the conditional variances, stochastic volatility models are defined in terms of $\ln(\sigma_t^2)$ instead of σ_t^2. A basic version of a stochastic volatility model is defined by $a_t = \sigma_t e_t$ as in (10.2.1) with $\ln(\sigma_t^2)$ satisfying

$$\ln(\sigma_t^2) = \alpha_0 + \beta_1 \ln(\sigma_{t-1}^2) + \cdots + \beta_r \ln(\sigma_{t-r}^2) + \upsilon_t \tag{10.2.14}$$

where e_t are iid normal $N(0, 1)$, υ_t are iid normal $N(0, \sigma_\upsilon^2)$, $\{e_t\}$ and $\{\upsilon_t\}$ are independent processes, and the roots of the characteristic equation $1 - \sum_{j=1}^{r} \beta_i B^j = 0$ are outside the unit circle. Note, for example, the stochastic volatility model equation for $r = 1$ is $\ln(\sigma_t^2) = \alpha_0 + \beta_1 \ln(\sigma_{t-1}^2) + \upsilon_t$, which is somewhat analogous to the GARCH(1, 1) model equation, $\sigma_t^2 = \alpha_0 + \beta_1\sigma_{t-1}^2 + \alpha_1 a_{t-1}^2$. Alternatively, replacing $g(e_{t-1})$ by υ_t in the EGARCH(1, 1) model, we obtain (10.2.14) with $r = 1$. Some properties of the stochastic volatility model for $r = 1$ are provided by Jacquier et al. (1994). Also note that we may write $a_t^2 = \sigma_t^2 e_t^2$ so that $\ln(a_t^2) = \ln(\sigma_t^2) + \ln(e_t^2)$. This allows the stochastic volatility model to be viewed as a state-space model, with the last relation representing the observation equation and the transition equation being developed from (10.2.14). Difficulty in parameter estimation is increased for stochastic volatility models, however, since likelihoods based on the state-space model are non-Gaussian. Quasi-likelihood methods may thus be needed. Jacquier et al. (1994) give a good summary of estimation techniques, including quasi-likelihood methods with Kalman filtering and the expectation maximization (EM) algorithm and Markov chain Monte Carlo (MCMC) methods. They also provide a comparison of estimation results between the different methods.

A discussion and examples of the use of Markov chain Monte Carlo methods for parameter estimation can also be found in Tsay (2010, Chapter 12). A general overview of the stochastic volatility literature is given by a collection of articles in the books edited by Shephard (2005) and Andersen et al. (2009).

10.3 NONLINEAR TIME SERIES MODELS

Many processes occurring in the natural sciences, engineering, finance, and economics exhibit some form of nonlinear behavior. This includes features that can not be modeled using Gaussian linear processes such as lack of time reversibility evidenced, for example, by pseudocyclical patterns where the values slowly rise to a peak and then quickly

decline to a trough. Time series that exhibit occasional bursts of outlying values are also unlikely under the linear Gaussian assumption. The prevalence of such series has led to an interest in developing nonlinear time series models that can account for such behavior. Nonlinear models proposed in the literature include bilinear models, threshold autoregressive (TAR) models, exponential autoregressive (EXPAR) models, and stochastic or random coefficient models. These models describe nonlinearities in the conditional mean as opposed to nonlinearities in the conditional variance as discussed in Section 10.2. When nonlinearities are present, model identification and estimation become more complicated, including the fundamental problem of which type of nonlinear model might be useful for a particular time series. This section presents a brief description of some nonlinear models that have been proposed in the literature. More comprehensive discussions are available in texts such as Tong (1983, 1990), Priestley (1988), Franses and van Dijk (2000), Fan and Yao (2003), Tsay (2010, Chapter 4), and Teräsvirta et al. (2010).

10.3.1 Classes of Nonlinear Models

Many nonlinear ARMA models can be viewed as special cases of the following general form:

$$\begin{aligned} z_t - \phi_1(\boldsymbol{Y}_{t-1})z_{t-1} - \cdots - \phi_p(\boldsymbol{Y}_{t-1})z_{t-p} \\ = \theta_0(\boldsymbol{Y}_{t-1}) + a_t - \theta_1(\boldsymbol{Y}_{t-1})a_{t-1} - \cdots - \theta_q(\boldsymbol{Y}_{t-1})a_{t-q} \end{aligned} \tag{10.3.1}$$

where

$$\boldsymbol{Y}_{t-1} = (z_{t-1}, \ldots, z_{t-p}, a_{t-1}, \ldots, a_{t-q})'$$

and $\phi_i(\boldsymbol{Y}_{t-1})$ and $\theta_i(\boldsymbol{Y}_{t-1})$ are functions of the ''state vector'' $\boldsymbol{Y}_{t-1}$ at time $t-1$. For specific cases, we mention the following models.

1. *Bilinear Models.* Let the ϕ_i be constants, and set $\theta_j(\boldsymbol{Y}_{t-1}) = b_j + \Sigma_{i=1}^{k} b_{ij} z_{t-i}$. Then we have the model

$$z_t - \phi_1 z_{t-1} - \cdots - \phi_p z_{t-p} = \theta_0 + a_t - \sum_{j=1}^{q} b_j a_{t-j} - \sum_{i=1}^{k}\sum_{j=1}^{q} b_{ij} z_{t-i} a_{t-j} \tag{10.3.2}$$

Equivalently, with the notations $p^* = \max(p, k)$, $\phi_i = 0$, $i > p$, $b_{ij} = 0$, $i > k$, and $\alpha_i(t) = \Sigma_{j=1}^{q} b_{ij} a_{t-j}$, (10.3.2) can be expressed in the form

$$z_t - \sum_{i=1}^{p^*} [\phi_i - \alpha_i(t)] z_{t-i} = \theta_0 + a_t - \sum_{j=1}^{q} b_j a_{t-j}$$

and be viewed in the form of an ARMA model with random coefficients for the AR parameters, which are linear functions of past values of the innovations process a_t. The statistical properties of bilinear models were studied extensively by Granger and Anderson (1978). Methods for analysis and parameter estimation were also studied by Subba Rao (1981) and Subba Rao and Gabr (1984), and various special cases of these models have been examined by subsequent authors.

Conditions for stationarity and other properties have been studied for the general bilinear model by Tuan (1985, 1986) and Liu and Brockwell (1988), in particular. For example, consider the simple first-order bilinear model $z_t - \phi_1 z_{t-1} = a_t - b_{11} z_{t-1} a_{t-1}$. It is established that a condition for second-order stationarity of such a process $\{z_t\}$ is $\phi_1^2 + \sigma_a^2 b_{11}^2 < 1$, and that the autocovariances of z_t under stationarity will satisfy $\gamma_j = \phi_1 \gamma_{j-1}$ for $j > 1$. Thus, this process will have essentially the same autocovariance structure as an ARMA(1, 1) process. This example highlights the fact that moments higher than the second order are typically needed in order to distinguish between linear and nonlinear models.

2. *Amplitude-Dependent Exponential AR Models.* Let $\theta_i = 0$, and set $\phi_i(\boldsymbol{Y}_{t-1}) = b_i + \pi_i e^{-c z_{t-1}^2}$, where $c > 0$ is a constant. Then we have

$$z_t - \sum_{i=1}^{p} (b_i + \pi_i e^{-c z_{t-1}^2}) z_{t-i} = a_t \tag{10.3.3}$$

This class of models was introduced by Haggan and Ozaki (1981), with an aim to construct models that reproduce features of nonlinear random vibration theory.

3. *Threshold AR, or TAR, Models.* Let $\theta_i = 0, i \geq 1$, and for some integer time lag d and some ''threshold'' constant c, let

$$\phi_i(\boldsymbol{Y}_{t-1}) = \begin{cases} \phi_i^{(1)} & \text{if } z_{t-d} \leq c \\ \phi_i^{(2)} & \text{if } z_{t-d} > c \end{cases}$$

$$\theta_0(\boldsymbol{Y}_{t-1}) = \begin{cases} \theta_0^{(1)} & \text{if } z_{t-d} \leq c \\ \phi_0^{(2)} & \text{if } z_{t-d} > c \end{cases}$$

Then we have the model

$$z_t = \begin{cases} \theta_0^{(1)} + \sum_{i=1}^{p} \phi_i^{(1)} z_{t-i} + a_t^{(1)} & \text{if } z_{t-d} \leq c \\ \theta_0^{(2)} + \sum_{i=1}^{p} \phi_i^{(2)} z_{t-i} + a_t^{(2)} & \text{if } z_{t-d} > c \end{cases} \tag{10.3.4}$$

where $\{a_t^{(1)}\}$ and $\{a_t^{(2)}\}$ are each white noise processes with variances σ_1^2 and σ_2^2, respectively (e.g., we can take $a_t^{(j)} = \sigma_j a_t$). The value c is called the threshold parameter and d is the delay parameter. A special case arises when the parameter c is replaced by a lagged value of the series itself, resulting in a model called the self-exciting TAR (SETAR) model.

The model (10.3.4) readily extends to an ''l-threshold'' model of the form

$$z_t = \theta_0^{(j)} + \sum_{i=1}^{p} \phi_i^{(j)} z_{t-i} + a_t^{(j)} \qquad \text{if} \qquad c_{j-1} < z_{t-d} \leq c_j \qquad j = 1, \ldots, l$$

with threshold parameters $c_1 < c_2 < \cdots < c_{l-1}$ (and $c_0 = -\infty, c_l = +\infty$), which define a partition of the real line into l subintervals. The first-order threshold model,

$$z_t = \theta_0^{(j)} + \phi^{(j)} z_{t-1} + a_t^{(j)} \qquad \text{if} \qquad c_{j-1} < z_{t-1} \le c_j$$

for example, may thus be regarded as a piecewise linear approximation to a general nonlinear first-order model $z_t = g(z_{t-1}) + a_t$, where $g(\cdot)$ is some general nonlinear function.

The TAR models were introduced by Tong (1978) and Tong and Lim (1980) and discussed in detail by Tong (1983, 1990). Tong (2007) gives a brief discussion of their origin. The basic threshold AR model can be seen as a piecewise linear AR model, with a somewhat abrupt change from one equation or ''regime'' to another dependent on whether or not a threshold value c_j is exceeded by z_{t-d}. A generalization that allows for less abrupt transition from one regime to another has been developed as a class of models known as smooth transition AR (STAR) models; see, for example, Teräsvirta (1994) and Teräsvirta et al. (2010). For the case of a single threshold $l = 1$, the basic form of a STAR model is

$$z_t = \theta_0^{(1)} + \sum_{i=1}^{p} \phi_i^{(1)} z_{t-i} + \left(\theta_0^{(2)} + \sum_{i=1}^{p} \phi_i^{(2)} z_{t-i} \right) F(z_{t-d}) + a_t$$

where $F(z) = 1/[1 + \exp\{-\gamma(z - c)\}]$ in the case of a logistic STAR model and in the normal STAR model $F(z) = \Phi(\gamma(z - c))$, with $\Phi(\cdot)$ equal to the cumulative distribution function of the standard normal distribution. By letting $\gamma \to \infty$, we see that $F(z)$ tends to the indicator function, and the usual two-regime TAR model (10.3.4) is obtained as a special case. The TAR model and its extensions have been used to model nonlinear series in many diverse areas such as finance and economics, the environmental sciences, hydrology, neural science, population dynamics, and physics; for selected references, see Fan and Yao (2003, p. 126).

Other types of nonlinear models include the stochastic or random coefficient models. For example, in the simple AR(1) model we consider $z_t = \phi_t z_{t-1} + a_t$, where ϕ_t is not a constant but is a stochastic parameter. Possible assumptions on the mechanism generating the ϕ_t include (i) the ϕ_t are iid random variables with mean ϕ and variance σ_ϕ^2, independent of the process $\{a_t\}$, and (ii) the ϕ_t follow an AR(1) process themselves,

$$\phi_t - \phi = \alpha(\phi_{t-1} - \phi) + e_t$$

where ϕ is the mean of the ϕ_t process and the e_t are iid random variables with mean 0 and variance σ_e^2, independent of a_t. Estimation for the first case was considered in detail by Nicholls and Quinn (1982), while the second case may in principle be estimated using state-space methods (e.g., Ledolter, 1981).

Additional classes of nonlinear models include the general state-dependent model form (10.3.1) examined extensively by Priestley (1980, 1988), or more general nonparametric autoregressive model forms such as nonlinear additive autoregressive models considered by Chen and Tsay (1993), and adaptive spline threshold autoregressive models used by Lewis and Stevens (1991). Nonparametric and semiparametric methods such as kernel regression and artificial neural networks have also been used to model nonlinearity. A review of nonlinear time series models with special emphasis on nonparametric methods was provided by Tjøstheim (1994). More recent discussions of the developments in this

area can be found in Fan and Yao (2003), Gao (2007), and Teräsvirta et al. (2010). A discussion of nonlinear models with applications to finance is provided by Tsay (2010, Chapter 4).

10.3.2 Detection of Nonlinearity

Many methods have been proposed to detect nonlinearity of a time series. In addition to informal graphical methods and inspection of higher order moments, such as third- and fourth-order moments, these include more formal test procedures by Hinich (1982), Subba Rao and Gabr (1980), McLeod and Li (1983), Keenan (1985), Tsay (1986a), Petruccelli and Davies (1986), Luukkonen et al. (1988a), and others. Some of these tests exploit the nonlinear dependence structure that is reflected in the higher order moments, and many of the tests are developed as portmanteau tests based on a linear model, with an alternative not explicitly specified. Other tests are Lagrange multiplier or score-type procedures against specified alternative models. For example, the tests of Luukkonen et al. (1988a) are score-type tests against STAR alternatives. The tests of Subba Rao and Gabr (1980) and Hinich (1982) are nonparametric tests that use a bispectral approach, while the test of Petruccelli and Davies (1986) is based on cumulative sums of standardized residuals from autoregressive fitting to the data. The portmanteau test statistic (10.2.12) of McLeod and Li (1983) is based on sample autocorrelations of squared residuals $\hat{a}_t^2$ from a fitted linear ARMA model. This test was introduced as a test for nonlinearity, although simulations suggest that it may be more powerful against ARCH alternatives. A modest gain in power may be possible by basing the nonlinearity checks on the portmanteau statistics proposed by Peña and Rodríguez (2002, 2006).

Keenan (1985) proposed an F-test for nonlinearity using an analogue of Tukey's single-degree-of-freedom test for nonadditivity. The test is also similar to the regression specification error test (RESET) proposed by Ramsey (1969) for linear regression models. The test can be implemented by first fitting an AR(m) model to the observed series z_t, where m is a suitably selected order. The fitted values are retained and their squares are added as a predictor variable to the AR(m) model. This model is then refitted and the coefficient associated with the predictor variable is tested for significance. This procedure thus amounts to determining whether inclusion of the squared predicted values helps improve the prediction.

Tsay (1986a) proposed an extension based on testing whether second-order terms have additional predictive ability. The procedure can be carried out as follows: First fit a linear AR(m) model and obtain the residuals $\hat{a}_t$ from this fit. Then consider the $M = \frac{1}{2}m(m+1)$ component vector

$$\boldsymbol{Z}_t = (z_{t-1}^2, \ldots, z_{t-m}^2, z_{t-1}z_{t-2}, \ldots, z_{t-m+1}z_{t-m})'$$

consisting of all squares and distinct cross-products of the lagged values $z_{t-1}, \ldots, z_{t-m}$. Now perform a multivariate least-squares regression of the elements of $\boldsymbol{Z}_t$ on the set of regressors $\{1, z_{t-1}, \ldots, z_{t-m}\}$ and obtain the multivariate residual vectors $\hat{\boldsymbol{U}}_t$, for $t = m+1, \ldots, n$. Finally, perform a least-squares regression $\hat{a}_t = \hat{\boldsymbol{U}}_t'\boldsymbol{\beta} + e_t$ of the AR(m) model residuals $\hat{a}_t$ on the M-dimensional vectors $\hat{\boldsymbol{U}}_t$ as regressor variables, and let $\hat{F}$ be the F ratio of the

regression mean square to the error mean square from that regression, so that

$$\hat{F} = \frac{(\sum_t \hat{a}_t \hat{U}_t')(\sum_t \hat{U}_t \hat{U}_t')^{-1}(\sum_t \hat{U}_t \hat{a}_t)/M}{\sum_{t=m+1}^{n} \hat{e}_t^2/(n-m-M-1)} \tag{10.3.5}$$

Under the assumption of linearity, $\hat{F}$ has, for large n, an approximate F distribution with M and $n-m-M-1$ degrees of freedom, and the null hypothesis of linearity is rejected for large values of $\hat{F}$. Extension to a procedure for residuals $\hat{a}_t$ from a fitted ARMA(p, q) model was also mentioned by Tsay (1986a).

If one aggregates or condenses the information in the M-dimensional vector $\boldsymbol{Z}_t$ into a single variable $\hat{z}_t^2 = (\hat{\theta}_0 + \Sigma_{i=1}^{m} \hat{\phi}_i z_{t-i})^2$, which is the square of the fitted value from the AR(m) model, and performs the remaining steps outlined above, one obtains the earlier test by Keenan (1985). The associated test statistic is

$$\hat{F} = \frac{(\sum_t \hat{u}_t \hat{a}_t)^2/(\sum_t \hat{u}_t^2)}{\sum_{t=m+1}^{n} \hat{e}_t^2/(n-2m-2)}$$

with 1 and $n-2m-2$ degrees of freedom. Luukkonen et al. (1988b) and Tong (1990, Section 5.3) noted a score test interpretation of the procedures proposed by Keenan (1985) and Tsay (1986a). Both tests are available in the TSA package of R and can be implemented using the commands Keenan.test(z) and Tsay.test(z). For further discussion, see Tsay (2010, Chapter 4).

10.3.3 An Empirical Example

For illustration, we consider modeling of the Canadian lynx dataset, consisting of annual numbers of Canadian lynx trapped in the MacKenzie River district for the period 1821 to 1934. The series is available in the R datasets package. For several reasons, the $\log_{10}$ transformation of the data is used in the analysis, denoted as z_t, $t = 1, \ldots, n$, with $n = 114$. Examination of the time series plot of z_t in Figure 10.5 shows a very strong cyclical behavior, with period around 10 years. It also shows an asymmetry or lack of time reversibility in that the sample values rise to their peak or maximum values more slowly than they fall away to their minimum values (typically, about 6-year segments of rising and 4-year segments of falling). This is a feature exhibited by many nonlinear processes. There are biological/population reasons that would also support a nonlinear process, especially one involving a threshold mechanism; see, for example, Tong (1990).

The sample ACF and PACF of the series $\{z_t\}$ are shown in Figure 10.6. The ACF exhibits the cyclic feature clearly, and based on features of the sample PACF a linear AR(4) model is initially fitted to the series, with $\hat{\sigma}_a^2 = 0.0519$. The presence of some moderate autocorrelation at higher lags, around lags 10 and 12, in the residuals from the fitted AR(4) model suggested the following more refined model that was estimated by conditional LS:

$$\begin{aligned} z_t = {} & 1.149 + 1.038 z_{t-1} - 0.413 z_{t-2} + 0.252 z_{t-3} - 0.229 z_{t-4} \\ & + 0.188 z_{t-9} - 0.232 z_{t-12} + a_t \end{aligned} \tag{10.3.6}$$

with residual variance estimate $\hat{\sigma}_a^2 = 0.0380$.

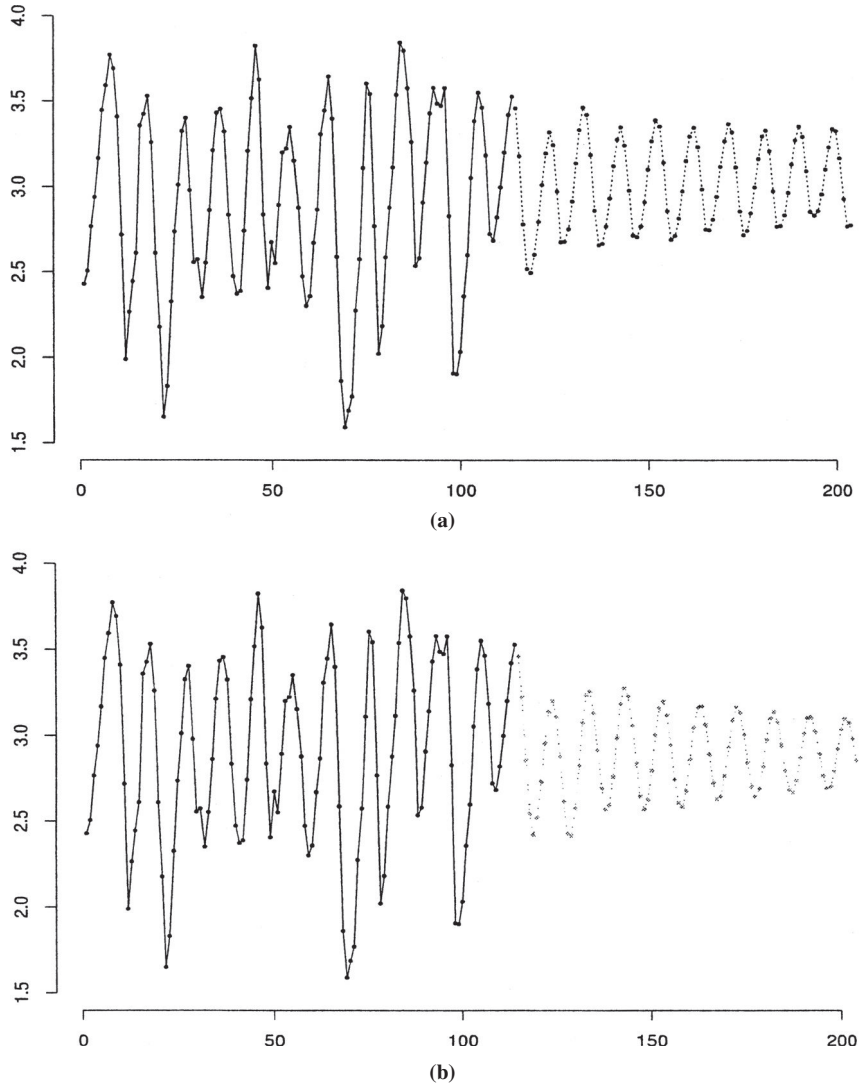

FIGURE 10.5 Logarithms (base 10) of the Canadian lynx time series for 1821–1934, with forecasts for 90 periods ahead from (a) the TAR model and (b) the linear subset AR(12) model.

Some diagnostics of this fitted model suggest possible nonlinearity. Specifically, there is strong autocorrelation in the squared residuals $\hat{a}_t^2$ at lag 2, with $r_2(\hat{a}^2) = 0.401$, and nonlinear features exist in scatter plots of the ''fitted values'' $\hat{z}_t \equiv \hat{z}_{t-1}(1)$ and residuals $\hat{a}_t = z_t - \hat{z}_{t-1}(1)$ versus lagged values z_{t-j}, for lags $j = 2, 3, 4$. But the tests by Keenan (1985) and Tsay (1986a), implemented in the TSA package of R, are inconclusive in that the Keenan test rejects linearity whereas the Tsay test does not (see the output below). However, it appears that the failure of the Tsay test to detect the nonlinearity may be due to the way the package computes the Tsay statistic. This computation uses 77 parameters and results in an observation/parameter ratio of $114/77 < 2$, which is too small for valid inference.

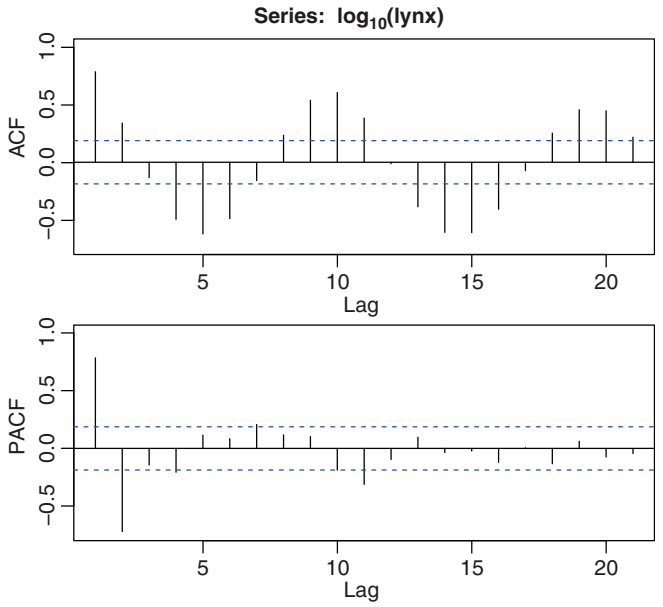

FIGURE 10.6 Autocorrelation and partial autocorrelation functions for the logarithm of the Canadian lynx series.

```
> library(TSA)
> data(lynx)
> z=log10(lynx)
> Keenan.test(z)
    $test.stat: 11.66997
    $p.value:  0.000955
    $order: 11
> Tsay.test(z)
    $test.stat: 1.316
    $p.value:  0.2256
    $order: 11
```

Tong (1990) specified a TAR model, with time delay of $d = 2$ and threshold value of about $c \approx 3.10$ for this series. A threshold version of the AR model in (10.3.6), with two phases and terms at lags 1, 2, 3, 4, 9, and 12, was estimated by conditional LS. After eliminating nonsignificant parameter estimates, we arrived at the following estimated threshold AR model:

$$\begin{aligned} z_t &= 1.3206 + 0.9427 z_{t-1} - 0.2161 z_{t-4} \\ &\quad - 0.1411 z_{t-12} + a_t^{(1)} \quad \text{if} \quad z_{t-2} \le 3.10 \\ &= 1.8259 + 1.1971 z_{t-1} - 0.7266 z_{t-2} + 0.1667 z_{t-9} \\ &\quad - 0.2229 z_{t-12} + a_t^{(2)} \qquad \text{if} \quad z_{t-2} > 3.10 \end{aligned}$$

with residual variance estimates $\hat{\sigma}_1^2 = 0.0249$ and $\hat{\sigma}_2^2 = 0.0386$ (pooled $\hat{\sigma}^2 = 0.0328$).

The approximate ''eventual'' forecast function from this model will lead to periodic limit cycle behavior with an approximate period of 9 years (see Tong (1990) for discussion of limit cycles). Although exact minimum MSE forecasts $\hat{z}_n(l)$ for lead times $l > 2$ are not easily computed for the fitted threshold AR model, approximate forecasts for larger l can be obtained by projecting series values forward with future white noise terms $a_t^{(i)}$ set to 0 (see Teräsvirta et al. (2010, Chapter 14) for other options). Values obtained in this way for the eventual forecast function from the TAR model are depicted for 90 years, $l = 1, \ldots, 90$, in Figure 10.5(a). These values exhibit a limit cycle with a period of essentially 9 years (in fact, the period is 28 years with 3 ''subcycles''), and the asymmetric feature of slower rise to peak values and faster fall to minimum values is visible. In contrast, the stationary linear AR model will give a forecast function in the form of very slowly damped sinusoidal oscillations that will eventually decay to the mean value of the process, 2.90. This forecast function is shown in Figure 10.5(b).

Other nonlinear models have been considered for the Canadian lynx data. For examples, Subba Rao and Gabr (1984) have estimated a bilinear model for these data, an AR(2) model with random coefficients was fitted by Nicholls and Quinn (1982), and an amplitude-dependent exponential AR model of order 11 was fitted to the mean-adjusted log lynx data by Haggan and Ozaki (1981).

10.4 LONG MEMORY TIME SERIES PROCESSES

The autocorrelation function ρ_k of a stationary ARMA(p, q) process decreases rapidly as $k \to \infty$, since the autocorrelation function is geometrically bounded so that

$$|\rho_k| \leq CR^k, \qquad k = 1, 2, \ldots$$

where $C > 0$ and $0 < R < 1$. Processes with this property are often referred to as *short memory* processes. Stationary processes with much more slowly decreasing autocorrelation function, known as *long memory* processes, have

$$\rho_k \sim Ck^{2d-1} \qquad \text{as} \qquad k \to \infty \tag{10.4.1}$$

where $C > 0$ and $-0.5 < d < 0.5$. Empirical evidence suggests that long memory processes are common in fields as diverse as hydrology (e.g., Hurst, 1951; McLeod and Hipel, 1978), geophysics, and financial economics. The sample autocorrelations of such processes are not necessarily large, but tend to persist over a long period. The latter could suggest a need for differencing to achieve stationarity, although taking a first difference may be too extreme. This motivates the notion of fractional differencing and consideration of the class of fractionally integrated processes.

10.4.1 Fractionally Integrated Processes

A notable class of stationary long memory processes z_t is the *fractionally integrated ARMA*, or ARFIMA, processes defined for $-0.5 < d < 0.5$ by the relation

$$\phi(B)(1 - B)^d z_t = \theta(B)a_t \tag{10.4.2}$$

where $\{a_t\}$ is a white noise sequence with zero mean and variance σ_a^2, and $\phi(B) = 0$ and $\theta(B) = 0$ have all roots greater than one in absolute value. The class of models in (10.4.2) was initially proposed and studied by Granger and Joyeux (1980) and Hosking (1981) as an intermediate compromise between fully integrated ARIMA processes and short memory ARMA processes. More comprehensive treatments of these models can be found in texts by Beran (1994), Robinson (2003), and Palma (2007).

For $d > -1$, the operator $(1 - B)^d$ in (10.4.2) is defined by the binomial expansion

$$(1 - B)^d = \sum_{j=0}^{\infty} \pi_j B^j \tag{10.4.3}$$

where $\pi_0 = 1$ and

$$\pi_j = \frac{\Gamma(j - d)}{\Gamma(j + 1)\Gamma(-d)} = \prod_{0<k\leq j} \frac{k - 1 - d}{k} \qquad j = 1, 2, \ldots \tag{10.4.4}$$

and $\Gamma(x)$ is the gamma function. Hence, the π_j follow the simple recursion

$$\pi_j = \left(\frac{j - 1 - d}{j}\right) \pi_{j-1}$$

A particular special case is the *fractionally integrated white noise* process w_t, defined by

$$(1 - B)^d w_t = a_t$$

For $-0.5 < d < 0.5$, since the power series expansion of $\psi(B) = (1 - B)^{-d} \equiv \Sigma_{j=0}^{\infty} \psi_j B^j$ converges for $|B| \leq 1$, it follows that such a process $\{w_t\}$ is stationary and has the infinite MA representation

$$w_t = (1 - B)^{-d} a_t = \sum_{j=0}^{\infty} \psi_j a_{t-j} \tag{10.4.5}$$

where

$$\psi_j = \frac{\Gamma(j + d)}{\Gamma(j + 1)\Gamma(d)} = \prod_{0<k\leq j} \frac{k - 1 + d}{k} \sim \frac{1}{\Gamma(d)} j^{d-1} \qquad \text{as} \qquad j \to \infty \tag{10.4.6}$$

It can also be shown (Hosking, 1981; Brockwell and Davis, 1991, Chapter 12) that the fractionally integrated white noise process has variance

$$\gamma_0(w) = \text{var}[w_t] = \frac{\sigma^2{}_a \Gamma(1 - 2d)}{[\Gamma(1 - d)]^2}$$

and ACF

$$\rho_h(w) = \frac{\Gamma(h + d)\Gamma(1 - d)}{\Gamma(h - d + 1)\Gamma(d)} = \prod_{0<k\leq h} \frac{k - 1 + d}{k - d} \qquad h = 1, 2, \ldots \tag{10.4.7}$$

In particular, we have $\rho_1(w) = d/(1 - d)$, and $\rho_h(w) = [(h - 1 + d)/(h - d)]\rho_{h-1}(w)$. It follows, using Stirling's formula $\Gamma(x) \sim \sqrt{2\pi} e^{-x+1}(x - 1)^{x-1/2}$ as $x \to \infty$, that the ACF

behaves like

$$\rho_h(w) \sim h^{2d-1}\frac{\Gamma(1-d)}{\Gamma(d)} \qquad \text{as} \qquad h \to \infty$$

the characteristic feature of the ACF of a long memory process. In addition, by use of the Levinson–Durbin recursion algorithm described in Appendix A3.2, values for the partial autocorrelations of the fractionally integrated white noise process can be determined by induction and shown to be $\phi_{kk} = d/(k-d), k = 1, \ldots$.

The fractionally integrated white noise process itself may be of limited use in modeling long memory behavior since the single parameter d can allow for only a restrictive class of autocorrelation function forms. This process can be useful, however, in building of the more general class of long memory processes. In fact, we can see from the above definition that a fractionally integrated ARMA(p, d, q) process, $\phi(B)(1-B)^d z_t = \theta(B)a_t$, can be interpreted as an ''ARMA(p, q) process driven by fractionally integrated white noise,'' that is, $\{z_t\}$ satisfies $\phi(B)z_t = \theta(B)w_t$, with $(1-B)^d w_t = a_t$. From general results on linear filtering, we see that the exact autocovariance function of $\{z_t\}$ can be expressed in terms of the autocovariance function of the fractionally integrated white noise process $\{w_t\}$ as

$$\gamma_h(z) = \sum_{j=0}^{\infty}\sum_{k=0}^{\infty}\psi_j\psi_k\gamma_{h+j-k}(w) \tag{10.4.8}$$

where the ψ_j are the coefficients in $\psi(B) = \phi(B)^{-1}\theta(B) = \sum_{j=0}^{\infty}\psi_j B^j$ and

$$\begin{aligned}\gamma_h(w) = \gamma_0(w)\rho_h(w) &= \sigma_a^2\frac{\Gamma(1-2d)\Gamma(h+d)}{\Gamma(h-d+1)\Gamma(d)\Gamma(1-d)} \\ &\equiv \sigma_a^2\frac{(-1)^h\Gamma(1-2d)}{\Gamma(h-d+1)\Gamma(1-h-d)}\end{aligned}$$

is the autocovariance function of the fractionally integrated white noise process $\{w_t\}$.

In terms of the spectrum, from (3.1.12) the spectrum of a fractionally integrated ARIMA (p, d, q) process $\{z_t\}$ is

$$p_z(f) = 2\sigma_a^2|1-e^{-i2\pi f}|^{-2d}\frac{|\theta(e^{-i2\pi f})|^2}{|\phi(e^{-i2\pi f})|^2} \qquad 0 \le f \le \frac{1}{2} \tag{10.4.9}$$

where $p_w(f) = 2\sigma_a^2|1-e^{-i2\pi f}|^{-2d} \equiv 2\sigma_a^2[2\sin(\pi f)]^{-2d}$ is the spectrum of the fractionally integrated white noise process. In particular, we see that $p_z(f)$ does not remain finite as $f \to 0$ for $0 < d < \frac{1}{2}$. Since $\sin(x) \sim x$ as $x \to 0$, we have the behavior that

$$p_z(f) \sim 2\sigma_a^2\left[\frac{|\theta(1)|^2}{|\phi(1)|^2}\right](2\pi f)^{-2d} \equiv C^* f^{-2d} \qquad \text{as} \qquad f \to 0$$

which is a distinguishing feature of the spectrum of long memory processes, for $0 < d < \frac{1}{2}$.

Two Simple Special Cases. In practice, ARIMA(p, d, q) models are likely to be most useful for small values of p and q. So, we mention a few specific details given by Hosking (1981) about characteristics of two of the simplest such models. First, consider the fractional ARIMA$(1, d, 0)$ model, $(1-\phi B)(1-B)^d z_t = a_t$, with AR parameter $-1 < \phi < 1$. Then

$(1-\phi B)z_t = w_t$ or $z_t = (1-\phi B)^{-1}w_t = \sum_{j=0}^{\infty}\phi^j w_{t-j}$, so using (10.4.7) and (10.4.8) with $\psi_j = \phi^j$ it follows that the autocorrelation function of $\{z_t\}$ is

$$\rho_l(z) = \frac{\rho_l(w)}{1-\phi}\frac{F(d+l,1;1-d+l;\phi)+F(d-l,1;1-d-l;\phi)-1}{F(1+d,1;1-d;\phi)}$$

where $F(a,b;c;x)$ is the hypergeometric function defined by

$$\begin{aligned}F(a,b;c;x) &= 1+\frac{ab}{c\cdot 1}x+\frac{a(a+1)b(b+1)}{c(c+1)\cdot 1\cdot 2}x^2+\cdots\\ &= \frac{\Gamma(c)}{\Gamma(a)\Gamma(b)}\sum_{k=0}^{\infty}\frac{\Gamma(a+k)\Gamma(b+k)}{\Gamma(c+k)k!}x^k\end{aligned}$$

and

$$\begin{aligned}\gamma_0(z) &= \gamma_0(w)\sum_{j=0}^{\infty}\sum_{k=0}^{\infty}\phi^{j+k}\rho_{j-k}(w)\\ &= \frac{\gamma_0(w)}{1-\phi^2}[2F(d,1;1-d;\phi)-1] = \frac{\sigma_a^2\Gamma(1-2d)}{\Gamma(1-d)^2}\frac{F(1+d,1;1-d;\phi)}{1+\phi}\end{aligned}$$

Given ϕ and d, values of $F(d+l,1;1-d+l;\phi)$ required in computing the $\gamma_l(z) = \gamma_0(z)\rho_l(z)$ may be obtained more conveniently using the recurrence relation

$$F(d+l-1,1;1-d+l-1;\phi) = \frac{d+l-1}{1-d+l-1}\phi F(d+l,1;1-d+l;\phi)+1$$

Second, for the fractional ARIMA$(0,d,1)$ model, $(1-B)^d z_t = (1-\theta B)a_t$, with $-1<\theta<1$, we have $z_t = (1-\theta B)w_t$. So again using (10.4.7) and (10.4.8), now with $\psi_0 = 1, \psi_1 = -\theta$, and $\psi_j = 0$ for $j>1$, we find that

$$\gamma_l(z) = \gamma_0(w)[(1+\theta^2)\rho_l(w)-\theta\rho_{l+1}(w)-\theta\rho_{l-1}(w)]$$

and the ACF of $\{z_t\}$ is

$$\rho_l(z) = \rho_l(w)\frac{al^2-(1-d)^2}{l^2-(1-d)^2}$$

where

$$a = (1-\theta)^2\left[1+\theta^2-\frac{2\theta d}{1-d}\right]^{-1}$$

with

$$\gamma_0(z) = \gamma_0(w)[1+\theta^2-2\theta\rho_1(w)] = \left[\frac{\sigma_a^2\Gamma(1-2d)}{\Gamma(1-d)^2}\right]\left[1+\theta^2-\frac{2\theta d}{1-d}\right]$$

10.4.2 Estimation of Parameters

We first briefly mention the sampling properties of the sample mean

$$\bar{z} = \left(\frac{1}{n}\right)\sum_{t=1}^{n} z_t$$

for estimation of the mean $\mu = E[z_t]$ from a fractionally integrated ARMA process. From the general result that $\text{var}[\bar{z}] = (\gamma_0(z)/n)[1 + 2\sum_{h=1}^{n-1}\{(n-h)/n\}\rho_h(z)]$ and the property that $\rho_h(z) \sim Ch^{2d-1}$ as $h \to \infty$, it follows that

$$n^{1-2d}\text{var}[\bar{z}] \to C^*$$

for $-0.5 < d < 0.5$, where $C^* > 0$ is a certain constant. Hence, we see that $\text{var}[\bar{z}] \simeq C^*/n^{1-2d}$, whereas for short memory processes ($d = 0$), the variance of the sample mean behaves like $\text{var}[\bar{z}] \simeq C^*/n$. Thus, for $0 < d < 0.5$, the process mean μ can be much less accurately estimated by the sample mean. Equivalently, a much longer series length n is required for accurate estimation of μ for long memory processes. Hosking (1996) derived asymptotic distribution results for sample autocorrelations $\hat{\rho}_l(z)$ of long memory processes.

Estimation of the parameters $d, \boldsymbol{\phi}, \boldsymbol{\theta}$, and σ_a^2 in a fractionally integrated ARIMA (p, d, q) process can be performed by maximum likelihood (e.g., Sowell, 1992). However, direct evaluation of the exact likelihood function is rather slow due partly to the complicated nature of the autocovariance function of the process. Therefore, approximate ML estimation methods have been considered by Beran (1994, 1995) and others. Another convenient approach is to obtain an estimate of the parameter d initially by certain methods (e.g., using a frequency-domain nonparametric approach; see Geweke and Porter-Hudak (1983)), and then estimate $\boldsymbol{\phi}, \boldsymbol{\theta}$, and σ_a^2 by relatively standard ML methods for the given estimate of d. Asymptotic normality and the form of limiting covariance matrix of (approximate) ML estimators have been established by Beran (1995) and argued by Li and McLeod (1986). Notice that for $d \geq 0.5$, the fractionally integrated ARMA process is nonstationary. For such cases, in practice the typical procedure is to first difference the nonstationary process in the usual way, thus reducing it to a fractionally integrated process with a parameter d in the ''stationary'' range $-0.5 \leq d < 0.5$.

One approximate maximum likelihood estimation method is suggested by expressing the general fractional ARIMA process z_t in (10.4.2) in the infinite AR form as

$$z_t - \sum_{j=1}^{\infty} \pi_j^* z_{t-j} = a_t \tag{10.4.10}$$

where

$$\pi^*(B) = 1 - \sum_{j=1}^{\infty} \pi_j^* B^j = \theta^{-1}(B)\phi(B)(1-B)^d$$

The π_j^* coefficients can be obtained recursively based on the relation $\theta(B)\pi^*(B) = \phi(B)(1-B)^d \equiv \varphi(B)$, similar to Section 4.2.3, as

$$\pi_j^* - \theta_1\pi_{j-1}^* - \cdots - \theta_q\pi_{j-q}^* = \varphi_j \qquad j = 1, 2, \ldots$$

where $\varphi(B) = \phi(B)(1-B)^d = 1 - \sum_{j=1}^{\infty} \varphi_j B^j$. For example, in an ARIMA$(1, d, 1)$ model, the π_j^* satisfy $\pi_j^* - \theta_1 \pi_{j-1}^* = \varphi_j$, with $\varphi_j = \pi_j - \phi_1 \pi_{j-1}$ for $j \geq 1$, where the π_j are the coefficients in (10.4.3) and (10.4.4). In the approximate maximum likelihood or least-squares method, the truncated errors

$$\varepsilon_t(\boldsymbol{\beta}) = z_t - \sum_{j=1}^{t-1} \pi_j^* z_{t-j} \qquad t = 1, \ldots, n \tag{10.4.11}$$

are considered as a function of $\boldsymbol{\beta} = (\boldsymbol{\phi}', \boldsymbol{\theta}', d)'$, and the estimate $\hat{\boldsymbol{\beta}}$ is determined by minimizing the sum of squares $S(\boldsymbol{\beta}) = \sum_{t=1}^{n} \varepsilon_t^2(\boldsymbol{\beta})$. The corresponding approximate ML estimate of σ_a^2 is then taken as $\hat{\sigma}_a^2 = S(\hat{\boldsymbol{\beta}})/n$. For very long time series, it might be advisable to discard the first several $\varepsilon_t^2(\boldsymbol{\beta})$ terms in the sum-of-squares function to be minimized (e.g., the first 10–20 values), to avoid the effects of the inaccuracy in the approximation (10.4.11) for small values of t.

For practical implementation of the approximate maximum likelihood method, we might consider the following modification suggested because the series $(1-B)^d z_t$ follows the ARMA(p, q) model. Construct the series of truncated values of $(1-B)^d z_t \equiv \pi(B) z_t$ as

$$\tilde{z}_t(d) = z_t + \sum_{j=1}^{t-1} \pi_j(d) z_{t-j} \qquad t = 1, \ldots, n$$

for each d a grid of values within $-0.5 \leq d < 0.5$, where the $\pi_j(d)$ are the coefficients in (10.4.3) and (10.4.4). Then for *each* (fixed) value of d on the grid, obtain ML estimates of the ARMA parameters $\boldsymbol{\phi}, \boldsymbol{\theta}$, and σ_a^2, for the time series $\tilde{z}_t(d), \ldots, \bar{z}_n(d)$, by the usual likelihood and sum-of-squares methods of Chapter 7. The estimate $\hat{d}$ is then taken as the value of d that gives the minimum $\hat{\sigma}_a^2$ or the maximum of the likelihood, and the estimates $\hat{\boldsymbol{\phi}}, \hat{\boldsymbol{\theta}}$ associated with this value of d are the corresponding approximate ML estimates.

Estimation procedures directly extend to the more practical case of the fractional ARIMA model with an unknown nonzero mean μ,

$$\phi(B)(1-B)^d (z_t - \mu) = \theta(B) a_t$$

Although asymptotic theory is established to show that estimation of the additional unknown mean parameter μ does not affect the limiting distribution of the ARIMA parameter estimates $\hat{\boldsymbol{\phi}}, \hat{\boldsymbol{\theta}}, \hat{d}$, empirical simulation evidence (e.g., Hauser, 1999; Cheang and Reinsel, 2003) suggests that sampling properties of these estimates can be adversely affected even for moderately large sample lengths. This behavior may be related to previous discussion concerning the lower accuracy in estimation of the mean μ of a fractional ARIMA process. A possible remedy to obtain improved estimates of the ARIMA model parameters in the case of an unknown mean μ, or in situations of more general regression models with fractional ARIMA noise, is use of the restricted maximum likelihood estimation method as discussed in Section 9.5.2.

Forecasting. As with parameter estimation, forecasting for fractionally integrated ARMA processes (10.4.2) is not as convenient as for ARIMA processes with nonnegative *integer* value of d, because of the higher complexity of the differencing operator $(1-B)^d$ in the fractional case. Unlike the standard ARIMA model, forecasts cannot be obtained

conveniently directly from a *finite-order* difference equation form. For the fractional ARIMA model, it is simpler to consider forecasts based on the infinite AR form (10.4.10). Then, similar to (5.3.5) and (5.3.6), from this form we obtain that the l-step-ahead forecast of z_{t+l} based on the infinite past observations through origin t, z_t, z_{t-1}, …, is

$$\hat{z}_t(l) = \sum_{j=1}^{\infty} \pi_j^* \hat{z}_t(l-j) \tag{10.4.12}$$

where $\hat{z}_t(l-j) = z_{t+l-j}$ for $j \geq l$ as usual. For practical use, with forecasts based on a finite series of n available observations $z_1, \ldots, z_n$ and n sufficiently large, the sum in (10.4.12) must be truncated as $\hat{z}_n(l) = \sum_{j=1}^{n+l-1} \pi_j^* \hat{z}_n(l-j)$.

Conversely, the process z_t has the infinite MA form

$$z_t = \psi(B)a_t = \sum_{j=0}^{\infty} \psi_j a_{t-j}$$

where $\psi(B) = \Sigma_{j=0}^{\infty} \psi_j B^j = \phi^{-1}(B)(1-B)^{-d}\theta(B) \equiv \varphi^{-1}(B)\theta(B)$. From the same reasoning as in Chapter 5, we also have the equivalent representation of the lead-l forecast in (10.4.12) as

$$\hat{z}_t(l) = \sum_{j=l}^{\infty} \psi_j a_{t+l-j} \tag{10.4.13}$$

So the forecast error is $e_t(l) = z_{t+l} - \hat{z}_t(l) = \sum_{j=0}^{l-1} \psi_j a_{t+l-j}$, with variance

$$\sigma^2(l) = \text{var}[e_t(l)] = \sigma_a^2 \sum_{j=0}^{l-1} \psi_j^2$$

Example: Series A. Consider again Series A, which is a time series of chemical process concentration readings with $n = 197$ observations. Two possible models were proposed for this series in Chapters 6 and 7. One was the ''nearly nonstationary'' ARMA(1, 1) model, $(1-\phi B)z_t = \theta_0 + (1-\theta B)a_t$, with estimates $\hat{\phi} = 0.92$, $\hat{\theta} = 0.58$, $\hat{\theta}_0 = 1.45$, and $\hat{\sigma}_a^2 = 0.0974$. The second was the nonstationary IMA(0, 1, 1) model, $(1-B)z_t = (1-\theta B)a_t$, with estimates $\hat{\theta} = 0.71$ and $\hat{\sigma}_a^2 = 0.1004$. The unit root test performed in Section 10.1 suggests that the nonstationary IMA(0, 1, 1) model may be more appropriate. Beran (1995) also examined these data and found that an ARIMA$(0, d, 0)$ model, that is, a fractionally integrated white noise model, $(1-B)^d(z_t - \mu) = a_t$, fits the series well, with estimates $\hat{d} = 0.41$ and $\hat{\sigma}_a^2 = 0.0978$. Notice that the estimate of d is less than, but close to, the nonstationary boundary of $d < 0.5$ for an ARIMA$(0, d, 0)$ process, giving further support to the notion that it is very difficult to determine whether this process is stationary or not based on the series length of only $n = 197$ observations. In certain respects, especially in terms of long memory characteristics, the fractional ARIMA$(0, d, 0)$ model of Beran (1995) may be viewed as intermediate between the two models suggested earlier. For comparison, in Table 10.1 we display the first 30 ψ_j coefficients of the ''infinite'' MA representation for each of the three models considered. Notice that while the ψ_j, for ≥ 2, are initially smaller for the ARIMA$(0, d, 0)$ model than for the ARMA(1, 1) model, they decay relatively more slowly and become larger than those of the ARMA(1, 1) for all lags $j \geq 18$. In contrast,

TABLE 10.1 Coefficients ψ_j of the "Infinite" MA Representations for Three ARIMA Models Fitted to the Chemical Process Concentration Readings in Series A.

j	ARMA (1, 1)	IMA (0, 1, 1)	ARMA $(0, d, 0)$	j	ARMA (1, 1)	IMA (0, 1, 1)	ARMA $(0, d, 0)$
1	0.34000	0.290	0.41000	16	0.09734	0.290	0.08938
2	0.31280	0.290	0.28905	17	0.08955	0.290	0.08628
3	0.28778	0.290	0.23220	18	0.08239	0.290	0.08345
4	0.26475	0.290	0.19795	19	0.07580	0.290	0.08086
5	0.24357	0.290	0.17460	20	0.06974	0.290	0.07848
6	0.22409	0.290	0.15743	21	0.06416	0.290	0.07627
7	0.20616	0.290	0.14416	22	0.05902	0.290	0.07423
8	0.18967	0.290	0.13353	23	0.05430	0.290	0.07232
9	0.17449	0.290	0.12477	24	0.04996	0.290	0.07054
10	0.16054	0.290	0.11741	25	0.04596	0.290	0.06888
11	0.14769	0.290	0.11111	26	0.04228	0.290	0.06732
12	0.13588	0.290	0.10565	27	0.03890	0.290	0.06585
13	0.12501	0.290	0.10086	28	0.03579	0.290	0.06446
14	0.11501	0.290	0.09661	29	0.03293	0.290	0.06315
15	0.10581	0.290	0.09281	30	0.03029	0.290	0.06190

for the IMA(0, 1, 1) model we know that the $\psi_j = 1 - \theta$, for all $j > 1$, do not decay, which may not be an appropriate feature of a model for this process.

Remark. The parameters of the ARIMA$(0, d, 0)$ model can be estimated using the fracdiff package in R as shown below. From the partial output included, we see that the estimates $\hat{d} = 0.40$ and $\hat{\sigma}_a^2 = (0.3123734)^2 = 0.0976$ are close to the values quoted above.

```
> library(fracdiff)
> fracdiff(seriesA, nar=0, nma=0, M=30)
  Call:  fracdiff(x = numA, nar=0, nma=0, M=30)
  Coefficients:  d = 0.4001903
  sigma[eps] = 0.3123734
```

EXERCISES

10.1 Download from the Internet the daily stock prices of a company of your choosing.

(a) Plot the data using the graphics capabilities in R. Are there any unusual features worth noting? Perform a statistical test to determine the presence of a unit root in the series.

(b) Compute and plot the series of daily log returns. Does the graph show evidence of volatility clustering? Perform a statistical analysis to determine whether an AR–ARCH model would be appropriate for your series. If so, fit the model to the returns.

10.2 Daily closing prices of four major European stock indices are available for the period 1991–1998 in the file ''EuStockMarkets'' in the R datasets package; see help(EuStockMarkets) for details.

(a) Select two series and plot the data using R. Are there any unusual features worth noting? Perform a statistical test to determine the presence of a unit root in these series.

(b) Compute and plot the series of daily log returns. Do the graphs show evidence of volatility clustering? Perform a statistical analysis to determine whether AR–ARCH models would be appropriate for your series. State the final models selected.

10.3 Consider the ARCH(1) process $\{a_t\}$ defined by $a_t = \sigma_t e_t$, with $\sigma_t^2 = \alpha_0 + \alpha_1 a_{t-1}^2$, where the e_t are independent, identically distributed variates with mean 0 and variance 1, and assume that $0 < \alpha_1 < 1$.

(a) Verify that $a_t^2 = \alpha_0 \sum_{j=0}^{\infty} \alpha_1^j e_t^2 e_{t-1}^2 \cdots e_{t-j}^2 = e_t^2 \alpha_0 \left(1 + \sum_{j=1}^{\infty} \alpha_1^j e_{t-1}^2 \cdots e_{t-j}^2\right)$ or

$$a_t = e_t \left\{ \alpha_0 \left(1 + \sum_{j=1}^{\infty} \alpha_1^j e_{t-1}^2 \cdots e_{t-j}^2 \right) \right\}^{1/2}$$

provides a causal (strictly) stationary representation (solution) of the ARCH model equations, that is, such that $\sigma_t^2 = \alpha_0 \left(1 + \sum_{j=1}^{\infty} \alpha_1^j e_{t-1}^2 \cdots e_{t-j}^2\right)$ satisfies $\sigma_t^2 = \alpha_0 + \alpha_1 a_{t-1}^2 \equiv \alpha_0 + \alpha_1 e_{t-1}^2 \sigma_{t-1}^2$.

(b) Use the representation for a_t in (a) to show that $E[a_t] = 0$, $E[a_t^2] = \text{var}[a_t] = \alpha_0/(1 - \alpha_1)$, and $E[a_t a_{t-k}] = \text{cov}[a_t, a_{t-k}] = 0$ for $k \neq 0$.

(c) Define $X_t = a_t^2$ and assume, in addition, that $\alpha_1^2 < \frac{1}{3}$, so that $E[a_t^4] < \infty$, that is, $E[X_t^2] < \infty$. Show that the process $\{X_t\}$ satisfies the relation $X_t = e_t^2(\alpha_0 + \alpha_1 X_{t-1})$, and deduce from this that the autocovariances of $\{X_t\}$ satisfy $\text{cov}[X_t, X_{t-k}] = \alpha_1 \text{cov}[X_{t-1}, X_{t-k}]$ for $k \geq 1$. Hence, conclude that $\{X_t\}$ has the same autocorrelation function as an AR(1) process with AR parameter $\phi = \alpha_1$.

10.4 Consider the GARCH(1, 1) model $a_t = \sigma_t e_t$, where the e_t are iid random variables with mean 0 and variance 1, and $\sigma_t^2 = \alpha_0 + \alpha_1 a_{t-1}^2 + \beta_1 \sigma_{t-1}^2$. Show that the unconditional variance of a_t equals $\text{var}[a_t] = \alpha_0/[1 - (\alpha_1 + \beta_1)]$.

10.5 Derive the five-step-ahead forecast of the conditional variance σ_t^2 from a time origin h for the GARCH(1, 1) process. Repeat the derivation for a GARCH(2, 1) process.

10.6 Suppose that a time series of stock returns $\{r_t\}$ can be represented using an ARCH(1)-M process $r_t = \delta \sigma_t^2 + a_t$, $a_t = \sigma_t e_t$, and $\sigma_t^2 = \alpha_0 + \alpha_1 a_{t-1}^2$, where the e_t are iid Normal(0, 1).

(a) Derive the conditional and unconditional mean of the series.

(b) Show that the ARCH-in-mean effect makes the $\{r_t\}$ serially correlated and calculate the ACF $\rho_k, k = 1, 2, \ldots$.

10.7 Assume that $\{z_t\}$ is a stationary, zero mean, Gaussian process with autocovariance function $\gamma_k(z)$ and autocorrelation function $\rho_k(z)$. Use the property that for zero

mean Gaussian variates,

$$E[z_t z_{t+i} z_{t+j} z_{t+k}] = E[z_t z_{t+i}]E[z_{t+j} z_{t+k}] + E[z_t z_{t+j}]E[z_{t+i} z_{t+k}] + E[z_t z_{t+k}]\, E[z_{t+i} z_{t+j}]$$

to show that $\text{cov}[z_t^2, z_{t+k}^2] = 2\gamma_k^2(z)$ and hence that the autocorrelation function of the process of squared values $X_t = z_t^2$ is $\rho_k(X) = \rho_k^2(z)$.

10.8 Consider the first-order bilinear model $z_t = \phi z_{t-1} + a_t - b z_{t-1} a_{t-1}$, where the a_t are independent variates with mean 0 and variance σ_a^2. Assume the process $\{z_t\}$ is stationary, which involves the condition that $\phi^2 + \sigma_a^2 b^2 < 1$, and assume that $\{z_t\}$ has a causal stationary representation of the form $z_t = a_t + f(a_{t-1}, a_{t-2}, \ldots)$.

(a) Verify that $E[z_t a_t] = \sigma_a^2$, and so also that $\mu_z = E[z_t]$ satisfies $(1 - \phi)\mu_z = -b\sigma_a^2$.

(b) Establish that the autocovariances γ_k of $\{z_t\}$ satisfy $\gamma_k = \phi\gamma_{k-1}$ for $k > 1$, so that the process has the same autocovariance structure as an ARMA(1, 1) process.

10.9 Consider the annual sunspot series referred to as Series E in this text. The series is also available for a slightly longer time period as series ''sunspot.year'' in the R datasets package.

(a) Plot the time series and fit an AR(3) model to the series.

(b) Use the procedure described by McLeod and Li (1983) to test for nonlinearity in the series.

(c) Repeat part (b) using the Keenan and Tsay tests for nonlinearity.

(d) Describe how you might fit a nonlinear time series model to this series.

10.10 Measurements of the annual flow of the river Nile at Aswan from 1871 to 1970 are provided as series ''Nile'' in the R datasets package; type help(Nile) for details.

(a) Plot the data along with the ACF and PACF of the series. Fit an appropriate ARIMA model to this series and comment.

(b) Perform a statistical analysis to determine whether there is evidence of long memory dependence in this series.

(c) If the answer in (b) is affirmative, develop a fractionallly integrated ARMA (i.e. ARFIMA) model for the series.

PART THREE

TRANSFER FUNCTION AND MULTIVARIATE MODEL BUILDING

Suppose that X measures the level of an *input* to a dynamic system. For example, X might be the concentration of some constituent in the feed to a chemical process. Suppose that the level of X influences the level of a system *output* Y. For example, Y might be the yield of product from the chemical process. It will usually be the case that because of the inertia of the system, a change in X from one level to another will have no immediate effect on the output but, instead, will produce delayed response with Y eventually coming to equilibrium at a new level. We refer to such a change as a *dynamic* response. A model that describes this dynamic response is called a *transfer function model*. We shall suppose that observations of input and output are made at equispaced intervals of time. The associated transfer function model will then be called a *discrete* transfer function model.

Models of this kind can describe not only the behavior of industrial processes but also that of economic and business systems. Transfer function model building is important because it is only when the dynamic characteristics of a system are understood that intelligent direction, manipulation, and control of the system is possible.

Even under carefully controlled conditions, influences other than X will affect Y. We refer to the combined effect on Y of such influences as the *disturbance* or the *noise*. Such model that can be related to real data must take account of not only the dynamic relationship associating X and Y but also the noise infecting the system. Such joint models are obtained by combining a deterministic transfer function model with a stochastic noise model.

In Chapter 11 we introduce a class of linear transfer function models capable of representing many of the dynamic relationships commonly met in practice. In Chapter 12 we show how, taking account of corrupting noise, they may be related to data. Given the observed series X and Y, the development of the combined transfer function and noise model is accomplished by procedures of *identification, estimation*, and *diagnostic checking,*

Time Series Analysis: Forecasting and Control, Fifth Edition. George E. P. Box, Gwilym M. Jenkins, Gregory C. Reinsel, and Greta M. Ljung

which closely parallel those already described for univariate time series. In Chapter 13 we describe how simple pulse and step indicator variables can be used as inputs in transfer function models to represent and assess the effects of unusual *intervention* events on the behavior of a time series Y. In Chapter 14 the concepts and methods of bivariate time series analysis and transfer function modeling are extended to the general study of dynamic relationships among *several* time series through development of statistical models and methods of *multivariate* time series analysis.

11

TRANSFER FUNCTION MODELS

In this chapter, we introduce a class of discrete linear transfer function models. These models take advantage of the dynamic relationship between two time series for prediction, control, and other applications. The models considered can be used to represent commonly occurring dynamic situations and are parsimonious in their use of parameters.

11.1 LINEAR TRANSFER FUNCTION MODELS

We assume that pairs of observations (X_t, Y_t) are available at equispaced intervals of time of an input X and an output Y from some dynamic system, as illustrated in Figure 11.1. In some situations, both X and Y are essentially continuous but are observed only at discrete times. It then makes sense to consider not only what the data has to tell us about the model representing transfer from one discrete series to another, but also what the discrete model might be able to tell us about the corresponding continuous model. In other examples, the discrete series are all that exist, and there is no underlying continuous process. Where we relate continuous and discrete systems, we shall use the basic sampling interval as the unit of time. That is, periods of time will be measured by the number of sampling intervals they occupy. Also, a discrete observation X_t will be deemed to have occurred ''at time t.''

When we consider the value of a continuous variable, say Y at time t, we denote it by $Y(t)$. If t happens to be a time at which a discrete variable Y is observed, its value is denoted by Y_t. When we wish to emphasize the dependence of a discrete output Y, not only on time but also on the level of the input X, we write $Y_t(X)$.

Time Series Analysis: Forecasting and Control, Fifth Edition. George E. P. Box, Gwilym M. Jenkins, Gregory C. Reinsel, and Greta M. Ljung

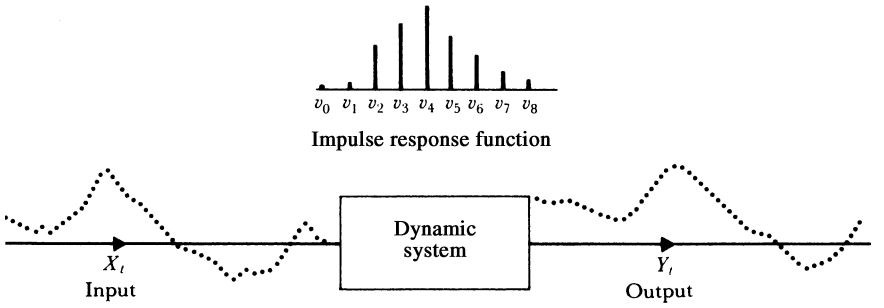

FIGURE 11.1 Input to, and output from, a dynamic system.

11.1.1 Discrete Transfer Function

With suitable inputs and outputs, which are left to the imagination of the reader, the dynamic system of Figure 11.1 might represent an industrial process, the economy of a country, or the behavior of a particular corporation or government agency.

From time to time, we refer to the *steady-state* level of the output obtained when the input is held at some fixed value. By this, we mean that the value $Y_\infty(X)$ at which the discrete output from a stable system *eventually* comes to equilibrium when the input is held at the fixed level X. Very often, over the range of interest, the relationship between $Y_\infty(X)$ and X will be approximately linear. Hence, if we use Y and X to denote *deviations* from convenient origins situated on the line, we can write the steady-state relationship as

$$Y_\infty = gX \tag{11.1.1}$$

where g is called the *steady-state gain*, and it is understood that Y_∞ is a function of X.

Now, suppose the level of the input is being varied and that X_t and Y_t represent *deviations* at time t from equilibrium. Then, it frequently happens that to an adequate approximation, the inertia of the system can be represented by a *linear filter* of the form

$$\begin{aligned} Y_t &= v_0 X_t + v_1 X_{t-1} + v_2 X_{t-2} + \cdots \\ &= (v_0 + v_1 B + v_2 B^2 + \cdots) X_t \\ &= v(B) X_t \end{aligned} \tag{11.1.2}$$

in which the output deviation at some time t is represented as a linear aggregate of input deviations at times $t, t-1, \ldots$. The operator $v(B)$ is called the *transfer function* of the filter.

Impulse Response Function. The weights $v_0, v_1, v_2, \ldots$ in (11.1.2) are called the *impulse response function* of the system. This is because the v_j may be regarded as the output or *response* at times $j \geq 0$ to a unit *pulse* input at time 0, that is, an input X_t such that $X_t = 1$ if $t = 0$, $X_t = 0$ otherwise. The impulse response function is shown in Figure 11.1 in the form of a bar chart. When there is no immediate response, one or more of the initial v's, say $v_0, v_1, \ldots, v_{b-1}$, will be equal to zero.

According to (11.1.2), the output deviation can be regarded as a linear aggregate of a series of superimposed impulse response functions scaled by the deviations X_t. This is illustrated in Figure 11.2, which shows a hypothetical impulse response function and the transfer it induces from the input to the output. In the situation illustrated, the input and

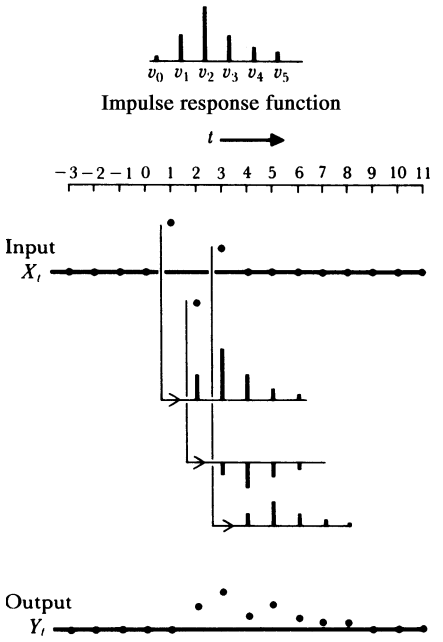

FIGURE 11.2 Linear transfer from input X_t to output Y_t.

output are initially in equilibrium. The deviations that occur in the input at times $t = 1$, $t = 2$, and $t = 3$ produce impulse response patterns of deviations in the output, which add together to produce the overall output response.

Relation Between the Incremental Changes. Denote by

$$y_t = Y_t - Y_{t-1} = \nabla Y_t$$

and by

$$x_t = X_t - X_{t-1} = \nabla X_t$$

the *incremental changes* in Y and X. We often wish to relate such changes. On differencing (11.1.2), we obtain

$$y_t = v(B)x_t$$

Thus, we see that the incremental changes y_t and x_t satisfy the same transfer function model as do Y_t and X_t.

Stability. If the infinite series $v_0 + v_1 B + v_2 B^2 + \cdots$ converges for $|B| \leq 1$, or equivalently, if the v_j are absolutely summable, so that $\sum_{j=0}^{\infty} |v_j| < \infty$, then the system is said to be *stable*. We shall be concerned here only with stable systems and consequently, impose this condition on the models we study. The stability condition implies that a finite incremental change in the input results in a finite incremental change in the output.

Now, suppose that X is held indefinitely at the value +1. Then, according to (11.1.1), Y will adjust and maintain itself at the value g. On substituting in (11.1.2) the values $Y_t = g$, $1 = X_t = X_{t-1} = X_{t-2} = \ldots$, we obtain

$$\sum_{j=0}^{\infty} v_j = g \tag{11.1.3}$$

Thus, for a stable system the sum of the impulse response weights converges and is equal to the steady-state gain of the system.

Parsimony. It would often be unsatisfactory to parameterize the system in terms of the v_j's of (11.1.2). The use of that many parameters could, at the estimation stage, lead to inaccurate and unstable estimation of the transfer function. Furthermore, it is usually inappropriate to estimate the weights v_j directly because for many real situations the v_j's would be functionally related, as we now see.

11.1.2 Continuous Dynamic Models Represented by Differential Equations

First-Order Dynamic System. Consider Figure 11.3. Suppose that at time t, $X(t)$ is the *volume* of water in tank A and $Y_1(t)$ the volume of water in tank B, which is connected to A by a pipe. For the time being we ignore tank C, shown by dashed lines. Now suppose that water can be forced in or out of A through pipe P and that mechanical devices are available that make it possible to force the level and hence the volume X in A to follow any desired pattern *irrespective* of what happens in B.

Now if the volume X in the first tank is held at some *fixed* level, water will flow from one tank to the other until the levels are equal. If we now reset the volume X to some other value, again a flow between the tanks will occur until equilibrium is reached. The volume in B at equilibrium as a function of the fixed volume in A yields the steady-state

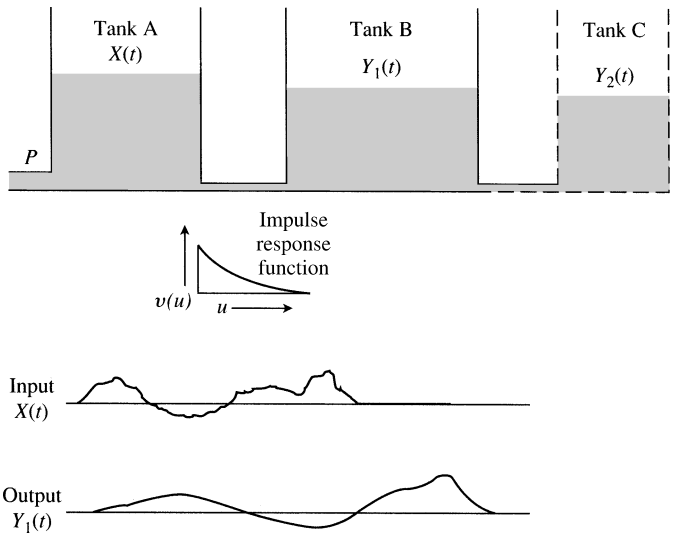

FIGURE 11.3 Representation of a simple dynamic system.

relationship

$$Y_{1\infty} = g_1 X \tag{11.1.4}$$

In this case the steady-state gain g_1 physically represents the ratio of the cross-sectional areas of the two tanks. If the levels are not in equilibrium at some time t, it is to be noted that the difference in the water level between the tanks is proportional to $g_1 X(t) - Y_1(t)$.

Suppose now that by forcing liquid in and out of pipe P, the volume $X(t)$ is made to follow a pattern like that labeled ''Input $X(t)$'' in Figure 11.3. Then, the volume $Y_1(t)$ in B will correspondingly change in some pattern such as that labeled on the figure as ''Output $Y_1(t)$.'' In general, the function $X(t)$ that is responsible for driving the system is called the *forcing function*.

To relate output to input, we note that to a close approximation, the rate of flow through the pipe will be proportional to the difference in head. That is,

$$\frac{dY_1}{dt} = \frac{1}{T_1}[g_1 X(t) - Y_1(t)] \tag{11.1.5}$$

where T_1 is a constant. The differential equation (11.1.5) may be rewritten in the form

$$(1 + T_1 D)Y_1(t) = g_1 X(t) \tag{11.1.6}$$

where $D = d/dt$. The dynamic system so represented by a first-order differential equation is often referred to as a first-order dynamic system. The constant T_1 is called the *time constant* of the system. The same first-order model can approximately represent the behavior of many simple systems. For example, $Y_1(t)$ might be the outlet temperature of water from a water heater, and $X(t)$ the flow rate of water into the heater.

It is possible to show (see, e.g., Jenkins and Watts, 1968) that the solution of a linear differential equation such as (11.1.6) can be written in the form

$$Y_1(t) = \int_0^\infty v(u)X(t-u)du \tag{11.1.7}$$

where in general $v(u)$ is the (continuous) impulse response function. We see that $Y_1(t)$ is generated from $X(t)$ as a continuously weighted aggregate, just as Y_t is generated from X_t as a discretely weighted aggregate in (11.1.2). Furthermore, we see that the role of weight function played by $v(u)$ in the continuous case is precisely parallel to that played by v_j in the discrete situation. For the particular first-order system defined by (11.1.6),

$$v(u) = g_1 T_1^{-1} e^{-u/T_1}$$

Thus, the impulse response in this case undergoes simple exponential decay, as indicated in Figure 11.3.

In the continuous case, determination of the output for a completely arbitrary forcing function, such as shown in Figure 11.3, is normally accomplished by simulation on an analog computer, or by using numerical procedures on a digital machine. Solutions are available analytically only for special forcing functions. Suppose, for example, that with the hydraulic system empty, $X(t)$ was suddenly raised to a level $X(t) = 1$ and maintained at that value. Then, we shall refer to the forcing function, which was at a steady level of zero and changed instantaneously to a steady level of unity, as a (unit) *step function*. The response of the system to such a function, called the *step response* to the system, is derived

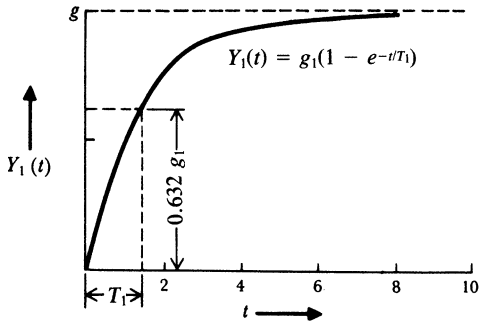

FIGURE 11.4 Response of a first-order system to a unit step change.

by solving the differential equation (11.1.6) with a unit step input, to obtain

$$Y_1(t) = g_1(1 - e^{-t/T_1}) \tag{11.1.8}$$

Thus, the level in tank B rises exponentially in the manner shown in Figure 11.4. Now, when $t = T_1, Y_1(t) = g_1(1 - e^{-1}) = 0.632g_1$. Thus, the time constant T_1 is the time required after the initiation of a step input for the first-order system (11.1.6) to reach 63.2% of its final equilibrium level.

Sometimes there is an initial period of pure *delay* or *dead time* before the response to a given input change begins to take effect. For example, if there were a long length of pipe between A and B in Figure 11.3, a sudden change in level in A could not begin to take effect until liquid had flowed down the pipe. Suppose that the delay thus introduced occupies τ units of time. Then, the response of the delayed system would be represented by a differential equation like (11.1.6), but with $t - \tau$ replacing t on the right-hand side, so that

$$(1 + T_1 D)Y_1(t) = g_1 X(t - \tau) \tag{11.1.9}$$

The corresponding impulse and step response functions for this system would be of precisely the same shape as for the undelayed system, but the functions would be translated along the horizontal axis a distance τ.

Second-Order Dynamic System. Consider Figure 11.3 once more. Imagine a three-tank system in which a pipe leads from tank B to a third tank C, the volume of liquid in which is denoted by $Y_2(t)$. Let T_2 be the time constant for the additional system and g_2 its steady-state gain. Then, $Y_2(t)$ and $Y_1(t)$ are related by the differential equation

$$(1 + T_2 D)Y_2(t) = g_2 Y_1(t)$$

After substitution in (11.1.6), we obtain a *second-order* differential equation linking the output from the third tank and the input to the first:

$$[1 + (T_1 + T_2)D + T_1 T_2 D^2]Y_2(t) = gX(t) \tag{11.1.10}$$

where $g = g_1 g_2$. For such a system, the impulse response function is a mixture of two exponentials

$$v(u) = \frac{g(e^{-u/T_1} - e^{-u/T_2})}{T_1 - T_2} \tag{11.1.11}$$

and the response to a unit step is given by

$$Y_2(t) = g\left(1 - \frac{T_1 e^{-t/T_1} - T_2 e^{-t/T_2}}{T_1 - T_2}\right) \tag{11.1.12}$$

The continuous curve R in Figure 11.5 shows the response to a unit step for the system

$$(1 + 3D + 2D^2)Y_2(t) = 5X(t)$$

for which $T_1 = 1$, $T_2 = 2$, $g = 5$. Note that unlike the first-order system, the second-order system has a step response that has zero slope initially.

A more general second-order system is defined by

$$(1 + \Xi_1 D + \Xi_2 D^2)Y(t) = gX(t) \tag{11.1.13}$$

where

$$\Xi_1 = T_1 + T_2 \qquad \Xi_2 = T_1 T_2 \tag{11.1.14}$$

and the constants T_1 and T_2 may be complex. If we write

$$T_1 = \frac{1}{\zeta} e^{i\lambda} \qquad T_2 = \frac{1}{\zeta} e^{-i\lambda} \tag{11.1.15}$$

then (11.1.13) becomes

$$\left(1 + \frac{2\cos\lambda}{\zeta} D + \frac{1}{\zeta^2} D^2\right) Y(t) = gX(t) \tag{11.1.16}$$

The impulse response function (11.1.11) then reduces to

$$v(u) = g \frac{\zeta e^{-\zeta u \cos\lambda} \sin(\zeta u \sin\lambda)}{\sin\lambda} \tag{11.1.17}$$

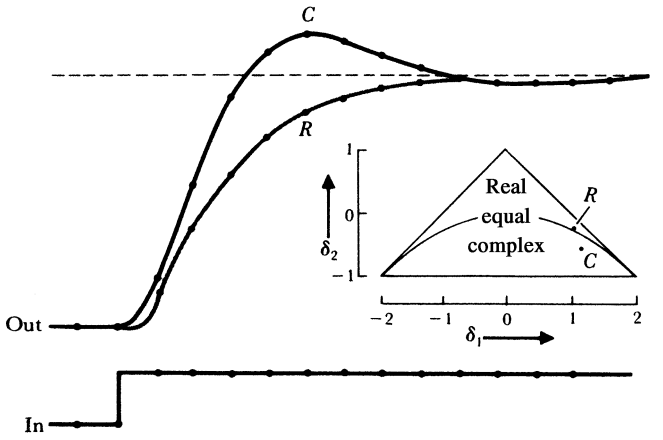

FIGURE 11.5 Step responses of coincident, discrete, and continuous second-order systems having characteristic equations with real roots (curve ***R***) and complex roots (curve ***C***).

and the response (11.1.12) to a unit step, to

$$Y(t) = g\left[1 - \frac{e^{-\zeta t \cos\lambda}\sin(\zeta t \sin\lambda + \lambda)}{\sin\lambda}\right] \tag{11.1.18}$$

The continuous curve C in Figure 11.5 shows the response to a unit step for the system

$$(1 + \sqrt{2}D + 2D^2)Y(t) = 5X(t)$$

for which $\lambda = \pi/3$ and $\zeta = \sqrt{2}/2$. It will be noticed that the response overshoots the value $g = 5$ and then comes to equilibrium as a damped sine wave. This behavior is typical of underdamped systems, as they are called. In general, a second-order system is said to be *overdamped, critically damped*, or *underdamped*, depending on whether the constants T_1 and T_2 are real, real and equal, or complex. The overdamped system has a step response that is a mixture of two exponentials, given by (11.1.12), and will always remain below the asymptote $Y(\infty) = g$. As with the first-order system, the response can be made subject to a period of dead time by replacing t on the right-hand side of (11.1.13) by $t - \tau$. Many quite complicated dynamic systems can be closely approximated by such second-order systems with delay.

More elaborate linear dynamic systems can be represented by allowing not only the level of the forcing function $X(t)$ but also its rate of change dX/dt and higher derivatives to influence the behavior of the system. Thus, a general model for representing (continuous) dynamic systems is the linear differential equation

$$(1 + \Xi_1 D + \cdots + \Xi_R D^R)Y(t) = g(1 + H_1 D + \cdots + H_S D^S)X(t - \tau) \tag{11.1.19}$$

11.2 DISCRETE DYNAMIC MODELS REPRESENTED BY DIFFERENCE EQUATIONS

11.2.1 General Form of the Difference Equation

Corresponding to the continuous representation (11.1.19), discrete dynamic systems are often parsimoniously represented by the general linear *difference* equation

$$(1 + \xi_1\nabla + \cdots + \xi_r\nabla^r)Y_t = g(1 + \eta_1\nabla + \cdots + \eta_s\nabla^s)X_{t-b} \tag{11.2.1}$$

which we refer to as a transfer function model of order (r, s). The difference equation (11.2.1) may also be written in terms of the backward shift operator B, with $\nabla = 1 - B$, as

$$(1 - \delta_1 B - \cdots - \delta_r B^r)Y_t = (\omega_0 - \omega_1 B - \cdots - \omega_s B^s)X_{t-b} \tag{11.2.2}$$

or as

$$\delta(B)Y_t = \omega(B)X_{t-b}$$

Equivalently, writing $\Omega(B) = \omega(B)B^b$, the model becomes

$$\delta(B)Y_t = \Omega(B)X_t \tag{11.2.3}$$

Comparing (11.2.3) with (11.1.2) we see that the transfer function for this model is

$$v(B) = \delta^{-1}(B)\Omega(B) \tag{11.2.4}$$

Thus, the transfer function is represented by the ratio of two polynomial operators in B.

Dynamics of ARIMA Stochastic Models. The ARIMA model

$$\varphi(B)z_t = \theta(B)a_t$$

used for the representation of a time series $\{z_t\}$ relates z_t and a_t by the linear filtering operation

$$z_t = \varphi^{-1}(B)\theta(B)a_t$$

where a_t is white noise. Thus, the ARIMA model postulates that a time series can be usefully represented as an output from a dynamic system to which the input is white noise and for which the transfer function can be parsimoniously expressed as the ratio of two polynomial operators in B.

Stability of the Discrete Models. The requirement of stability for the discrete transfer function models exactly parallels that of stationarity for the ARMA stochastic models. In general, for stability we require that the roots of the characteristic equation

$$\delta(B) = 0$$

with B regarded as a variable, lie outside the unit circle. In particular, this implies that for the first-order model with $\delta(B) = 1 - \delta_1 B$, the parameter δ_1 satisfies

$$-1 < \delta_1 < 1$$

and for the second-order model (see, e.g., Fig. 11.5), the parameters δ_1, δ_2 satisfy

$$\delta_2 + \delta_1 < 1$$

$$\delta_2 - \delta_1 < 1$$

$$-1 < \delta_2 < 1$$

On writing (11.2.2) in full as

$$Y_t = \delta_1 Y_{t-1} + \cdots + \delta_r Y_{t-r} + \omega_0 X_{t-b} - \omega_1 X_{t-b-1} - \cdots - \omega_s X_{t-b-s}$$

we see that if X_t is held indefinitely at a value $+1$, Y_t will eventually reach the value

$$g = \frac{\omega_0 - \omega_1 - \cdots - \omega_s}{1 - \delta_1 - \cdots - \delta_r} \tag{11.2.5}$$

which expresses the steady-state gain in terms of the parameters of the model.

11.2.2 Nature of the Transfer Function

If we employ a transfer function model defined by the difference equation (11.2.2), then substituting

$$Y_t = v(B)X_t \tag{11.2.6}$$

in (11.2.2), we obtain the identity

$$\begin{aligned}(1 - \delta_1 B - \delta_2 B^2 - \cdots - \delta_r B^r)(v_0 + v_1 B + v_2 B^2 + \cdots) \\ = (\omega_0 - \omega_1 B - \cdots - \omega_s B^s)B^b\end{aligned} \tag{11.2.7}$$

On equating coefficients of B, we find

$$v_j = \begin{cases} 0 & j < b \\ \delta_1 v_{j-1} + \delta_2 v_{j-2} + \cdots + \delta_r v_{j-r} + \omega_0 & j = b \\ \delta_1 v_{j-1} + \delta_2 v_{j-2} + \cdots + \delta_r v_{j-r} - \omega_{j-b} & j = b+1, b+2, \ldots, b+s \\ \delta_1 v_{j-1} + \delta_2 v_{j-2} + \cdots + \delta_r v_{j-r} & j > b+s \end{cases} \tag{11.2.8}$$

The weights $v_{b+s}, v_{b+s-1}, \ldots, v_{b+s-r+1}$ supply r starting values for the homogeneous difference equation

$$\delta(B)v_j = 0 \qquad j > b + s$$

The solution $v_j = f(\boldsymbol{\delta}, \boldsymbol{\omega}, j)$ of this difference equation applies to all values v_j for which $j \geq b + s - r + 1$.

Thus, in general, the impulse response weights v_j consist of:

1. b zero values $v_0, v_1, \ldots, v_{b-1}$.
2. A further $s - r + 1$ values $v_b, v_{b+1}, \ldots, v_{b+s-r}$ following no fixed pattern (no such values occur if $s < r$).
3. Values v_j with $j \geq b + s - r + 1$ following the pattern dictated by the rth-order difference equation, which has r starting values $v_{b+s}, v_{b+s-1}, \ldots, v_{b+s-r+1}$. Starting values v_j for $j < b$ will, of course, be zero.

Step Response. We now write $V(B)$ for the generating function of the step response weights V_j, which represent the *response* at times $j \geq 0$ to a unit *step* at time 0, $X_t = 1$ if $t \geq 0$, $X_t = 0$ if $t < 0$, so that $V_j = \sum_{i=0}^{j} v_i$ for $j \geq 0$. Thus,

$$\begin{aligned}V(B) &= V_0 + V_1 B + V_2 B^2 + \cdots \\ &= v_0 + (v_0 + v_1)B + (v_0 + v_1 + v_2)B^2 + \cdots\end{aligned} \tag{11.2.9}$$

and

$$v(B) = (1 - B)V(B) \tag{11.2.10}$$

Substitution of (11.2.10) in (11.2.7) yields the identity

$$(1 - \delta_1^* B - \delta_2^* B^2 - \cdots - \delta_{r+1}^* B^{r+1})(V_0 + V_1 B + V_2 B^2 + \cdots) = (\omega_0 - \omega_1 B - \cdots - \omega_s B^s) B^b \tag{11.2.11}$$

with

$$(1 - \delta_1^* B - \delta_2^* B^2 - \cdots - \delta_{r+1}^* B^{r+1}) = (1 - B)(1 - \delta_1 B - \cdots - \delta_r B^r) \tag{11.2.12}$$

The identity (11.2.11) for the step response weights V_j exactly parallels the identity (11.2.7) for the impulse response weights, except that the left-hand operator $\delta^*(B)$ is of order $r + 1$ instead of r.

Using the results (11.2.8), it follows that the step response function is defined by:

1. b zero values $V_0, V_1, \ldots, V_{b-1}$.
2. A further $s - r$ values $V_b, V_{b+1}, \ldots, V_{b+s-r-1}$ following no fixed pattern (no such values occur if $s < r + 1$).
3. Values V_j, with $j \geq b + s - r$, which follow the pattern dictated by the $(r + 1)$th-order difference equation $\delta^*(B)V_j = 0$, which has $r + 1$ starting values V_{b+s}, $V_{b+s-1}, \ldots, V_{b+s-r}$. Starting values V_j for $j < b$ will, of course, be zero.

11.2.3 First- and Second-Order Discrete Transfer Function Models

Details of transfer function models for all combinations of $r = 0, 1, 2$ and $s = 0, 1, 2$ are shown in Table 11.1. Specific examples of the models, with bar charts showing step response and impulse response, are given in Figure 11.6. The equations at the end of Table 11.1 allow the parameters ξ, g, η of the ∇ form of the model to be expressed in terms of the parameters $\boldsymbol{\delta}, \boldsymbol{\omega}$ of the B form. These equations are given for the most general of the models considered, namely that for which $r = 2$ and $s = 2$. All the other models are special cases of this one, and the corresponding equations for these are obtained by setting appropriate parameters to zero. For example, if $r = 1$ and $s = 1, \xi_2 = \eta_2 = \delta_2 = \omega_2 = 0$, then

$$\delta_1 = \frac{\xi_1}{1 + \xi_1} \qquad \omega_0 = \frac{g(1 + \eta_1)}{1 + \xi_1} \qquad \omega_1 = \frac{g\eta_1}{1 + \xi_1}$$

In Figure 11.6, the starting values for the difference equations satisfied by the impulse and step responses, respectively, are indicated by circles on the bar charts.

Discussion of the Models in Table 11.1. The models, whose properties are summarized in Table 11.1 and Figure 11.6, will require careful study, since they are useful in representing many commonly met dynamic systems. In all the models the operator B^b on the right ensures that the first nonzero term in the impulse response function is v_b. In the examples in Figure 11.6, the value of g is assumed to equal 1, and b is assumed to equal 3.

Models with $r = 0$. With r and s both equal to zero, the impulse response consists of a single nonzero value $v_b = \omega_0 = g$. The output is proportional to the input but is displaced by b time intervals. More generally, if we have an operator of order s on the right, the instantaneous input will be delayed b intervals and will be spread over $s + 1$ values in proportion to $v_b = \omega_0, v_{b+1} = -\omega_1, \ldots, v_{b+s} = -\omega_s$. The step response is obtained by summing the impulse

TABLE 11.1 Impulse Response Functions for Transfer Function Models of the Form $\delta_r(B)Y_t = \omega_s(B)B^bX_t$

rsb	∇ Form	B Form	Impulse Response V_j	
00b	$Y_t = gX_{t-b}$	$Y_t = \omega_0 B^b X_t$	0	$j < b$
			ω_0	$j = b$
			0	$j > b$
01b	$Y_t = g(1 + \eta_1\nabla)X_{t-b}$	$Y_t = (\omega_0 - \omega_1 B)B^b X_t$	0	$j < b$
			ω_0	$j = b$
			$-\omega_1$	$j = b + 1$
			0	$j > b + 1$
02b	$Y_t = g(1 + \eta_1\nabla + \eta_2\nabla^2)X_{t-b}$	$Y_t = (\omega_0 - \omega_1 B - \omega_2 B^2)B^b X_t$	0	$j < b$
			ω_0	$j = b$
			$-\omega_1$	$j = b + 1$
			$-\omega_2$	$j = b + 2$
			0	$j > b + 2$
10b	$(1 + \xi_1\nabla)Y_t = gX_{t-b}$	$(1 - \delta_1 B)Y_t = \omega_0 B^b X_t$	0	$j < b$
			ω_0	$j = b$
			$\delta_1 v_{j-1}$	$j > b$
11b	$(1 + \xi_1\nabla)Y_t = g(1 + \eta_1\nabla)X_{t-b}$	$(1 - \delta_1 B)Y_t = (\omega_0 - \omega_1 B)B^b X_t$	0	$j < b$
			ω_0	$j = b$
			$\delta_1\omega_0 - \omega_1$	$j = b + 1$
			$\delta_1 v_{j-1}$	$j > b + 1$
12b	$(1 + \xi_1\nabla)Y_t = g(1 + \eta_1\nabla + \eta_2\nabla^2)X_{t-b}$	$(1 - \delta_1 B)Y_t = (\omega_0 - \omega_1 B - \omega_2 B^2)B^b X_t$	0	$j < b$
			ω_0	$j = b$
			$\delta_1\omega_0 - \omega_1$	$j = b + 1$
			$\delta_1^2\omega_0 - \delta_1\omega_1 - \omega_2$	$j = b + 2$
			$\delta_1 v_{j-1}$	$j > b + 2$

(*continued*)

TABLE 11.1 Impulse Response Functions for Transfer Function Models of the Form $\delta_r(B)Y_t = \omega_s(B)B^bX_t$ (*continued*)

rsb	∇ Form	B Form	Impulse Response V_j	
20*b*	$(1+\xi_1\nabla+\xi_2\nabla^2)Y_t = gX_{t-b}$	$(1-\delta_1B-\delta_2B^2)Y_t = \omega_0B^bX_t$	0	$j<b$
			ω_0	$j=b$
			$\delta_1v_{j-1}+\delta_1v_{j-2}$	$j>b$
21*b*	$(1+\xi_1\nabla+\xi_2\nabla^2)Y_t = g(1+\eta_1\nabla)X_{t-b}$	$(1-\delta_1B-\delta_2B^2)Y_t = (\omega_0-\omega_1B)B^bX_t$	0	$j<b$
			ω_0	$j=b$
			$\delta_1\omega_0-\omega_1$	$j=b+1$
			$\delta_1v_{j-1}+\delta_2v_{j-2}$	$j>b+1$
22*b*	$(1+\xi_1\nabla+\xi_2\nabla^2)Y_t = g(1+\eta_1\nabla+\eta_2\nabla^2)X_{t-b}$	$(1-\delta_1B-\delta_2B^2)Y_t = (\omega_0-\omega_1B-\omega_2B^2)B^bX_t$	0	$j<b$
			ω_0	$j=b$
			$\delta_1\omega_0-\omega_1$	$j=b+1$
			$(\delta_1^2+\delta_2)\omega_0-\delta_1\omega_1-\omega_2$	$j=b+2$
			$\delta_1v_{j-1}+\delta_2v_{j-2}$	$j=b+2$

$$\xi_1 = \frac{\delta_1+2\delta_2}{1-\delta_1-\delta_2}, \quad \xi_2 = \frac{-\delta_2}{1-\delta_1-\delta_2} \qquad \delta_1 = \frac{\xi_1+2\xi_2}{1+\xi_1+\xi_2}, \quad \delta_2 = \frac{-\xi_2}{1+\xi_1+\xi_2}$$

$$g = \frac{\omega_0-\omega_1-\omega_2}{1-\delta_1-\delta_2} \qquad \omega_0 = \frac{g(1+\eta_1+\eta_2)}{1+\xi_1+\xi_2}$$

$$\eta_1 = \frac{\omega_1+2\omega_2}{\omega_0-\omega_1-\omega_2} \qquad \omega_1 = \frac{g(\eta_1+2\eta_2)}{1+\xi_1+\xi_2}$$

$$\eta_2 = \frac{-\omega_2}{\omega_0-\omega_1-\omega_2} \qquad \omega_2 = \frac{-g\eta_2}{1+\xi_1+\xi_2}$$

$$1-\delta_1-\delta_2 = (1+\xi_1+\xi_2)^{-1}$$

r, s, b	∇ Form	B Form	Impulse Response v_j	Step Response $V_j = \sum_{i=0}^{j} v_i$
003	$Y_t = X_{t-3}$	$Y_t = B^3 X_t$	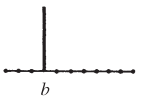	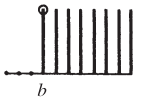
013	$Y_t = (1 - 0.5\nabla)\, X_{t-3}$	$Y_t = (0.5 + 0.5B)\, B^3 X_t$	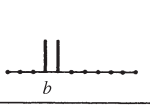	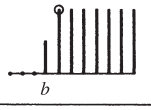
023	$Y_t = (1 - \nabla + 0.25\nabla^2)\, X_{t-3}$	$Y_t = (0.25 + 0.50B + 0.25B^2)\, B^3 X_t$	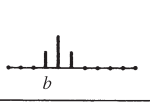	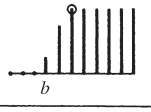
103	$(1+\nabla)\, Y_t = X_{t-3}$	$(1 - 0.5B)\, Y_t = 0.5B^3 X_t$	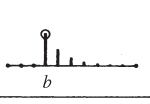	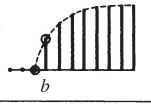
113	$(1+\nabla)\, Y_t = (1 - 0.5\nabla)\, X_{t-3}$	$(1 - 0.5B)\, Y_t = (0.25 + 0.25B)\, B^3 X_t$	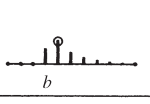	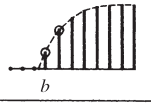
123	$(1+\nabla)\, Y_t = (1 - \nabla + 0.25\nabla^2)\, X_{t-3}$	$(1 - 0.5B)\, Y_t = (0.125 + 0.25B + 0.125B^2)\, B^3 X_t$	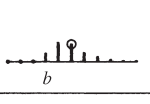	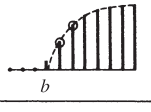
203	$(1 - 0.25\nabla + 0.5\nabla^2)\, Y_t = X_{t-3}$	$(1 - 0.6B + 0.4B^2)\, Y_t = 0.8B^3 X_t$	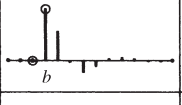	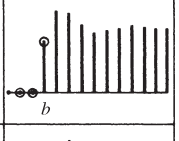
213	$(1 - 0.25\nabla + 0.5\nabla^2)\, Y_t = (1 - 0.5\nabla)\, X_{t-3}$	$(1 - 0.6B + 0.4B^2)\, Y_t = (0.4 + 0.4B)\, B^3 X$	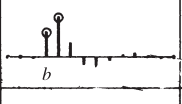	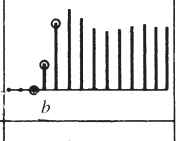
223	$(1 - 0.25\nabla + 0.5\nabla^2)\, Y_t = (1 - \nabla + 0.25\nabla^2)\, X_{t-3}$	$(1 - 0.6B + 0.4B^2)\, Y_t = (0.2 + 0.4B + 0.2B^2)\, B^3 X_t$	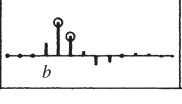	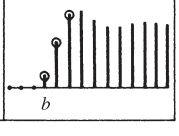

FIGURE 11.6 Examples of impulse and step response functions with gain $g = 1$.

response and eventually satisfies the difference equation $(1 - B)V_j = 0$ with starting values $V_{b+s} = g = \omega_0 - \omega_1 - \cdots - \omega_s$.

Models with $r = 1$. With $s = 0$, the impulse response tails off exponentially (geometrically) from the initial starting value $v_b = \omega_0 = g/(1 + \xi_1) = g(1 - \delta_1)$. The step re-

sponse increases exponentially until it attains the value $g = 1$. If the exponential step response is extrapolated backwards as indicated by the dashed line, it cuts the time axis at time $b - 1$. This corresponds to the fact that $V_{b-1} = 0$ as well as $V_b = v_b$ are starting values for the appropriate difference equation $(1 - \delta_1 B)(1 - B)V_j = 0$.

With $s = 1$, there is an initial value $v_b = \omega_0 = g(1 + \eta_1)/(1 + \xi_1)$ of the impulse response, which does not follow a pattern. The exponential pattern induced by the difference equation $v_j = \delta_1 v_{j-1}$ associated with the left-hand operator begins with the starting value $v_{b+1} = (\delta_1 \omega_0 - \omega_1) = g(\xi_1 - \eta_1)/(1 + \xi_1)^2$. The step response function follows an exponential curve, determined by the difference equation $(1 - \delta_1 B)(1 - B)V_j = 0$, which approaches g asymptotically from the starting value $V_b = v_b$ and $V_{b+1} = v_b + v_{b+1}$. An exponential curve projected by the dashed line backwards through the points will, in general, cut the time axis at some intermediate point in the time interval. We show in Section 11.3 that certain discrete models, which approximate continuous first-order systems having *fractional* periods of delay, may in fact be represented by a first-order difference equation with an operator of order $s = 1$ on the right.

With $s = 2$, there are two values v_b and v_{b+1} for the impulse response that do not follow a pattern, followed by exponential fall off beginning with v_{b+2}. Correspondingly, there is a single preliminary value V_b in the step response that does not coincide with the exponential curve projected by the dashed line. This curve is, as before, determined by the difference equation $(1 - \delta_1 B)(1 - B)V_j = 0$ but with starting values V_{b+1} and V_{b+2}.

Models with r = 2. The flexibility of the model with $s = 0$ is limited because the first starting value of the impulse response is fixed to be zero. More useful models are obtained for $s = 1$ and $s = 2$. The use of these models in approximating continuous second-order systems is discussed in Section 11.3 and in Appendix A11.1.

The behavior of the dynamic weights v_j, which eventually satisfy

$$v_j - \delta_1 v_{j-1} - \delta_2 v_{j-2} = 0 \qquad j > b + s \tag{11.2.13}$$

depends on the nature of the roots S_1^{-1} and S_2^{-1}, of the *characteristic equation*

$$1 - \delta_1 B - \delta_2 B^2 = (1 - S_1 B)(1 - S_2 B) = 0$$

This dependence is shown in Table 11.2. As in the continuous case, the model may be overdamped, critically damped, or underdamped, depending on the nature of the roots of the characteristic equation.

When the roots are complex, the solution of (11.2.13) will follow a damped sine wave, as in the examples of second-order systems in Figure 11.6. When the roots are real, the solution will be the sum of two exponentials. As in the continuous case considered in

TABLE 11.2 Dependence of Nature of Second-Order System on the Roots of $1 - \delta_1 B - \delta_2 B^2 = 0$

Roots (S_1^{-1}, S_2^{-1})	Condition	Damping
Real	$\delta_1^2 + 4\delta_2 > 0$	Overdamped
Real and equal	$\delta_1^2 + 4\delta_2 = 0$	Critically damped
Complex	$\delta_1^2 + 4\delta_2 < 0$	Underdamped

Section 11.1.2, the system can then be thought of as equivalent to two discrete first-order systems arranged in series and having parameters S_1 and S_2.

The weights V_j for the step response eventually satisfy a difference equation

$$(V_j - g) - \delta_1(V_{j-1} - g) - \delta_2(V_{j-2} - g) = 0$$

which is of the same form as (11.2.13). Thus, the behavior of the step response V_j about its asymptotic value g parallels the behavior of the impulse response about the time axis. In the situation where there are complex roots, the step response ''overshoots'' the value g and then oscillates about this value until it reaches equilibrium. When the roots are real and positive, the step response, which is the sum of two exponential terms, approaches its asymptote g without crossing it. However, if there are negative real roots, the step response may overshoot and oscillate as it settles down to its equilibrium value.

In Figure 11.5, the dots indicate two discrete step responses, labeled R and C, respectively, in relation to a discrete step input indicated by dots at the bottom of the figure. The difference equation models[1] corresponding to R and C are

$$\text{R}: \quad (1 - 0.97B + 0.22B^2)Y_t = 5(0.15 + 0.09B)X_{t-1}$$

$$\text{C}: \quad (1 - 1.15B + 0.49B^2)Y_t = 5(0.19 + 0.15B)X_{t-1}$$

Also shown in Figure 11.5 is a diagram of the stability region with the parameter points (δ_1, δ_2) marked for each of the two models. Note that the system described by model R, which has real positive roots, has no overshoot while that for model C, which has complex roots, does have overshoot.

11.2.4 Recursive Computation of Output for Any Input

It would be extremely tedious if it were necessary to use the impulse response form (11.1.2) of the model to compute the output for a given input. Fortunately, this is not necessary. Instead, we may employ the difference equation model directly. In this way it is a simple matter to compute the output recursively for any input. For example, consider the model with $r = 1, s = 0, b = 1$, and with $\xi = 1$ and $g = 5$. Thus,

$$(1 + \nabla)Y_t = 5X_{t-1}$$

or equivalently,

$$(1 - 0.5B)Y_t = 2.5X_{t-1} \tag{11.2.14}$$

Table 11.3 shows the calculation of Y_t when the input X_t is (a) a unit pulse input, (b) a unit step input, and (c) a ''general'' input. In all cases, it is assumed that the output has the initial value $Y_0 = 0$. To perform the recursive calculation, the difference equation is written out with Y_t on the left. Thus,

$$Y_t = 0.5Y_{t-1} + 2.5X_{t-1}$$

[1]The parameters in these models were in fact selected, in a manner to be discussed in Section 11.3.2, so that at the discrete points, the step responses exactly matched those of the continuous systems introduced in Section 11.1.2.

TABLE 11.3 Calculation of Output from Discrete First-Order System for Impulse, Step, and General Input

	(a) Impulse Input		(b) Step Input		(c) General Input	
t	Input X_t	Output Y_t	Input X_t	Output Y_t	Input X_t	Output Y_t
0	0	0	0	0	0	0
1	1	0	1	0	1.5	0
2	0	2.50	1	2.50	0.5	3.75
3	0	1.25	1	3.75	2.0	3.12
4	0	0.62	1	4.38	1.0	6.56
5	0	0.31	1	4.69	−2.5	5.78
6	0	0.16	1	4.84	0.5	−3.36

and, for example, in the case of the ''general'' input

$$Y_1 = 0.5 \times 0 + 2.5 \times 0 = 0$$
$$Y_2 = 0.5 \times 0 + 2.5 \times 1.5 = 3.75$$
$$Y_3 = 0.5 \times 3.75 + 2.5 \times 0.5 = 3.125$$

and so on. These inputs and outputs are plotted in Figure 11.7(a), (b), and (c).

In general, we see that having written the transfer function model in the form

$$Y_t = \delta_1 Y_{t-1} + \cdots + \delta_r Y_{t-r} + \omega_0 X_{t-b} - \omega_1 X_{t-b-1} - \cdots - \omega_s X_{t-b-s}$$

it is an easy matter to compute the discrete output for any discrete input. To start off the recursion, we need to know certain initial values. This need is not, of course, a shortcoming of the method of calculation but comes about because with a transfer function model, the initial values of Y *will* depend on values of X that occurred before observation was begun. In practice, when the necessary initial values are not known, we can substitute mean values for unknown Y's and X's (zeros if these quantities are considered as deviations from their means). The early calculated values will then depend upon this choice of the starting values. However, for a stable system, the effect of this choice will be negligible after a period sufficient for the impulse response to become negligible. If this period is p_o time intervals, an alternative procedure is to compute $Y_{p_o}, Y_{p_o+1}, \ldots$ directly from the impulse response until enough values are available to set the recursion going.

11.2.5 Transfer Function Models with Added Noise

In practice, the output Y could not be expected to follow exactly the pattern determined by the transfer function model, even if that model were entirely adequate. Disturbances of various kinds other than X normally corrupt the system. A disturbance might originate at any point in the system, but it is often convenient to consider it in terms of its net effect on the output Y, as indicated in Figure 1.5. If we assume that the disturbance, or noise N_t, is independent of the level of X and is additive with respect to the influence of X,

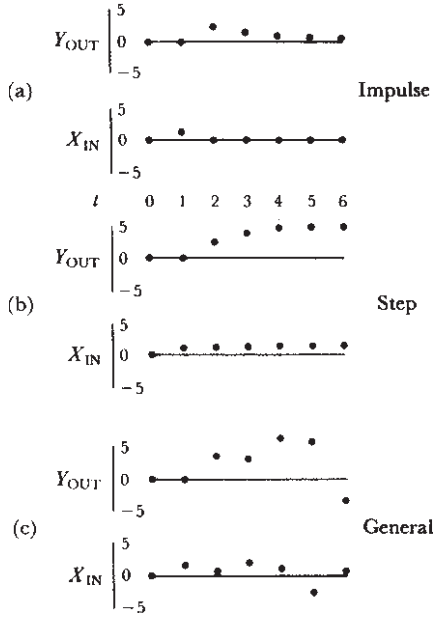

FIGURE 11.7 Response of a first-order system to (a) an impulse, (b) a step, and (c) a ''general'' input.

we can write

$$Y_t = \delta^{-1}(B)\omega(B)X_{t-b} + N_t \tag{11.2.15}$$

If the noise process N_t can be represented by an ARIMA(p, d, q) model

$$N_t = \varphi^{-1}(B)\theta(B)a_t$$

where a_t is white noise, the model (11.2.15) can be written finally as

$$Y_t = \delta^{-1}(B)\omega(B)X_{t-b} + \varphi^{-1}(B)\theta(B)a_t \tag{11.2.16}$$

In Chapter 12, we describe methods for identifying, fitting, and checking combined transfer function–noise models of the form (11.2.16).

11.3 RELATION BETWEEN DISCRETE AND CONTINUOUS MODELS

The discrete dynamic model, defined by a linear difference equation, is of importance in its own right. It provides a sensible class of transfer functions and needs no other justification. In many examples, no question will arise of attempting to relate the discrete model to a supposed underlying continuous model because no underlying continuous series properly exists. However, in some cases, for example, where instantaneous observations are taken periodically on a chemical reactor, the discrete record can be used to tell us something about the continuous system. In particular, control engineers are used to thinking in terms

of the time constants and dead times of continuous systems and may best understand the results of the discrete model analysis when so expressed.

As before, we denote a continuous output and input at time t by $Y(t)$ and $X(t)$, respectively. Suppose that the output and input are related by the linear filtering operation

$$Y(t) = \int_0^\infty v(u)X(t-u)du$$

Suppose now that only discrete observations $(X_t, Y_t), (X_{t-1}, Y_{t-1}), \ldots$ of output and input are available at equispaced intervals of time $t, t-1, \ldots$ and that the discrete output and input are related by the discrete linear filter

$$Y_t = \sum_{j=0}^{\infty} v_j X_{t-j}$$

Then, for certain special cases, and with appropriate assumptions, useful relationships may be established between the discrete and continuous models.

11.3.1 Response to a Pulsed Input

A special case, which is of importance in the design of the discrete control schemes discussed in Part Four, arises when the opportunity for adjustment of the process occurs immediately after observation of the output, so that the input variable is allowed to remain at the same level between observations. The typical appearance of the resulting square wave, or *pulsed input* as we shall call it, is shown in Figure 11.8. We denote the fixed level at which the input is held during the period $t-1 < \tau < t$ by X_{t-1+}.

Consider a continuous linear system that has b whole periods of delay plus a fractional period c of further delay. Thus, in terms of previous notation, $b + c = \tau$. Then, we can represent the output from the system as

$$Y(t) = \int_0^\infty v(u)X(t-u)du$$

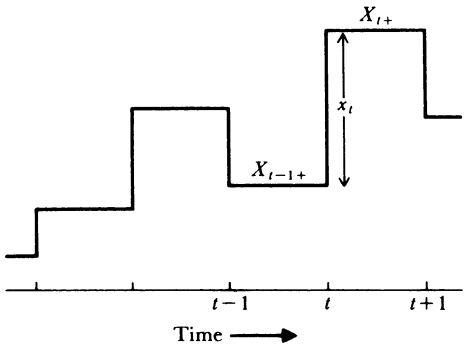

FIGURE 11.8 Example of a pulsed input.

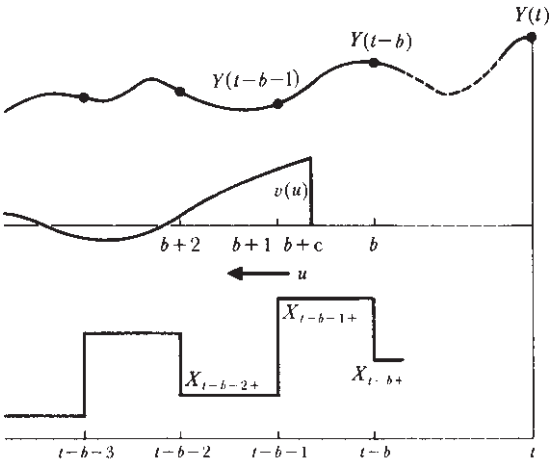

FIGURE 11.9 Transfer to output from a pulsed input.

where the impulse response function $v(u)$ is zero for $u < b + c$. Now for a pulsed input, as shown in Figure 11.9, the output at time t will be given exactly by

$$Y(t) = \left[\int_{b+c}^{b+1} v(u)du\right] X_{t-b-1+} + \left[\int_{b+1}^{b+2} v(u)du\right] X_{t-b-2+} + \cdots$$

Thus,

$$Y(t) = Y_t = v_b X_{t-b-1+} + v_{b+1} X_{t-b-2+} + \cdots$$

Therefore, for a *pulsed input*, there exists a discrete linear filter that is such that at times $t, t-1, t-2, \ldots$, the continuous output $Y(t)$ *exactly* equals the discrete output.

Given a pulsed input, consider the output Y_t from a discrete model

$$\xi(\nabla)Y_t = \eta(\nabla)X_{t-b-1+} \tag{11.3.1}$$

of order (r, r) in relation to the continuous output from the Rth-order model

$$(1 + \Xi_1 D + \Xi_2 D^2 + \cdots + \Xi_R D^R)Y(t) = X(t - b - c) \tag{11.3.2}$$

subject to the same input. It is shown in Appendix A11.1 that for suitably chosen values of the parameters $(\boldsymbol{\Xi}, c)$, the outputs will coincide exactly if $R = r$. Furthermore, if $c = 0$, the output from the continuous model (11.3.2) will be identical at the discrete times with that of a discrete model (11.3.1) of order $(r, r-1)$. We refer to the related continuous and discrete models as *discretely coincident* systems. If, then, a discrete model of the form (11.3.1) of order (r, r) has been obtained, then on the assumption *that the continuous model would be represented by the rth-order differential equation (11.3.2)*, the parameters, and in particular the time constants for the discretely coincident continuous system, may be written explicitly in terms of the parameters of the discrete model.

The parameter relationships for a delayed second-order system have been derived in Appendix A11.1. From these, the corresponding relationships for simpler systems may be obtained by setting appropriate constants equal to zero, as we shall now discuss.

11.3.2 Relationships for First- and Second-Order Coincident Systems

Undelayed First-Order System.

B Form. The continuous system satisfying

$$(1 + TD)Y(t) = gX(t) \tag{11.3.3}$$

is, for a pulsed input, discretely coincident with the discrete system satisfying

$$(1 - \delta B)Y_t = \omega_0 X_{t-1+} \tag{11.3.4}$$

where

$$\delta = e^{-1/T} \qquad T = (-\ln \delta)^{-1} \qquad \omega_0 = g(1 - \delta) \tag{11.3.5}$$

∇ ***Form***. Alternatively, the difference equation may be written

$$(1 + \xi\nabla)Y_t = gX_{t-1+} \tag{11.3.6}$$

where

$$\xi = \frac{\delta}{1 - \delta} \tag{11.3.7}$$

To illustrate, we reconsider the example of Section 11.2.4 for the ''general'' input. The output for this case is calculated in Table 11.3(c) and plotted in Figure 11.7(c). Suppose that, in fact, we had a continuous system:

$$(1 + 1.44D)Y(t) = 5X(t)$$

Then this would be discretely coincident with the discrete model (11.2.14) actually considered, namely,

$$(1 - 0.5B)Y_t = 2.5X_{t-1+}$$

If the input and output were continuous and the input were pulsed, the actual course of the response would be that shown by the continuous lines in Figure 11.10. The output would in fact follow a series of exponential curves. Each dashed line shows the further course that the response would take if no further change in the input were made. The curves correspond exactly at the discrete sample points with the discrete output already calculated in Table 11.3(c) and plotted in Figure 11.7(c).

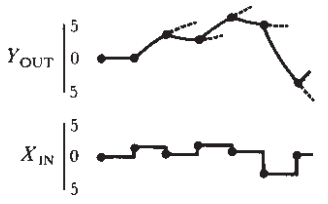

FIGURE 11.10 Continuous response of the system $(1 + 1.44D)Y(t) = 5X(t)$ to a pulsed input.

Delayed First-Order System.

B Form. The continuous system satisfying

$$(1 + TD)Y(t) = gX(t - b - c) \tag{11.3.8}$$

is, for a pulsed input, discretely coincident with the discrete system satisfying

$$(1 - \delta B)Y_t = (\omega_0 - \omega_1 B)X_{t-b-1+} \tag{11.3.9}$$

where

$$\delta = e^{-1/T} \qquad \omega_0 = g(1 - \delta^{1-c}) \qquad \omega_1 = g(\delta - \delta^{1-c}) \tag{11.3.10}$$

∇ ***Form***. Alternatively, the difference equation may be written

$$(1 + \xi\nabla)Y_t = g(1 + \eta\nabla)X_{t-b-1+} \tag{11.3.11}$$

where

$$\xi = \frac{\delta}{1 - \delta} \qquad -\eta = \frac{\delta(\delta^{-c} - 1)}{1 - \delta} \tag{11.3.12}$$

Now

$$(1 + \eta\nabla)X_{t-b-1+} = (1 + \eta)X_{t-b-1+} - \eta X_{t-b-2+} \tag{11.3.13}$$

can be regarded as an interpolation at an increment $(-\eta)$ between X_{t-b-1+} and X_{t-b-2+}. Table 11.4 allows the corresponding parameters $(\xi, -\eta)$ and (T, c) of the discrete and continuous models to be determined for a range of alternatives.

Undelayed Second-Order System.

B Form. The continuous system satisfying

$$(1 + T_1 D)(1 + T_2 D)Y(t) = gX(t) \tag{11.3.14}$$

TABLE 11.4 Values of $-\eta$ for Various Values of T and c for a First-Order System with Delay; Corresponding Values of ξ and δ

			$-\eta$ for				
δ	ξ	T	$c = 0.9$	$c = 0.7$	$c = 0.5$	$c = 0.3$	$c = 0.1$
0.9	9.00	9.49	0.90	0.69	0.49	0.29	0.10
0.8	4.00	4.48	0.89	0.68	0.47	0.28	0.09
0.7	2.33	2.80	0.88	0.66	0.46	0.26	0.09
0.6	1.50	1.95	0.88	0.64	0.44	0.25	0.08
0.5	1.00	1.44	0.87	0.62	0.41	0.23	0.07
0.4	0.67	1.09	0.85	0.60	0.39	0.21	0.06
0.3	0.43	0.83	0.84	0.57	0.35	0.19	0.05
0.2	0.25	0.62	0.82	0.52	0.31	0.15	0.04
01	0.11	0.43	0.77	0.45	0.24	0.11	0.03

is, for a pulsed input, discretely coincident with the system

$$(1 - \delta_1 B - \delta_2 B^2)Y_t = (\omega_0 - \omega_1 B)X_{t-1+} \tag{11.3.15}$$

or equivalently, with the system

$$(1 - S_1 B)(1 - S_2 B)Y_t = (\omega_0 - \omega_1 B)X_{t-1+} \tag{11.3.16}$$

where

$$\begin{aligned} S_1 &= e^{-1/T_1} \qquad S_2 = e^{-1/T_2} \\ \omega_0 &= g(T_1 - T_2)^{-1}[T_1(1 - S_1) - T_2(1 - S_2)] \\ \omega_1 &= g(T_1 - T_2)^{-1}[T_1 S_2(1 - S_1) - T_2 S_1(1 - S_2)] \end{aligned} \tag{11.3.17}$$

∇ *Form*. Alternatively, the difference equation may be written

$$(1 + \xi_1 \nabla + \xi_2 \nabla^2)Y_t = g(1 + \eta_1 \nabla)X_{t-1+} \tag{11.3.18}$$

where

$$-\eta_1 = (1 - S_1)^{-1}(1 - S_2)^{-1}(T_1 - T_2)^{-1}[T_2 S_1(1 - S_2) - T_1 S_2(1 - S_1)] \tag{11.3.19}$$

may be regarded as the increment of an interpolation between X_{t-1+} and X_{t-2+}. Values for ξ_1 and ξ_2 in terms of the δ's can be obtained directly using the results given in Table 11.1.

As a specific example, Figure 11.5 shows the step response for two discrete systems we have considered before, together with the corresponding continuous responses from the discretely coincident systems.

The pair of models are, for curve C,

$$\begin{aligned} &\text{Continuous}: \quad (1 + 1.41D + 2D^2)Y(t) = 5X(t) \\ &\text{Discrete}: \quad (1 - 1.15B + 0.49B^2)Y_t = 5(0.19 + 0.15B)X_{t-1+} \end{aligned}$$

and for curve R,

$$\begin{aligned} &\text{Continuous}: \quad (1 + 2D)(1 + D)Y(t) = 5X(t) \\ &\text{Discrete}: \quad (1 - 0.97B + 0.22B^2)Y_t = 5(0.15 + 0.09B)X_{t-1+} \end{aligned}$$

The continuous curves were drawn using (11.1.18) and (11.1.12), which give the continuous step responses for second-order systems having, respectively, complex and real roots.

The discrete representation of the response of a second-order continuous system with delay to a pulsed input is given in Appendix A11.1.

11.3.3 Approximating General Continuous Models by Discrete Models

Perhaps we should emphasize once more that the discrete transfer function models do not need to be justified in terms of, or related to, continuous systems. They are of importance in their own right in allowing a discrete output to be calculated from a discrete input. However, in some instances, such relationships are of interest.

For continuous systems, the pulsed input arises of itself in control problems when the convenient way to operate is to make an observation on the output Y and then immediately

to make any adjustment that may be needed on the input variable X. Thus, the input variable stays at a fixed level between observations, and we have a pulsed input. The relationships established in the previous sections may then be applied immediately. In particular, these relationships indicate that with the notation we have used, the *undelayed* discrete system is represented by

$$\xi(\nabla)Y_t = \eta(\nabla)X_{t-1+}$$

in which the subscript $t-1+$ on X is one step behind the subscript t on Y.

Use of Discrete Models When Continuous Records Are Available. Even though we have a continuous record of input and output, it may be convenient to determine the dynamic characteristics of the system by discrete methods, as we describe in Chapter 12. Thus, if pairs of values are read off with a sufficiently short sampling interval, very little is lost by replacing the continuous record by the discrete one.

One way in which the discrete results may then be used to approximate the continuous transfer function is to treat the input as though it were pulsed, that is, to treat the input record as if the discrete input observed at time j extended from just after $j-\frac{1}{2}$ to $j+\frac{1}{2}$. Thus, $X(t) = X_j(j-\frac{1}{2} < t \le j+\frac{1}{2})$. We can then relate the discrete result to that of the continuous record by using the pulsed input equations with X_t replacing X_{t+} and with $b+c-\frac{1}{2}$ replacing $b+c$, that is, with one half a time period subtracted from the delay. The continuous record will normally be read at a sufficiently small sampling interval so that sudden changes do not occur between the sampled points. In this case, the approximation will be very close.

APPENDIX A11.1 CONTINUOUS MODELS WITH PULSED INPUTS

We showed in Section 11.3.1 (see also Fig. 11.9) that for a pulsed input, the output from any delayed continuous linear system

$$Y(t) = \int_0^\infty v(u)X(t-u)du$$

where $v(u) = 0, u < b+c$, exactly given at the discrete times $t, t-1, t-2, \ldots$ by the discrete linear filter

$$Y_t = v(B)X_{t-1+}$$

where the weights $v_0, v_1, \ldots, v_{b-1}$ are zero and the weights $v_b, v_{b+1}, \ldots$ are given by

$$v_b = \int_{b+c}^{b+1} v(u)du \tag{A11.1.1}$$

$$v_{b+j} = \int_{b+j}^{b+j+1} v(u)du \qquad j \ge 1 \tag{A11.1.2}$$

Now suppose that the dynamics of the continuous system is represented by the Rth-order linear differential equation

$$\Xi(D)Y(t) = gX(t-b-c) \tag{A11.1.3}$$

which may be written in the form

$$\prod_{h=1}^{R}(1+T_hD)Y(t) = gX(t-b-c)$$

where $T_1, T_2, \ldots, T_R$ may be real or complex. We now show that for a pulsed input, the output from this continuous system is discretely coincident with that from a discrete difference equation model of order (r, r), or of order $(r, r-1)$ if $c = 0$. Now $v(u)$ is zero for $u < b + c$ and for $u \geq b + c$ is in general nonzero and satisfies the differential equation

$$\prod_{h=1}^{R}(1+T_hD)v(u-b-c) = 0 \qquad u \geq b+c$$

Thus,

$$v(u) = 0 \qquad u < b+c$$
$$v(u) = \alpha_1 e^{-(u-b-c)/T_1} + \alpha_2 e^{-(u-b-c)/T_2} + \cdots + \alpha_R e^{-(u-b-c)/T_R} \qquad u \geq b+c$$

Hence, using (A11.1.1) and (A11.1.2),

$$v_b = \sum_{h=1}^{R} \alpha_h T_h [1 - e^{-(1-c)/T_h}] \tag{A11.1.4}$$

$$v_{b+j} = \sum_{h=1}^{R} \alpha_h T_h (1 - e^{-1/T_h}) e^{c/T_h} e^{-j/T_h} \qquad j \geq 1 \tag{A11.1.5}$$

It will be noted that in the particular case when $c = 0$, the weights v_{b+j} are given by (A11.1.2) for $j = 0$ as well as for $j > 0$.

Now consider the difference equation model of order (r, s),

$$\delta(B)Y_t = \omega(B)B^b X_{t-1+} \tag{A11.1.6}$$

If we write

$$\Omega(B) = \omega(B)B^b$$

the discrete transfer function $v(B)$ for this model satisfies

$$\delta(B)v(B) = \Omega(B) \tag{A11.1.7}$$

As we have observed in (11.2.8), by equating coefficients in (A11.1.7) we obtain b zero weights $v_0, v_1, \ldots, v_{b-1}$, and if $s \geq r$, a further $s - r + 1$ values $v_b, v_{b+1}, \ldots, v_{b+s-r}$ which do not follow a pattern. The weights v_j eventually satisfy

$$\delta(B)v_j = 0 \qquad j > b+s \tag{A11.1.8}$$

with $v_{b+s}, v_{b+s-1}, \ldots, v_{b+s-r+1}$ supplying the required r starting values. Now write

$$\delta(B) = \prod_{h=1}^{r}(1 - S_h B)$$

where $S_1^{-1}, S_2^{-1}, \ldots, S_r^{-1}$ are the roots of the equation $\delta(B) = 0$. Then, the solution of (A11.1.8) is of the form

$$v_j = A_1(\boldsymbol{\omega})S_1^j + A_2(\boldsymbol{\omega})S_2^j + \cdots + A_r(\boldsymbol{\omega})S_r^j \qquad j > b + s - r \tag{A11.1.9}$$

where the coefficients $A_h(\boldsymbol{\omega})$ are suitably chosen so that the solutions of (A11.1.9) for $j = s - r + 1, s - r + 2, \ldots, s$ generate the starting values $v_{b+s-r+1}, \ldots, v_{b+s}$, and the notation $A_h(\boldsymbol{\omega})$ is used as a reminder that the A_h's are functions of $\omega_0, \omega_1, \ldots, \omega_s$. Thus, if we set $s = r$, for given parameters $(\boldsymbol{\omega}, \boldsymbol{\delta})$ in (A11.1.6), and hence for given parameters $(\boldsymbol{\omega}, \mathbf{S})$, there will be a corresponding set of values $A_h(\boldsymbol{\omega})$ $(h = 1, 2, \ldots, r)$ that produce the appropriate r starting values $v_{b+1}, v_{b+2}, \ldots, v_{b+r}$. Furthermore, we know that $v_b = \omega_0$. Thus,

$$v_b = \omega_0 \tag{A11.1.10}$$

$$v_{b+j} = \sum_{h=1}^{r} A_h(\boldsymbol{\omega})S_h^j \tag{A11.1.11}$$

and we can equate the values of the weights in (A11.1.4) and (A11.1.5), which come from the differential equation, to those in (A11.1.10) and (A11.1.11), which come from the difference equation. To do this, we must set

$$R = r \qquad S_h = e^{-1/T_h}$$

and the remaining $r + 1$ equations

$$\omega_0 = \sum_{h=1}^{r} \alpha_h T_h (1 - S_h^{1-c})$$

$$A_h(\boldsymbol{\omega}) = \alpha_h T_h (1 - S_h) S_h^{-c}$$

determine $c, \alpha_1, \alpha_2, \ldots, \alpha_r$ in terms of the S_h's and ω_j's.

When $c = 0$, we set $s = r - 1$, and for given parameters $(\boldsymbol{\omega}, \mathbf{S})$ in the difference equation, there will then be a set of r values $A_h(\boldsymbol{\omega})$ that are functions of $\omega_0, \omega_1, \ldots, \omega_{r-1}$, which produce the r starting values $v_b, v_{b+1}, \ldots, v_{b+r-1}$ and which can be equated to the values given by (A11.1.5) for $j = 0, 1, \ldots, r - 1$. To do this, we set

$$R = r \qquad S_h = e^{-1/T_h}$$

and the remaining r equations

$$A_h(\boldsymbol{\omega}) = \alpha_h T_h (1 - S_h)$$

determine $\alpha_1, \alpha_2, \ldots, \alpha_r$, in terms of the S_h's and ω_j's.

It follows, in general, that for a pulsed input the output at times $t, t - 1, \ldots$ from the continuous rth-order dynamic system defined by

$$\Xi(D)Y(t) = gX(t - b - c) \tag{A11.1.12}$$

is identical to the output from a discrete model

$$\xi(\nabla)Y_t = g\eta(\nabla)X_{t-b-1+} \tag{A11.1.13}$$

of order (r, r) with the parameters suitably chosen. Furthermore, if $c = 0$, the output from the continuous model (A11.1.12) is identical at the discrete times to that of a model (A11.1.13) of order $(r, r-1)$.

We now derive the discrete model corresponding to the second-order system with delay, from which the results given in Section 11.3.2 may be obtained as special cases.

Second-Order System with Delay. Suppose that the differential equation relating input and output for a continuous system is given by

$$(1 + T_1 D)(1 + T_2 D)Y(t) = gX(t - b - c) \tag{A11.1.14}$$

Then, the continuous impulse response function is

$$v(u) = g(T_1 - T_2)^{-1}(e^{-(u-b-c)/T_1} - e^{-(u-b-c)/T_2}) \qquad u > b + c \tag{A11.1.15}$$

For a pulsed input, the output at discrete times $t, t-1, t-2, \ldots$ will be related to the input by the difference equation

$$(1 + \xi_1\nabla + \xi_2\nabla^2)Y_t = g(1 + \eta_1\nabla + \eta_2\nabla^2)X_{t-b-1+} \tag{A11.1.16}$$

with suitably chosen values of the parameters. This difference equation can also be written

$$(1 - \delta_1 B - \delta_2 B^2)Y_t = (\omega_0 - \omega_1 B - \omega_2 B^2)X_{t-b-1+}$$

or

$$(1 - S_1 B)(1 - S_2 B)Y_t = (\omega_0 - \omega_1 B - \omega_2 B^2)X_{t-b-1+} \tag{A11.1.17}$$

Using (A11.1.1) and (A11.1.2) and writing

$$S_1 = e^{-1/T_1} \qquad S_2 = e^{-1/t_2}$$

we obtain

$$v_b = \int_{b+c}^{b+1} v(u)\,du = g(T_1 - T_2)^{-1}[T_1(1 - S_1^{1-c}) - T_2(1 - S_2^{1-c})]$$

$$v_{b+j} = \int_{b+j}^{b+j+1} v(u)\,du = g(T_1 - T_2)^{-1}[T_1 S_1^{-c}(1 - S_1)S_1^j - T_2 S_2^{-c}(1 - S_2)S_2^j] \qquad j \geq 1$$

Thus,

$$\begin{aligned}(T_1 - T_2)v(B) = {} & gB^b T_1[1 - S_1^{1-c} + S_1^{-c}(1 - S_1)(1 - S_1 B)^{-1}S_1 B] \\ & - gB^b T_2[1 - S_2^{1-c} + S_2^{-c}(1 - S_2)(1 - S_2 B)^{-1}S_2 B]\end{aligned}$$

But from (A11.1.17),

$$v(B) = \frac{B^b(\omega_0 - \omega_1 B - \omega_2 B^2)}{(1 - S_1 B)(1 - S_2 B)}$$

Hence, we obtain

$$\begin{aligned}\omega_0 &= g(T_1 - T_2)^{-1}[T_1(1 - S_1^{1-c}) - T_2(1 - S_2^{1-c})] \\ \omega_1 &= g(T_1 - T_2)^{-1}[(S_1 + S_2)(T_1 - T_2) + T_2 S_2^{1-c}(1 + S_1) - T_1 S_1^{1-c}(1 + S_2)] \\ \omega_2 &= g S_1 S_2 (T_1 - T_2)^{-1}[T_2(1 - S_2^{-c}) - T_1(1 - S_1^{-c})]\end{aligned} \tag{A11.1.18}$$

and

$$\delta_1 = S_1 + S_2 = e^{-1/T_1} + e^{-1/T_2} \qquad \delta_2 = -S_1 S_2 = -e^{-(1/T_1)-(1/T_2)} \tag{A11.1.19}$$

Complex Roots. If T_1 and T_2 are complex, corresponding expressions are obtained by substituting

$$T_1 = \zeta^{-1} e^{i\lambda} \qquad T_2 = \zeta^{-1} e^{-i\lambda} \qquad (i^2 = -1)$$

yielding

$$\begin{aligned}\omega_0 &= g\left\{1 - \frac{e^{-\zeta(1-c)\cos\lambda}\sin[\zeta(1-c)\sin\lambda + \lambda]}{\sin\lambda}\right\} \\ \omega_2 &= g\delta_2\left[1 - \frac{e^{\zeta c\cos\lambda}\sin(-\zeta c\sin\lambda + \lambda)}{\sin\lambda}\right] \\ \omega_1 &= \omega_0 - \omega_2 - (1 - \delta_1 - \delta_2)g\end{aligned} \tag{A11.1.20}$$

where

$$\begin{aligned}\delta_1 &= 2e^{-\zeta\cos\lambda}\cos(\zeta\sin\lambda) \\ \delta_2 &= -e^{-2\zeta\cos\lambda}\end{aligned} \tag{A11.1.21}$$

APPENDIX A11.2 NONLINEAR TRANSFER FUNCTIONS AND LINEARIZATION

The linearity (or additivity) of the transfer function models we have considered implies that the overall response to the sum of a number of individual inputs will be the sum of the individual responses to those inputs. Specifically, that if $Y_t^{(1)}$ is the response at time t to an input history $\{X_t^{(1)}\}$ and $\{Y_t^{(2)}\}$ is the response at time t to an input history $\{X_t^{(2)}\}$ the response at time t to an input history $\{X_t^{(1)} + X_t^{(2)}\}$ would be $Y_t^{(1)} + Y_t^{(2)}$, and similarly for continuous inputs and outputs. In particular, if the input level is multiplied by some constant, the output level is multiplied by this same constant. In practice, this assumption is probably never quite true, but it supplies a useful approximation for many practical situations.

Models for nonlinear systems may sometimes be obtained by allowing the parameters to depend upon the level of the input in some prescribed manner. For example, suppose that a system were being studied over a range where Y had a maximum η, and for any X

the steady-state relation could be approximated by the quadratic expression

$$Y_\infty = \eta - \frac{1}{2}k(\mu - X)^2$$

where Y and X are, as before, deviations from a convenient origin. Then,

$$g(X) = \frac{dY_\infty}{dX} = k(\mu - X)$$

and the dynamic behavior of the system might then be capable of representation by the first-order difference equation (11.3.4) but with variable gain proportional to $k(\mu - X)$. Thus,

$$Y_t = \delta Y_{t-1} + k(\mu - X_{t-1+})(1 - \delta)X_{t-1+} \tag{A11.2.1}$$

Dynamics of a Simple Chemical Reactor. It sometimes happens that we can make a theoretical analysis of a physical problem that will yield the appropriate form for the transfer function. In particular, this allows us to see very specifically what is involved in the linearized approximation.

As an example, suppose that a pure chemical A is continuously fed through a stirred tank reactor, and in the presence of a catalyst a certain proportion of it is changed to a product B, with no change of overall volume; hence the material continuously leaving the reactor consists of a mixture of B and unchanged A.

Suppose that initially the system is in equilibrium and that with quantities measured in suitable units:

1. μ is the rate at which A is fed to the reactor (and consequently is also the rate at which the mixture of A and B leaves the reactor).
2. η is the proportion of unchanged A at the outlet, so that $1 - \eta$ is the proportion of the product B at the outlet.
3. V is the volume of the reactor.
4. k is a constant determining the rate at which the product B is formed.

Suppose that the reaction is ''first order'' with respect to A, which means that the rate at which B is formed and A is used up is proportional to the amount of A present. Then, the rate of formation of B is $kV\eta$, but the rate at which B is leaving the outlet is $\mu(1 - \eta)$, and since the system is in equilibrium,

$$\mu(1 - \eta) = kV\eta \tag{A11.2.2}$$

Now, suppose that the equilibrium of the system is disturbed, the rate of feed to the reactor at time t being $\mu + X(t)$ and the corresponding concentration of A in the outlet being $\eta + Y(t)$. Now, the rate of chemical formation of B, which now equals $kV[\eta + Y(t)]$, will in general no longer exactly balance the rate at which B is flowing out of the system, which now equals $[\mu + X(t)][1 - \eta - Y(t)]$. The difference in these two quantities is the rate of increase in the amount of B within the reactor, which equals $-V[dY(t)/dt]$. Thus,

$$-V\frac{dY(t)}{dt} = kV[\eta + Y(t)] - [\mu + X(t)][1 - \eta - Y(t)] \tag{A11.2.3}$$

Using (A11.2.2) and rearranging, (A11.2.3) may be written

$$(kV + \mu + VD)Y(t) = X(t)[1 - \eta - Y(t)]$$

or

$$(1 + TD)Y(t) = (1 - \frac{Y(t)}{1 - \eta})X(t) \tag{A11.2.4}$$

where

$$T = \frac{V}{kV + \mu} \qquad g = \frac{1 - \eta}{kV + \mu} \tag{A11.2.5}$$

Now (A11.2.4) is a nonlinear differential equation, since it contains a term $X(t)$ multiplied by $Y(t)$. However, in some practical circumstances, it could be adequately approximated by a linear differential equation, as we now show.

Processes operate under a wide range of conditions, but certainly a not unusual situation might be one where $100(1 - \eta)$, the percentage conversion of feed A to product B was, say, 80%, and $100Y(t)$, the percentage fluctuation that was of practical interest, was 4%. In this case, the factor $1 - Y(t)/(1 - \eta)$ would vary from 0.95 to 1.05 and, to a good approximation, could be replaced by unity. The nonlinear differential equation (A11.2.4) could then be replaced by the linear first-order differential equation

$$(1 + TD)Y(t) = gX(t)$$

where T and g are as defined in Section 11.1.2. If the system was observed at discrete intervals of time, this equation could be approximated by a linear difference equation.

Situations can obviously occur when nonlinearities are of importance. This is particularly true of optimization studies, where the range of variation for the variables may be large. A device that is sometimes useful when the linear assumption is not adequate is to represent the dynamics by a set of linear models applicable over different ranges of the input variables. This approach could lead to nonlinear transfer function models similar in spirit to the threshold AR stochastic models considered in Section 10.3. However, for discrete systems it is often less clumsy to work directly with a nonlinear difference equation that can be ''solved'' recursively rather than analytically. For example, we might replace the nonlinear differential equation (A11.2.4) by the nonlinear difference equation

$$(1 + \xi_1 \nabla)Y_t = g(1 + \eta_{12} Y_{t-1})X_{t-1}$$

which has a form analogous to a particular case of the bilinear stochastic models discussed in Section 10.3.

EXERCISES

11.1. In the following transfer function models, X_t is the methane gas feed rate to a gas furnace, measured in cubic feet per minute, and Y_t the percent carbon dioxide in the outlet gas:

(1) $Y_t = 10 + \dfrac{25}{1 - 0.7B} X_{t-1}$

(2) $Y_t = 10 + \dfrac{22 - 12.5B}{1 - 0.85B} X_{t-2}$

(3) $Y_t = 10 + \dfrac{20 - 8.5B}{1 - 1.2B + 0.4B^2} X_{t-3}$

(a) Verify that the models are stable.

(b) Calculate the steady-state gain g, expressing it in the appropriate units.

11.2. For each of the models of Exercise 11.1, calculate from the difference equation and plot the responses to:

(a) A unit impulse $(0, 1, 0, 0, 0, 0, \ldots)$ applied at time $t = 0$

(b) A unit step $(0, 1, 1, 1, 1, 1, \ldots)$ applied at time $t = 0$

(c) A ramp input $(0, 1, 2, 3, 4, 5, \ldots)$ applied at time $t = 0$

(d) A periodic input $(0, 1, 0, -1, 0, 1, \ldots)$ applied at time $t = 0$

Estimate the period and damping factor of the step response to model (3).

11.3. Use equation (11.2.8) to obtain the impulse weights v_j for each of the models of Exercise 11.1, and check that they are the same as the impulse response obtained in Exercise 11.2(a).

11.4. Express the models of Exercise 11.1 in ∇ form.

11.5. **(a)** Calculate and plot the response of the two-input system

$$Y_t = 10 + \frac{6}{1 - 0.7B} X_{1,t-1} + \frac{8}{1 - 0.5B} X_{2,t-2}$$

to the orthogonal and randomized input sequences shown below.

t	X_{1t}	X_{2t}	t	X_{1t}	X_{2t}
0	0	0	5	1	−1
1	−1	1	6	1	1
2	1	−1	7	−1	−1
3	−1	−1	8	−1	1
4	1	1			

(b) Calculate the gains g_1 and g_2 of Y with respect to X_1 and X_2, respectively, and express the model in ∇ form.

12

IDENTIFICATION, FITTING, AND CHECKING OF TRANSFER FUNCTION MODELS

In Chapter 11, a parsimonious class of discrete linear transfer function models was introduced:

$$Y_t - \delta_1 Y_{t-1} - \cdots - \delta_r Y_{t-r} = \omega_0 X_{t-b} - \omega_1 X_{t-b-1} - \cdots - \omega_s X_{t-b-s}$$

or

$$Y_t = \delta^{-1}(B)\omega(B)X_{t-b}$$

where X_t and Y_t are deviations from equilibrium of the system input and output. In practice, the system will be infected by disturbances, or noise, whose net effect is to corrupt the output predicted by the transfer function model by an amount N_t. The combined transfer function–noise model may then be written as

$$Y_t = \delta^{-1}(B)\omega(B)X_{t-b} + N_t$$

In this chapter, methods are described for identifying, fitting, and checking transfer function–noise models when simultaneous pairs of observations (X_1, Y_1), $(X_2, Y_2), \ldots, (X_N, Y_N)$ of the input and output are available at discrete equispaced times $1, 2, \ldots, N$.

Engineering methods for estimating transfer functions are usually based on the choice of special inputs to the system, for example, step and sine wave inputs (Young, 1955) and ''pulse'' inputs (Hougen, 1964). These methods have been useful when the system is affected by small amounts of noise but are less satisfactory otherwise. In the presence of

Time Series Analysis: Forecasting and Control, Fifth Edition. George E. P. Box, Gwilym M. Jenkins, Gregory C. Reinsel, and Greta M. Ljung

appreciable noise, it is necessary to use statistical methods for estimating the transfer function. Two previous approaches that have been tried for this problem are direct estimation of the impulse response in the time domain and direct estimation of the gain and phase characteristics in the frequency domain, as described, for example, by Briggs et al. (1965), Hutchinson and Shelton (1967), and Jenkins and Watts (1968). These methods are often unsatisfactory because they involve the estimation of too many parameters. For example, to determine the gain and phase characteristics, it is necessary to estimate two parameters at each frequency. The approach adopted in this chapter is to estimate the parameters in parsimonious difference equation models. Throughout most of the chapter we assume that the input X_t is itself a stochastic process. Models of the kind discussed are useful in representing and forecasting certain multiple time series.

12.1 CROSS-CORRELATION FUNCTION

In the same way that the autocorrelation function was used to identify stochastic models for univariate time series, the data analysis tool employed for the identification of transfer function models is the *cross-correlation function* between the input and output. In this section, we describe the basic properties of the cross-correlation function and in the next section show how it can be used to identify transfer function models.

12.1.1 Properties of the Cross-Covariance and Cross-Correlation Functions

Bivariate Stochastic Processes. We have seen in Chapter 2 that to analyze a time series, it is useful to regard it as a realization of a hypothetical population of time series called a stochastic process. Now, suppose that we want to describe an input time series X_t and the corresponding output time series Y_t from some physical system. For example, Figure 12.1 shows continuous data representing the (coded) input gas feed rate and corresponding output CO_2 concentration from a gas furnace. Then we can regard this pair of time series as realizations of a hypothetical population of pairs of time series, called *a bivariate stochastic process* (X_t, Y_t). We will assume that the data are read off at equispaced times yielding a pair of discrete time series, generated by a discrete bivariate process, and that values of the time series at times $t_0 + h, t_0 + 2h, \ldots, t_0 + Nh$ are denoted by $(X_1, Y_1), (X_2, Y_2), \ldots, (X_N, Y_N)$.

In this chapter, we will use the gas furnace data read at intervals of 9 seconds for illustration. The resulting time series (X_t, Y_t) consist of 296 observations and are listed as Series J in the Collection of Time Series section in Part Five. Further details about the data will be given in Section 12.2.2.

Cross-Covariance and Cross-Correlation Functions. We have seen in Chapter 2 that a stationary Gaussian stochastic process can be described by its mean μ and autocovariance function γ_k, or, equivalently, by its mean μ, variance σ^2, and autocorrelation function ρ_k. Moreover, since $\gamma_k = \gamma_{-k}$ and $\rho_k = \rho_{-k}$, the autocovariance and autocorrelation functions need to be considered only for nonnegative values of the lag $k = 0, 1, 2, \ldots$.

In general, a bivariate stochastic process (X_t, Y_t) need not be stationary. However, as in Chapter 4, we assume that the appropriately differenced process (x_t, y_t), where $x_t = \nabla^{d_x} X_t$ and $y_t = \nabla^{d_y} Y_t$, is stationary. The stationarity assumption implies in particular that the two processes x_t and y_t have constant means μ_x and μ_y and constant variances σ_x^2 and σ_y^2. If, in addition, it is assumed that the bivariate process is Gaussian, or normal, it is uniquely

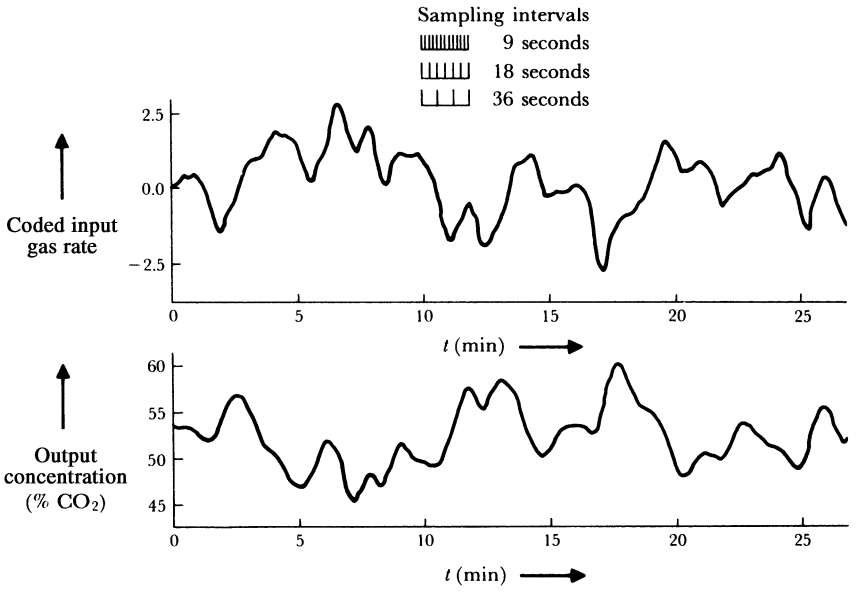

FIGURE 12.1 Input gas rate and output CO_2 concentration from a gas furnace.

characterized by its means μ_x and μ_y and its covariance matrix. Figure 12.2 shows the different kinds of covariances that need to be considered.

The autocovariance coefficients of each of the two series at lag k are defined by the usual formula:

$$\gamma_{xx}(k) = E[(x_t - \mu_x)(x_{t+k} - \mu_x)] = E[(x_t - \mu_x)(x_{t-k} - \mu_x)]$$
$$\gamma_{yy}(k) = E[(y_t - \mu_y)(y_{t+k} - \mu_y)] = E[(y_t - \mu_y)(y_{t-k} - \mu_y)]$$

where we now use the extended notation $\gamma_{xx}(k)$ and $\gamma_{yy}(k)$ for the autocovariances of the x_t and y_t series. The only other covariances that can appear in the covariance matrix are the *cross-covariance* coefficients between x_t and y_t series at lag $+k$:

$$\gamma_{xy}(k) = E[(x_t - \mu_x)(y_{t+k} - \mu_y)] \qquad k = 0, 1, 2, \ldots \tag{12.1.1}$$

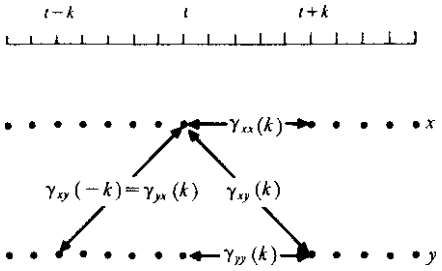

FIGURE 12.2 Autocovariances and cross-covariances of a bivariate stochastic process.

and the cross-covariance coefficients between the y_t and x_t series at lag $+k$:

$$\gamma_{yx}(k) = E[(y_t - \mu_y)(x_{t+k} - \mu_x)] \qquad k = 0, 1, 2, \ldots \tag{12.1.2}$$

Under (bivariate) stationarity, these cross-covariances must be the same for all t and hence are functions only of the lag k.

Note that, in general, $\gamma_{xy}(k)$ will not be the same as $\gamma_{yx}(k)$. However, since

$$\gamma_{xy}(k) = E[(x_{t-k} - \mu_x)(y_t - \mu_y)] = E[(y_t - \mu_y)(x_{t-k} - \mu_x)] = \gamma_{yx}(-k)$$

we need to define only one function $\gamma_{xy}(k)$ for $k = 0, \pm 1, \pm 2, \ldots$. The function $\gamma_{xy}(k) = \text{cov}[x_t, y_{t+k}]$, as defined in (12.1.1) for $k = 0, \pm 1, \pm 2, \ldots$, is called the *cross-covariance function* of the stationary bivariate process. Similarly, the correlation between x_t and y_{t+k}, which is the dimensionless quantity given by

$$\rho_{xy}(k) = \frac{\gamma_{xy}(k)}{\sigma_x \sigma_y} \qquad k = 0, \pm 1, \pm 2, \ldots \tag{12.1.3}$$

is called the *cross-correlation* coefficient at lag k, and the function $\rho_{xy}(k)$, defined for $k = 0, \pm 1, \pm 2, \ldots$, the *cross-correlation function* of the stationary bivariate process.

Since $\rho_{xy}(k)$ is not in general equal to $\rho_{xy}(-k)$, the cross-correlation function, in contrast to the autocorrelation function, is not symmetric about $k = 0$. In fact, it will sometimes happen that the cross-correlation function is zero over some range $-\infty$ to i or i to $+\infty$. For example, consider the cross-covariance function between the series a_t and z_t for the ''delayed'' first-order autoregressive process:

$$(1 - \phi B)\tilde{z}_t = a_{t-b} \qquad -1 < \phi < 1 \qquad b > 0$$

where a_t is white noise with zero mean and variance σ_a^2. Then since

$$\tilde{z}_{t+k} = a_{t+k-b} + \phi a_{t+k-b-1} + \phi^2 a_{t+k-b-2} + \cdots$$

the cross-covariance function between the series a_t and z_t is

$$\gamma_{az}(k) = E[a_t \tilde{z}_{t+k}] = \begin{cases} \phi^{k-b}\sigma_a^2 & k \geq b \\ 0 & k < b \end{cases}$$

Hence, for the delayed autoregressive process, the cross-correlation function is

$$\rho_{az}(k) = \begin{cases} \phi^{k-b}\dfrac{\sigma_a}{\sigma_z} = \phi^{k-b}(1 - \phi^2)^{1/2} & k \geq b \\ 0 & k < b \end{cases}$$

Figure 12.3 shows this cross-correlation function when $b = 2$ and $\phi = 0.6$.

12.1.2 Estimation of the Cross-Covariance and Cross-Correlation Functions

We assume that after differencing the original input and output time series d times, there are $n = N - d$ pairs of values $(x_1, y_1), (x_2, y_2), \ldots, (x_n, y_n)$ available for analysis. Then it is shown, for example, in Jenkins and Watts (1968), that an estimate $c_{xy}(k)$ of the

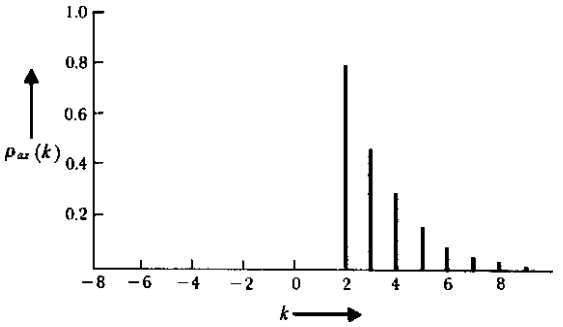

FIGURE 12.3 Cross-correlation function between a_t and z_t for delayed autoregressive process $\tilde{z}_t - 0.6\tilde{z}_{t-1} = a_{t-2}$.

cross-covariance coefficient at lag k is provided by

$$c_{xy}(k) = \begin{cases} \dfrac{1}{n}\displaystyle\sum_{t=1}^{n-k}(x_t - \bar{x})(y_{t+k} - \bar{y}) & k = 0, 1, 2, \ldots \\ \dfrac{1}{n}\displaystyle\sum_{t=1}^{n+k}(y_t - \bar{y})(x_{t-k} - \bar{x}) & k = 0, -1, -2, \ldots \end{cases} \tag{12.1.4}$$

where $\bar{x}$ and $\bar{y}$ are the sample means of the x_t series and y_t series, respectively. Similarly, the estimate $r_{xy}(k)$ of the cross-correlation coefficient $\rho_{xy}(k)$ at lag k may be obtained by substituting in (12.1.3) the estimates $c_{xy}(k)$ for $\gamma_{xy}(k)$, $s_x = \sqrt{c_{xx}(0)}$ for σ_x, and $s_y = \sqrt{c_{yy}(0)}$ for σ_y, yielding

$$r_{xy}(k) = \frac{c_{xy}(k)}{s_x s_y} \qquad k = 0, \pm 1, \pm 2, \ldots \tag{12.1.5}$$

The top graph in Figure 12.4 shows the estimated cross-correlation function $r_{xy}(k)$ between the input and output series for the discrete gas furnace data obtained by reading the continuous data of Figure 12.1 at intervals of 9 seconds. Note that the cross-correlation function is not symmetrical about zero and has a well-defined peak at $k = +5$, indicating that the output lags behind the input. The cross-correlations are negative. This is to be expected since an *increase* in the coded input produces a *decrease* in the output as seen from Figure 12.1. The autocorrelation functions of the input and output variables are also included in Figure 12.4. Both variables are highly autocorrelated and the slowly decaying patterns are indicative of an autoregressive dependence structure in these series.

Figure 12.4 can be reproduced in R as follows:

```
> gasfur = read.table('SeriesJ.txt',header=T)
> X = gasfur[,1]
> Y = gasfur[,2]
> CCF=ccf(Y,X)
> ACF.y=acf(Y)
> ACF.x=acf(X)
> par(mfrow=c(3,1))
> plot(CCF,ylab="CCF",main="Cross Correlation Between
```

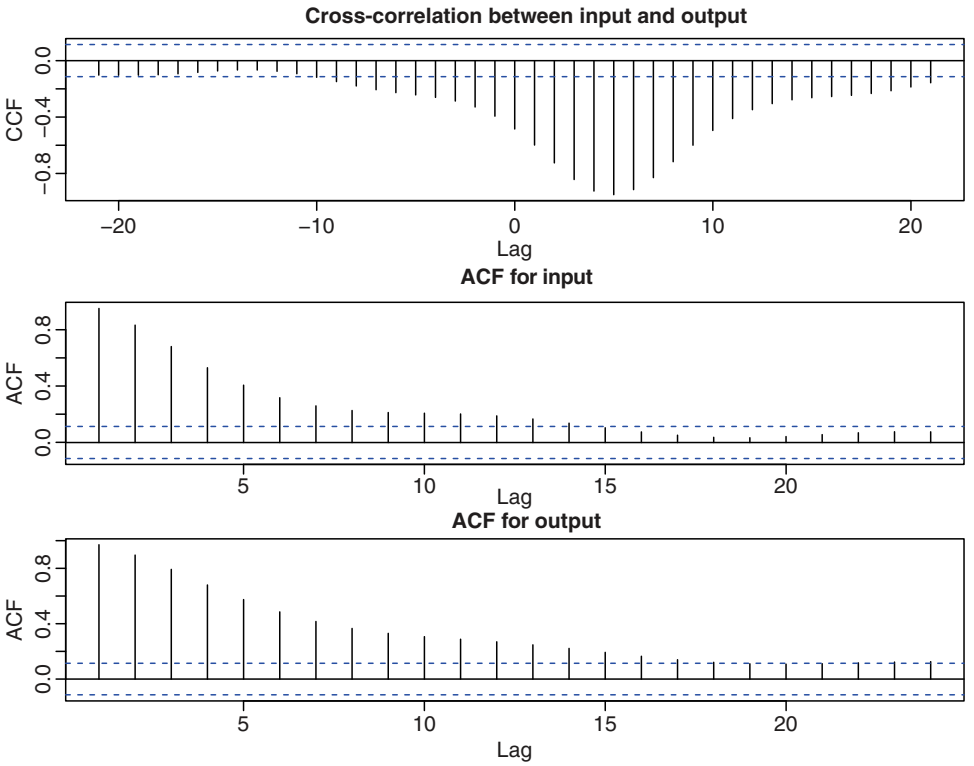

FIGURE 12.4 Estimated cross-correlation function between input and output for coded gas furnace data read at 9-second intervals along with the autocorrelation functions for the individual series.

```
    Input and Output")
> plot(ACF.x,main="ACF for Input")
> plot(ACF.y,main="ACF for Output")
```

12.1.3 Approximate Standard Errors of Cross-Correlation Estimates

A crude check as to whether certain values of the cross-correlation function $\rho_{xy}(k)$ could be effectively zero may be made by comparing the corresponding cross-correlation estimates with their approximate standard errors. Bartlett (1955) showed that the covariance between two cross-correlation estimates $r_{xy}(k)$ and $r_{xy}(k+l)$ is, on the normal assumption, and $k \geq 0$, given by

$$\begin{aligned}
&\operatorname{cov}[r_{xy}(k), r_{xy}(k+l)] \\
&\quad \simeq (n-k)^{-1} \sum_{\upsilon=-\infty}^{\infty} \{\rho_{xx}(\upsilon)\rho_{yy}(\upsilon+l) + \rho_{xy}(-\upsilon)\rho_{xy}(\upsilon+2k+l) \\
&\qquad\qquad + \rho_{xy}(k)\rho_{xy}(k+l)[\rho_{xy}^2(\upsilon) + \tfrac{1}{2}\rho_{xx}^2(\upsilon) + \tfrac{1}{2}\rho_{yy}^2(\upsilon)] \\
&\qquad\qquad - \rho_{xy}(k)[\rho_{xx}(\upsilon)\rho_{xy}(\upsilon+k+l) + \rho_{xy}(-\upsilon)\rho_{yy}(\upsilon+k+l)] \\
&\qquad\qquad - \rho_{xy}(k+l)[\rho_{xx}(\upsilon)\rho_{xy}(\upsilon+k) + \rho_{xy}(-\upsilon)\rho_{yy}(\upsilon+k)]\} \quad (12.1.6)
\end{aligned}$$

In particular, setting $l = 0$,

$$\begin{aligned}\operatorname{var}[r_{xy}(k)] &\simeq (n-k)^{-1}\sum_{v=-\infty}^{\infty}\{\rho_{xx}(v)\rho_{yy}(v)+\rho_{xy}(k+v)\rho_{xy}(k-v)\\ &\quad+\rho_{xy}^2(k)[\rho_{xy}^2(v)+\tfrac{1}{2}\rho_{xx}^2(v)+\tfrac{1}{2}\rho_{yy}^2(v)]\\ &\quad-2\rho_{xy}(k)[\rho_{xx}(v)\rho_{xy}(v+k)+\rho_{xy}(-v)\rho_{yy}(v+k)]\}\end{aligned} \tag{12.1.7}$$

Formulas that apply to important special cases can be derived from these general expressions. For example, if we assume that $x_t \equiv y_t$, it becomes appropriate to set

$$\rho_{xx}(v) = \rho_{yy}(v) = \rho_{xy}(v) = \rho_{xy}(-v)$$

On making this substitution in (12.1.6) and (12.1.7), we obtain an expression for the covariance between two autocorrelation estimates and, more particularly, the expression for the variance of an autocorrelation estimate given earlier in (2.1.13).

It is often the case that two processes are appreciably cross-correlated only over some rather narrow range of lags. Suppose it is postulated that $\rho_{xy}(v)$ is nonzero *only* over some range $Q_1 \le v \le Q_2$. Then,

1. If neither $k, k+l$, nor $k+\frac{1}{2}l$ are included in this range, all terms in (12.1.6) except the first are zero, and

$$\operatorname{cov}[r_{xy}(k), r_{xy}(k+l)] \simeq (n-k)^{-1}\sum_{v=-\infty}^{\infty}\rho_{xx}(v)\rho_{yy}(v+l) \tag{12.1.8}$$

2. If k is not included in this range, then in a similar way (12.1.7) reduces to

$$\operatorname{var}[r_{xy}(k)] \simeq (n-k)^{-1}\sum_{v=-\infty}^{\infty}\rho_{xx}(v)\rho_{yy}(v) \tag{12.1.9}$$

In particular, on the hypothesis that the two processes have *no cross-correlation*, that is, cross-correlations are zero for all lags, it follows that the simple formulas (12.1.8) and (12.1.9) apply for *all* lags k and $k+l$.

Another special case of some interest occurs when two processes are *not cross-correlated and one is white noise*. Suppose that $x_t = a_t$ is generated by a white noise process but y_t is autocorrelated. Then from (12.1.8),

$$\operatorname{cov}[r_{ay}(k), r_{ay}(k+l)] \simeq (n-k)^{-1}\rho_{yy}(l) \tag{12.1.10}$$

$$\operatorname{var}[r_{ay}(k)] \simeq (n-k)^{-1} \tag{12.1.11}$$

Hence, it follows that

$$\rho[r_{ay}(k), r_{ay}(k+l)] \simeq \rho_{yy}(l) \tag{12.1.12}$$

Thus, in this case the cross-correlations have the *same* autocorrelation function as the process generating the output y_t. Thus, even though a_t and y_t are *not* cross-correlated, the sample cross-correlation function can be expected to vary about zero with standard deviation $(n-k)^{-1/2}$ *in a systematic pattern* typical of the behavior of the autocorrelation

function $\rho_{yy}(l)$. Finally, if two processes are *both* white noise and are not cross-correlated, the covariance between cross-correlation estimates at different lags will be zero.

12.2 IDENTIFICATION OF TRANSFER FUNCTION MODELS

We now show how to *identify* a combined transfer function–noise model

$$Y_t = \delta^{-1}(B)\omega(B)X_{t-b} + N_t$$

for a linear system corrupted by noise N_t at the output and assumed to be generated by an ARIMA process that is statistically independent[1] of the input X_t. Specifically, the objective at this stage is to obtain some idea of the orders r and s of the denominator and numerator operators in the transfer function model and to derive initial guesses for the parameters $\boldsymbol{\delta}, \boldsymbol{\omega}$, and the delay parameter b. In addition, we aim to make initial guesses of the orders p, d, q of the ARIMA process describing the noise at the output and to obtain initial estimates of the parameters $\boldsymbol{\phi}$ and $\boldsymbol{\theta}$ in that model. The tentative transfer function and noise models so obtained can then be used as a starting point for more efficient estimation methods described in Section 12.3.

Outline of the Identification Procedure. Suppose that the transfer function model

$$Y_t = \upsilon(B)X_t + N_t \tag{12.2.1}$$

may be parsimoniously parameterized in the form

$$Y_t = \delta^{-1}(B)\omega(B)X_{t-b} + N_t \tag{12.2.2}$$

where $\delta(B) = 1 - \delta_1 B - \delta_2 B^2 - \cdots - \delta_r B^r$ and $\omega(B) = \omega_0 - \omega_1 B - \omega_2 B^2 - \cdots - \omega_s B^s$. The identification procedure is as follows:

1. Derive rough estimates $\hat{\upsilon}_j$ of the impulse response weights υ_j in (12.2.1).
2. Use the estimates $\hat{\upsilon}_j$ so obtained to make guesses of the orders r and s of the denominator and numerator operators in (12.2.2) and of the delay parameter b.
3. Substitute the estimates $\hat{\upsilon}_j$ in equations (11.2.8) with values of r, s, and b obtained from step 2 to obtain initial estimates of the parameters $\boldsymbol{\delta}$ and $\boldsymbol{\omega}$ in (12.2.2).

Knowing the $\hat{\upsilon}_j$, values of b, r, and s may be guessed using the following facts established in Section 11.2.2. For a model of the form of (12.2.2), the impulse response weights υ_j consist of:

1. b zero values $\upsilon_0, \upsilon_1, \ldots, \upsilon_{b-1}$.
2. A further $s - r + 1$ values $\upsilon_b, \upsilon_{b+1}, \ldots, \upsilon_{b+s-r}$ following no fixed pattern (no such values occur if $s < r$).

[1]When the input is at our choice, we can guarantee that it is independent of N_t by *generating* X_t according to some random process.

3. Values v_j with $j \geq b + s - r + 1$ that follow the pattern dictated by an rth-order difference equation that has r starting values $v_{b+s}, \ldots, v_{b+s-r+1}$. Starting values v_j for $j < b$ will, of course, be zero.

Differencing of the Input and Output. The basic tool that is employed here in the identification procedure is the cross-correlation function between input and output. When the processes are nonstationary, it is assumed that stationarity can be induced by suitable differencing. Nonstationary behavior is suspected if the estimated auto- and cross-correlation functions of the (X_t, Y_t) series fail to damp out quickly. We assume that a degree of differencing[2] d necessary to induce stationarity has been achieved when the estimated auto- and cross-correlations $r_{xx}(k)$, $r_{yy}(k)$, and $r_{xy}(k)$ of $x_t = \nabla^d X_t$ and $y_t = \nabla^d Y_t$ damp out quickly. In practice, d is usually 0, 1, or 2.

Identification of the Impulse Response Function Without Prewhitening. Suppose that after differencing d times, the model (12.2.1) can be written in the form

$$y_t = v_0 x_t + v_1 x_{t-1} + v_2 x_{t-2} + \cdots + n_t \tag{12.2.3}$$

where $y_t = \nabla^d Y_t$, $x_t = \nabla^d X_t$, and $n_t = \nabla^d N_t$ are stationary processes with zero means. Then, on multiplying throughout in (12.2.3) by x_{t-k} for $k \geq 0$, we obtain

$$x_{t-k} y_t = v_0 x_{t-k} x_t + v_1 x_{t-k} x_{t-1} + \cdots + x_{t-k} n_t \tag{12.2.4}$$

If we make the further assumption that x_{t-k} is uncorrelated with n_t for all k, taking expectations in (12.2.4) yields the set of equations

$$\gamma_{xy}(k) = v_0 \gamma_{xx}(k) + v_1 \gamma_{xx}(k-1) + \cdots \qquad k = 0, 1, 2, \ldots \tag{12.2.5}$$

Suppose that the weights v_j are effectively zero beyond $k = K$. Then the first $K + 1$ of the equations (12.2.5) can be written as

$$\boldsymbol{\gamma}_{xy} = \boldsymbol{\Gamma}_{xx} \mathbf{v} \tag{12.2.6}$$

where

$$\boldsymbol{\gamma}_{xy} = \begin{bmatrix} \gamma_{xy}(0) \\ \gamma_{xy}(1) \\ \vdots \\ \gamma_{xy}(K) \end{bmatrix} \qquad \mathbf{v} = \begin{bmatrix} v_0 \\ v_1 \\ \vdots \\ v_K \end{bmatrix}$$

$$\boldsymbol{\Gamma}_{xx} = \begin{bmatrix} \gamma_{xx}(0) & \gamma_{xx}(1) & \cdots & \gamma_{xx}(K) \\ \gamma_{xx}(1) & \gamma_{xx}(0) & \cdots & \gamma_{xx}(K-1) \\ \vdots & \vdots & \ddots & \vdots \\ \gamma_{xx}(K) & \gamma_{xx}(K-1) & \cdots & \gamma_{xx}(0) \end{bmatrix}$$

[2]The procedures outlined can equally well be used when different degrees of differencing are employed for input and output.

Substituting estimates $c_{xx}(k)$ of the autocovariance function of the input x_t and estimates $c_{xy}(k)$ of the cross-covariance function between the input x_t and output y_t, (12.2.6) provides $K+1$ linear equations for the first $K+1$ weights. However, these equations, which do not in general provide efficient estimates, are cumbersome to solve for large K and in any case require knowledge of the point K beyond which the v_j are effectively zero. The sample version of equations (12.2.6) represents essentially, apart from ''end effects,'' the least-squares normal equations from linear regression of y_t on $x_t, x_{t-1}, \ldots, x_{t-K}$, in which it is assumed, implicitly, that the noise n_t in (12.2.3) is not autocorrelated. This is one source of the inefficiency in this identification method, which may be called the *regression method*. To improve the efficiency of this method, Liu and Hanssens (1982) (see also Pankratz (1991, Chapter 5)) suggest performing generalized least-squares estimation of the regression equation $y_t = v_0 x_t + v_1 x_{t-1} + \cdots + v_K x_{t-K} + n_t$ assuming the noise n_t follows some autocorrelated time series ARMA model. They also discuss generalization of this method of identification of impulse response functions to the case with multiple input processes $X_{1,t}, X_{2,t}, \ldots, X_{m,t}$ in the model, that is, $Y_t = v_1(B)X_{1,t} + \cdots + v_m(B)X_{m,t} + N_t$.

12.2.1 Identification of Transfer Function Models by Prewhitening the Input

Considerable simplification in the identification process would occur if the input to the system were white noise. Indeed, as discussed in more detail in Section 12.5, when the choice of the input is at our disposal, there is much to recommend such an input. When the original input follows some other stochastic process, simplification is possible by *prewhitening*.

Suppose that the suitably differenced input process x_t is stationary and is capable of representation by some member of the general linear class of autoregressive–moving average models. Then, given a set of data, we can carry out our usual identification and estimation methods to obtain a model for the x_t process:

$$\theta_x^{-1}(B)\phi_x(B)x_t = \alpha_t \tag{12.2.7}$$

which, to a close approximation, transforms the correlated input series x_t to the uncorrelated white noise series α_t. At the same time, we can obtain an estimate s_α^2 of σ_α^2 from the sum of squares of the $\hat{\alpha}_t$'s. If we now apply this *same* transformation to y_t to obtain

$$\beta_t = \theta_x^{-1}(B)\phi_x(B)y_t$$

then the model (12.2.3) may be written as

$$\beta_t = v(B)\alpha_t + \varepsilon_t \tag{12.2.8}$$

where ε_t is the transformed noise series defined by

$$\varepsilon_t = \theta_x^{-1}(B)\phi_x(B)\eta_t \tag{12.2.9}$$

On multiplying (12.2.8) on both sides by α_{t-k} and taking expectations, we obtain

$$\gamma_{\alpha\beta}(k) = v_k\sigma_\alpha^2 \tag{12.2.10}$$

where $\gamma_{\alpha\beta}(k) = E[\alpha_{t-k}\beta_t]$ is the cross-covariance at lag $+k$ between the series α_t and β_t. Thus,

$$v_k = \frac{\gamma_{\alpha\beta}(k)}{\sigma_\alpha^2}$$

or, in terms of the cross-correlations,

$$v_k = \frac{\rho_{\alpha\beta}(k)\sigma_\beta}{\sigma_\alpha} \qquad k = 0, 1, 2, \ldots \tag{12.2.11}$$

Hence, after prewhitening the input, the cross-correlation function between the prewhitened input and correspondingly transformed output is directly proportional to the impulse response function. We note that the effect of prewhitening is to convert the nonorthogonal set of equation (12.2.6) into the orthogonal set (12.2.10).

In practice, we do not know the theoretical cross-correlation function $\rho_{\alpha\beta}(k)$, so we must substitute estimates in (12.2.11) to give

$$\hat{v}_k = \frac{r_{\alpha\beta}(k)s_\beta}{s_\alpha} \qquad k = 0, 1, 2, \ldots \tag{12.2.12}$$

The preliminary estimates $\hat{v}_k$ so obtained are again, in general, statistically inefficient but can provide a rough basis for selecting suitable operators $\delta(B)$ and $\omega(B)$ in the transfer function model. An additional feature of the prewhitening method is that because the prewhitened input series α_t is *white noise*, so that $\rho_{\alpha\alpha}(k) = 0$ for all $k \neq 0$, there are considerable simplifications in formulas (12.1.7) and (12.1.9) for $\text{var}[r_{\alpha\beta}(k)]$. In particular, on the assumption that the series α_t and β_t are not cross correlated, the result (12.1.11) applies to give simply $\text{var}[r_{\alpha\beta}(k)] \simeq (n-k)^{-1}$. We now illustrate this identification and preliminary estimation procedure with an actual example.

12.2.2 Example of the Identification of a Transfer Function Model

In an investigation on adaptive optimization (Kotnour et al., 1966), a gas furnace was employed in which air and methane combined to form a mixture of gases containing CO_2 (carbon dioxide). The air feed was kept constant, but the methane feed rate could be varied in any desired manner, and the resulting CO_2 concentration in the off-gases measured. The continuous data of Figure 12.1 were collected to provide information about the dynamics of the system over a region of interest where it was known that an approximately linear steady-state relationship applied. The continuous stochastic input series $X(t)$ shown in the top half of Figure 12.1 was generated by passing white noise through a linear filter. The process had mean zero and, during the realization that was used for this experiment, varied from -2.5 to $+2.5$. It was desired that the actual methane gas feed rate should cover a range from 0.5 to 0.7 ft^3/min. To ensure this, the input gas feed rate was caused to follow the process:

$$\text{Methane gas input feed} = 0.60 - 0.04X(t)$$

For simplicity, we will work throughout with the ''coded'' input $X(t)$. The final transfer function expressed in terms of the actual feed rate is readily obtained by substitution. Series J in the Collection of Time Series section in Part Five shows 296 successive pairs

TABLE 12.1 Estimated Cross-Correlation Function After Prewhitening and Approximate Impulse Response Function for Gas Furnace Data

k	$r_{\alpha\beta}(k)$	$\hat{\sigma}(r)$	$\hat{v}_k$	$r_{\beta\beta}(k)$	k	$r_{\alpha\beta}(k)$	$\hat{\sigma}(r)$	$\hat{v}_k$	$r_{\beta\beta}(k)$
0	−0.00	0.06	−0.02	1.00	6	−0.27	0.06	−0.52	0.12
1	0.05	0.06	0.10	0.23	7	−0.17	0.06	−0.32	0.05
2	−0.03	0.06	−0.06	0.36	8	−0.03	0.06	−0.06	0.09
3	−0.29	0.05	−0.53	0.13	9	0.03	0.06	0.06	0.01
4	−0.34	0.06	−0.63	0.08	10	−0.06	0.06	−0.10	0.10
5	−0.46	0.05	−0.88	0.01					

of observations (X_t, Y_t) read off from the continuous records at 9-second intervals. In this particular experiment, the nature of the input disturbance was known because it was deliberately induced. However, we proceed as if it were not known. As shown in Figure 12.4, the estimated auto- and cross-correlation functions of X_t and Y_t damp out fairly quickly, confirming that no differencing is necessary. The usual model identification and fitting procedures applied to the input series X_t indicate that it is well described by a third-order autoregressive process

$$(1 - \phi_1 B - \phi_2 B^2 - \phi_3 B^3)X_t = \alpha_t$$

with $\hat{\phi}_1 = 1.97$, $\hat{\phi}_2 = -1.37$, $\hat{\phi}_3 = 0.34$, and $s_\alpha^2 = 0.0353$. Hence, the transformations

$$\alpha_t = (1 - 1.97B + 1.37B^2 - 0.34B^3)X_t$$
$$\beta_t = (1 - 1.97B + 1.37B^2 - 0.34B^3)Y_t$$

are applied to the input and output series to yield the series α_t and β_t with $s_\alpha = 0.188$ and $s_\beta = 0.358$. The estimated cross-correlation function between α_t and β_t is listed in Table 12.1 and plotted in Figure 12.5. Table 12.1 also includes the estimate (12.2.12) of the impulse response function,

$$\hat{v}_k = \frac{0.358}{0.188} r_{\alpha\beta}(k)$$

The approximate standard errors $\hat{\sigma}(r)$ for the estimated cross-correlations $r_{\alpha\beta}(k)$ shown in Table 12.1 are the square roots of the variances obtained from expression (12.1.7):

1. With cross-correlations up to lag +2 and from lag +8 onward assumed equal to zero
2. With autocorrelations $\rho_{\alpha\alpha}(k)$ assumed zero for $k > 0$
3. With autocorrelations $\rho_{\beta\beta}(k)$ assumed zero for $k > 4$
4. With estimated correlations $r_{\alpha\beta}(k)$ and $r_{\beta\beta}(k)$ from Table 12.1 replacing theoretical values.

For this example, the standard errors $\hat{\sigma}(r)$ differ very little from the approximate values $(n-k)^{-1/2}$, or as a further approximation $n^{-1/2} = 0.06$, appropriate under the hypothesis that the series are uncorrelated. The estimated cross-correlations along with the approximate two standard error limits are plotted in Figure 12.5.

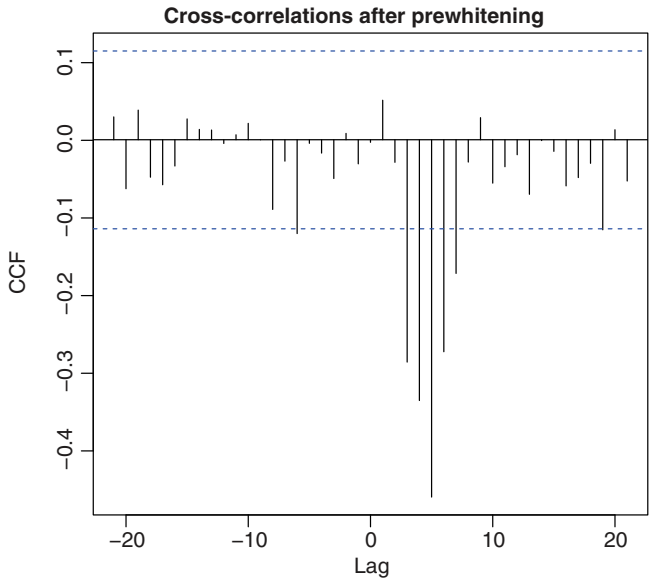

FIGURE 12.5 Estimated cross-correlation function for coded gas furnace data after prewhitening.

The values $\hat{v}_0, \hat{v}_1$, and $\hat{v}_2$ are small compared with their standard errors, suggesting that $b = 3$ (that there are two whole periods of delay). Using the results of Section 12.1.1, the subsequent pattern of the $\hat{v}$'s might be accounted for by a model with (r, s, b) equal to either (1, 2, 3) or (2, 2, 3). The first model would imply that v_3 and v_4 were preliminary values following no fixed pattern and that v_5 provided the starting value for an exponential decay determined by the difference equation $v_j - \delta v_{j-1} = 0, j > 5$. The second model would imply that v_3 was a single preliminary value and that v_4 and v_5 provided the starting values for a pattern of double exponential decay or damped sinusoidal decay determined by the difference equation $v_j - \delta_1 v_{j-1} - \delta_2 v_{j-2} = 0, j > 5$. Thus, the preliminary identification suggests a transfer function model

$$(1 - \delta_1 B - \delta_2 B^2) Y_t = (\omega_0 - \omega_1 B - \omega_2 B^2) X_{t-b} \tag{12.2.13}$$

or some simplification of it, probably with $b = 3$.

Calculations in R. The prewhitening, the calculation of $r_{\alpha\beta}(k)$, $\hat{v}_k$, and $r_{\beta\beta}(k)$ in Table 12.1, and the creation of Figure 12.5 can be performed using the R code provided below. Note, however, that the results from R differ very slightly from those shown in Table 12.1, possibly due to round-off and differences in the treatment of initial values in the series.

```
> mm1=arima(X,order=c(3,0,0))
> mm1  % Prints the AR(3) coefficients for X

   Call:  arima(x = X, order = c(3, 0, 0))
   Coefficients:
         ar1      ar2     ar3  intercept
      1.9691  -1.3651  0.3394    -0.0606
```

```
   s.e.  0.0544   0.0985  0.0543     0.1898
   sigma^2 estimated as 0.0353:log likelihood=72.6,aic=-135.1

> f1=c(1,-mm1$coef[1:3])        % Creates a filter to transform Y
> f1                    ar1         ar2        ar3
        1.000     -1.9691     1.3651    -0.3394

> Yf=filter(Y,f1,method=c("convolution"),sides=1)
> yprev=Yf[4:296]               % transformed Y
> xprev=mm1$residuals[4:296]    % transformed X
> CCF=ccf(yprev,xprev)          % computes the cross-correlations
> CCF                           % retrieves the cross-correlations
> vk=(sd(yprev)/sd(xprev))*CCF$acf    % impulse response function
> ACF=acf(yprev)                % autocorrelations of transformed Y
> plot(CCF,ylab='CCF',main='Cross-correlations after prewhitening')
```

Preliminary Estimates. Assuming the model (12.2.13) with $b = 3$, the equations (11.2.8) for the impulse response function are

$$\begin{aligned} v_j &= 0 \qquad j < 3 \\ v_3 &= \omega_0 \\ v_4 &= \delta_1 v_3 - \omega_1 \\ v_5 &= \delta_1 v_4 + \delta_2 v_3 - \omega_2 \\ v_6 &= \delta_1 v_5 + \delta_2 v_4 \\ v_7 &= \delta_1 v_6 + \delta_2 v_5 \end{aligned} \tag{12.2.14}$$

Substituting the estimates $\hat{v}_k$ from Table 12.1 in the last two of these equations, we obtain

$$\begin{aligned} -0.88\hat{\delta}_1 - 0.63\hat{\delta}_2 &= -0.52 \\ -0.52\hat{\delta}_1 - 0.88\hat{\delta}_2 &= -0.32 \end{aligned}$$

which give preliminary estimates $\hat{\delta}_1 = 0.57$ and $\hat{\delta}_2 = 0.02$. If these values are now substituted in the second, third, and fourth of equations (12.2.14), we obtain

$$\begin{aligned} \hat{\omega}_0 &= \hat{v}_3 = -0.53 \\ \hat{\omega}_1 &= \hat{\delta}_1 \hat{v}_3 - \hat{v}_4 = (0.57)(-0.53) + 0.63 = 0.33 \\ \hat{\omega}_2 &= \hat{\delta}_1 \hat{v}_4 + \hat{\delta}_2 \hat{v}_3 - \hat{v}_5 = (0.57)(-0.63) + (0.02)(-0.53) + 0.88 = 0.51 \end{aligned}$$

Thus, the preliminary identification suggests a tentative transfer function model:

$$(1 - 0.57B - 0.02B^2)Y_t = -(0.53 + 0.33B + 0.51B^2)X_{t-3}$$

The estimates so obtained can be used as starting values for the more efficient iterative estimation methods, which will be described in Section 12.3. Note that the estimate $\hat{\delta}_2$ is very small and suggests that this parameter may be omitted, but we will retain it for the time being.

12.2.3 Identification of the Noise Model

Reverting to the general case, suppose that (where necessary, after suitable differencing) the model could be written as

$$y_t = v(B)x_t + n_t$$

where $n_t = \nabla^d N_t$. Given that a preliminary estimate $\hat{v}(B)$ of the transfer function has been obtained in the manner discussed in Section 12.2.2, an estimate of the noise series is provided by

$$\hat{n}_t = y_t - \hat{v}(B)x_t$$

that is,

$$\hat{n}_t = y_t - \hat{v}_0 x_t - \hat{v}_1 x_{t-1} - \hat{v}_2 x_{t-2} - \cdots$$

Alternatively, $\hat{v}(B)$ may be replaced by the tentative transfer function model estimate $\hat{\delta}^{-1}(B)\hat{\omega}(B)B^b$ determined by preliminary identification. Thus,

$$\hat{n}_t = y_t - \hat{\delta}^{-1}(B)\hat{\omega}(B)x_{t-b}$$

and $\hat{n}_t$ may be computed by first calculating $\hat{y}_t = \hat{\delta}^{-1}(B)\hat{\omega}(B)x_{t-b}$ recursively through $\hat{\delta}(B)\hat{y}_t = \hat{\omega}(B)x_{t-b}$ as

$$\hat{y}_t = \hat{\delta}_1\hat{y}_{t-1} + \cdots + \hat{\delta}_r\hat{y}_{t-r} + \hat{\omega}_0 x_{t-b} - \hat{\omega}_1 x_{t-b-1} - \cdots - \hat{\omega}_s x_{t-b-s} \tag{12.2.15}$$

and then computing the noise series from $\hat{n}_t = y_t - \hat{y}_t$. In either case, study of the estimated autocorrelation function and partial autocorrelation function of $\hat{n}_t$ can lead to identification of the noise model.

It is also possible to identify the noise using the correlation functions for the input and output, after prewhitening, in the following way. Suppose that the input could be exactly prewhitened to give

$$\beta_t = v(B)\alpha_t + \varepsilon_t \tag{12.2.16}$$

where the known relationship

$$\varepsilon_t = \theta_x^{-1}(B)\phi_x(B)n_t \tag{12.2.17}$$

would link ε_t and n_t. If a stochastic model could be found for ε_t, then, using (12.2.17), a model could be deduced for n_t and hence for N_t. If we now write $v(B)\alpha_t = u_t$, so that $\beta_t = u_t + \varepsilon_t$, and provided that our independence assumption concerning x_t and n_t, and hence concerning u_t and ε_t, is justified, we can write

$$\gamma_{\beta\beta}(k) = \gamma_{uu}(k) + \gamma_{\varepsilon\varepsilon}(k) \tag{12.2.18}$$

Since α_t is white noise, $\gamma_{uu}(k)$ may be obtained using the result (3.1.8), which gives the autocorrelation function of a linear process. Thus,

$$\gamma_{uu}(k) = \sigma_\alpha^2 \sum_{j=0}^{\infty} v_j v_{j+k} = \frac{1}{\sigma_\alpha^2} \sum_{j=0}^{\infty} \gamma_{\alpha\beta}(j)\gamma_{\alpha\beta}(j+k)$$

TABLE 12.2 Estimated Autocorrelation and Partial Autocorrelation Functions of the Noise in Gas Furnace Data

k	r_k	$\hat{\phi}_{kk}$	k	r_k	$\hat{\phi}_{kk}$
1	0.89	0.89	7	0.01	−0.02
2	0.71	−0.43	8	−0.03	0.01
3	0.51	−0.13	9	−0.05	−0.01
4	0.32	0.02	10	−0.04	0.08
5	0.17	0.04	11	−0.03	−0.06
6	0.07	−0.02	12	−0.03	−0.10

using (12.2.10). Hence, using (12.2.18), the autocovariances of ε_t may be obtained from $\gamma_{\varepsilon\varepsilon}(k) = \gamma_{\beta\beta}(k) - \gamma_{uu}(k)$, with autocorrelations

$$\rho_{\varepsilon\varepsilon}(k) = \frac{\gamma_{\varepsilon\varepsilon}(k)}{\gamma_{\varepsilon\varepsilon}(0)} = \frac{\rho_{\beta\beta}(k) - \gamma_{uu}(k)/\gamma_{\beta\beta}(0)}{1 - \gamma_{uu}(0)/\gamma_{\beta\beta}(0)}$$
$$= \frac{\rho_{\beta\beta}(k) - \sum_{j=0}^{\infty} \rho_{\alpha\beta}(j)\rho_{\alpha\beta}(j+k)}{1 - \sum_{j=0}^{\infty} \rho_{\alpha\beta}^2(j)}$$

Now, in practice, it is necessary to *estimate* the prewhitening transformation. Having made the approximate prewhitening transformation, rough values for $\rho_{\varepsilon\varepsilon}(k)$ could be obtained by substituting the estimates $r_{\alpha\beta}(j)$ of the cross-correlation function between transformed input and output and $r_{\beta\beta}(j)$ of the autocorrelation function of the transformed output.

Application to the Gas Furnace Example. Table 12.2 shows the first 12 values of the sample autocorrelations and partial autocorrelations of the noise series $\hat{N}_t = Y_t - \hat{y}_t$, where $\hat{y}_t = \hat{\delta}^{-1}(B)\hat{\omega}(B)X_{t-3}$ is computed as in (12.2.15) using the preliminary estimates for the transfer function model obtained previously. That is, the values are computed as

$$\hat{y}_t = 0.57\hat{y}_{t-1} - (0.53X_{t-3} + 0.33X_{t-4} + 0.51X_{t-5})$$

The partial autocorrelations of $\hat{N}_t$ indicate that a second-order autoregressive model might be an adequate representation, and the least-squares estimates obtained from the $\hat{N}_t$ values for the AR(2) model yield

$$(1 - 1.54B + 0.64B^2)N_t = a_t \tag{12.2.19}$$

with $\hat{\sigma}_a^2 = 0.057$.

Thus, the analysis of this section and Section 12.1.2 suggests the identification

$$Y_t = \frac{\omega_0 - \omega_1 B - \omega_2 B^2}{1 - \delta_1 B - \delta_2 B^2} X_{t-3} + \frac{1}{1 - \phi_1 B - \phi_2 B^2} a_t \tag{12.2.20}$$

for the gas furnace model. Furthermore, the initial estimates $\hat{\omega}_0 = -0.53, \hat{\omega}_1 = 0.33, \hat{\omega}_2 = 0.51, \hat{\delta}_1 = 0.57, \hat{\delta}_2 = 0.02, \hat{\phi}_1 = 1.54$, and $\hat{\phi}_2 = -0.64$ can be used as rough starting values for the nonlinear estimation procedures that we describe in Section 12.3.

12.2.4 Some General Considerations in Identifying Transfer Function Models

Some general remarks can now be made concerning the procedure for identifying transfer function and noise models that we have just described.

1. For many practical situations, when the effect of noise is appreciable, a delayed first- or second-order system such as that given by (12.2.13), or some simplification of it, would often provide as elaborate a model as could be justified for the data.
2. Efficient estimation is only possible assuming the model *form* to be known. The estimates $\hat{v}_k$ given by (12.2.12) are in general *necessarily* inefficient therefore. They are employed at the identification stage because they are easily computed and can indicate a form of model worthy to be fitted by more elaborate means.
3. Even if these were efficient estimates, the number of $\hat{v}$'s required to trace out the impulse response function fully would typically be considerably larger than the number of parameters in a transfer function model. In cases where the δ's and ω's in an adequate transfer function model could be estimated accurately, nevertheless, the estimates of the corresponding v's could have large variances and be highly correlated.
4. The variance of

$$r_{\alpha\beta}(k) = \hat{v}_k \frac{s_\alpha}{s_\beta}$$

is of order $1/n$. Thus, we can expect that the estimates $r_{\alpha\beta}(k)$ and hence the $\hat{v}_k$ will be buried in noise unless σ_α is reasonably large compared with the residual noise, or unless n is large. Thus, the identification procedure requires the variation in the input X_t to be reasonably large compared with the variation due to the noise and/or a large volume of data is available. These requirements are satisfied by the gas furnace data for which, as we show in Section 12.3, the initial identification is remarkably good. When these requirements are not satisfied, the identification procedure may fail. Usually, this will mean that only very rough estimates are possible with the available data. However, some kind of rudimentary modeling may be possible by postulating a plausible but simple transfer function/noise model, fitting directly by the least-squares procedures of the next section, and applying diagnostic checks leading to elaboration of the model when this proves necessary.
5. It should, perhaps, be emphasized that the prewhitened series α_t and β_t, and their cross-correlation function, $r_{\alpha\beta}(k)$, in particular, are used only for the purpose of identification of the form of the transfer function model. Once the model form is identified, the original series X_t and Y_t, not the prewhitened series, are used for parameter estimation, forecasting, and so on.
6. An alternative method for identification of the transfer function–noise model was proposed by Haugh and Box (1977), and similar ideas were also discussed by Priestley (1981, Chapter 9). The method, which might be referred to as ''double prewhitening,'' involves prewhitening *both* input and output series. That is, separate univariate ARIMA models are built for both the input and the output processes, and then the cross-correlation structure of the resulting (univariate white noise) residuals from these models is examined. However, while sometimes useful, this procedure can

become overly complicated in terms of the final model specified, due to the use of two sets of prewhitening factors.

7. The above discussion has focused on transfer function models with a single input variable X_t. An alternative method of identifying transfer function models, which readily generalizes to deal with multiple inputs, is given in Appendix A12.1. Transfer function models can also be specified using methods developed for multivariate time series analysis as demonstrated by Tiao and Box (1981). A discussion of such methods is given in Chapter 14.

Lack of Uniqueness of the Model. Suppose that a particular dynamic system is represented by the model

$$Y_t = \delta^{-1}(B)\omega(B)X_{t-b} + \varphi^{-1}(B)\theta(B)a_t \tag{12.2.21}$$

Then it could equally well be represented by

$$L(B)Y_t = L(B)\delta^{-1}(B)\omega(B)X_{t-b} + L(B)\varphi^{-1}(B)\theta(B)a_t \tag{12.2.22}$$

where $L(B)$ could be an arbitrary common factor, and hence would be redundant. Similar to the discussion in Section 7.3.5 on parameter redundancy for ARMA models, for uniqueness of model parameterization in (12.2.21) it is clear that the possibility of common factors in the operators $\delta(B)$ and $\omega(B)$, or in the $\varphi(B)$ and $\theta(B)$ operators, must be avoided. The chance that we may iterate toward a model of unnecessarily complicated form is reduced if we base our strategy on the following considerations:

1. Since rather simple transfer function models of first or second order, with or without delay, are often adequate, iterative model building should begin with a fairly simple model, looking for further simplification if this is possible, and reverting to more complicated models only as the need is demonstrated.
2. One should be always on the look out for the possibility of removing a factor common to two or more of the operators on Y_t, X_t, and a_t. In practice, we will be dealing with estimated coefficients, which may be subject to rather large sampling errors, so that only approximate common factors in the factorizations can be expected. Thus, a very careful analysis may be needed to detect such factors. Of course, having removed what appears to be a common factor, the model can be refitted and checked to show whether the simplification can be justified.
3. When simplification by factorization is possible, but is overlooked, the least-squares estimation procedure may become extremely unstable since the minimum will tend to lie on a line or surface in the parameter space rather than at a point. Conversely, instability in the solution can point to the possibility of simplification of the model. As noted earlier, one reason for carrying out the identification procedure before fitting the model is to avoid redundancy or, conversely, to achieve *parsimony* in parameterization.

Remark. If the operator $L(B)$ in (12.2.22) were set equal to $\varphi(B)\delta(B)$, we would obtain

$$\varphi(B)\delta(B)Y_t = \varphi(B)\omega(B)X_{t-b} + \delta(B)\theta(B)a_t \tag{12.2.23}$$

which can be written as

$$\delta^*(B)Y_t = \omega^*(B)X_{t-b} + \theta^*(B)a_t \tag{12.2.23a}$$

Models of the general form of (12.2.23a) have been referred to as ARMAX models in the econometric literature (e.g., Hannan and Deistler, 1988; Hannan et al., 1979; Reinsel, 1979). As can be seen, care is needed to avoid the occurrence of common factors among the operators in this form.

12.3 FITTING AND CHECKING TRANSFER FUNCTION MODELS

12.3.1 Conditional Sum-of-Squares Function

We now consider the problem of efficiently and simultaneously estimating the parameters b, $\boldsymbol{\delta}, \boldsymbol{\omega}, \boldsymbol{\phi}$, and $\boldsymbol{\theta}$ in the tentatively identified model

$$y_t = \delta^{-1}(B)\omega(B)x_{t-b} + n_t \tag{12.3.1}$$

where $y_t = \nabla^d Y_t$, $x_t = \nabla^d X_t$, and $n_t = \nabla^d N_t$ are all stationary processes and

$$n_t = \phi^{-1}(B)\theta(B)a_t \tag{12.3.2}$$

It is assumed that $n = N - d$ pairs of values are available for the analysis and that Y_t and X_t (y_t and x_t if $d > 0$) denote deviations from expected values. These expected values may be estimated along with the other parameters, but for the lengths of time series normally worth analyzing it will usually be sufficient to use the sample means as estimates. When $d > 0$, it will frequently be true that expected values for y_t and x_t are zero.

If starting values $\mathbf{x}_0$, $\mathbf{y}_0$, and $\mathbf{a}_0$ prior to the commencement of the series were available, then given the data, for any choice of the parameters $(b, \boldsymbol{\delta}, \boldsymbol{\omega}, \boldsymbol{\phi}, \boldsymbol{\theta})$ and of the starting values $(\mathbf{x}_0, \mathbf{y}_0, \mathbf{a}_0)$ we could calculate, successively, values of

$$a_t = a_t(b, \boldsymbol{\delta}, \boldsymbol{\omega}, \boldsymbol{\phi}, \boldsymbol{\theta} | \mathbf{x}_0, \mathbf{y}_0, \mathbf{a}_0)$$

for $t = 1, 2, \ldots, n$. Under the normal assumption for the a_t's, a close approximation to the maximum likelihood estimates of the parameters can be obtained by minimizing the *conditional sum-of-squares function*,

$$S_0(b, \boldsymbol{\delta}, \boldsymbol{\omega}, \boldsymbol{\phi}, \boldsymbol{\theta}) = \sum_{t=1}^{n} a_t^2(b, \boldsymbol{\delta}, \boldsymbol{\omega}, \boldsymbol{\phi}, \boldsymbol{\theta} | \mathbf{x}_0, \mathbf{y}_0, \mathbf{a}_0) \tag{12.3.3}$$

Three-Stage Procedure for Calculating the a's. Given appropriate starting values, the generation of the a_t's *for any particular choice of the parameter values* may be accomplished using the following three-stage procedure.

First, the output y_t from the transfer function model may be computed from

$$y_t = \delta^{-1}(B)\omega(B)x_{t-b}$$

that is, from

$$\delta(B)y_t = \omega(B)x_{t-b}$$

or from

$$y_t - \delta_1 y_{t-1} - \cdots - \delta_r y_{t-r} = \omega_0 x_{t-b} - \omega_1 x_{t-b-1} - \cdots - \omega_s x_{t-b-s} \tag{12.3.4}$$

Having calculated the y_t series, then using (12.3.1), the noise series n_t can be obtained from

$$n_t = y_t - y_t \tag{12.3.5}$$

Finally, the a_t's can be obtained from (12.3.2) written in the form

$$\theta(B)a_t = \phi(B)n_t$$

that is,

$$a_t = \theta_1 a_{t-1} + \cdots + \theta_q a_{t-q} + n_t - \phi_1 n_{t-1} - \cdots - \phi_p n_{t-p} \tag{12.3.6}$$

Starting Values. As discussed in Section 7.1.3 for stochastic model estimation, the effect of transients can be minimized if the difference equations are started off from a value of t for which all previous x_t's and y_t's are known. Thus, y_t in (12.3.4) is calculated from $t = u + 1$ onward, where u is the larger of r and $s + b$. This means that n_t will be available from n_{u+1} onward; hence, if unknown a_t's are set equal to their unconditional expected values of zero, the a_t's may be calculated from a_{u+p+1} onward. Thus, the conditional sum-of-squares function is

$$S_0(b, \boldsymbol{\delta}, \boldsymbol{\omega}, \boldsymbol{\phi}, \boldsymbol{\theta}) = \sum_{t=u+p+1}^{n} a_t^2(b, \boldsymbol{\delta}, \boldsymbol{\omega}, \boldsymbol{\phi}, \boldsymbol{\theta} | \mathbf{x}_0, \mathbf{y}_0, \mathbf{a}_0) \tag{12.3.7}$$

Example Using the Gas Furnace Data. For these data, the model (12.2.20), namely

$$Y_t = \frac{\omega_0 - \omega_1 B - \omega_2 B^2}{1 - \delta_1 B - \delta_2 B^2} X_{t-3} + \frac{1}{1 - \phi_1 B - \phi_2 B^2} a_t$$

has been identified. Equations (12.3.4), (12.3.5), and (12.3.6) then become

$$y_t = \delta_1 y_{t-1} + \delta_2 y_{t-2} + \omega_0 X_{t-3} - \omega_1 X_{t-4} - \omega_2 X_{t-5} \tag{12.3.8}$$

$$N_t = Y_t - y_t \tag{12.3.9}$$

$$a_t = N_t - \phi_1 N_{t-1} - \phi_2 N_{t-2} \tag{12.3.10}$$

Thus, (12.3.8) can be used to generate y_t from $t = 6$ onward and (12.3.10) to generate a_t from $t = 8$ onward. The slight loss of information that results will not be important for a sufficiently long length of series. For example, since $N = 296$ for the gas furnace data, the loss of seven values at the beginning of the series is of little practical consequence.

In the example above, we have assumed that $b = 3$. To estimate b, the values of $\boldsymbol{\delta}, \boldsymbol{\omega}, \boldsymbol{\phi}$, and $\boldsymbol{\theta}$, which minimize the conditional sum of squares, can be calculated for each value of b in the likely range and the overall minimum with respect to $b, \boldsymbol{\delta}, \boldsymbol{\omega}, \boldsymbol{\phi}$, and $\boldsymbol{\theta}$ obtained.

12.3.2 Nonlinear Estimation

A nonlinear least-squares algorithm, analogous to that given for fitting the stochastic model in Section 7.2.4, can be used to obtain the least-squares estimates and their approximate

standard errors. The algorithm will behave well when the sum-of-squares function is roughly quadratic. However, the procedure can sometimes run into trouble, in particular if the parameter estimates are very highly correlated (if, for example, the model approaches singularity due to near-common factors in the factorizations of the operators), or, in some cases, if estimates are near a boundary of the permissible parameter space. In difficult cases, the estimation situation may be clarified by plotting sum-of-squares contours for selected two-dimensional sections of the parameter space.

The nonlinear least-squares algorithm can be implemented as follows: At any stage of the iteration, and for some fixed value of the delay parameter b, let the best guesses available for the remaining parameters be denoted by

$$\boldsymbol{\beta}_0' = (\delta_{1,0}, \ldots, \delta_{r,0};\ \omega_{0,0}, \ldots, \omega_{s,0}; \phi_{1,0}, \ldots, \phi_{p,0}; \theta_{1,0}, \ldots, \theta_{q,0})$$

Now let $a_{t,0}$ denote that value of a_t computed from the model, as in Section 12.3.1, for the guessed parameter values $\boldsymbol{\beta}_0$ and denote the negative of the derivatives of a_t with respect to the parameters as follows:

$$d_{i,t}^{(\delta)} = -\frac{\partial a_t}{\partial \delta_i}\bigg|_{\boldsymbol{\beta}_0} \qquad d_{j,t}^{(\omega)} = -\frac{\partial a_t}{\partial \omega_j}\bigg|_{\boldsymbol{\beta}_0} \qquad d_{g,t}^{(\phi)} = -\frac{\partial a_t}{\partial \phi_g}\bigg|_{\boldsymbol{\beta}_0} \qquad d_{h,t}^{(\theta)} = -\frac{\partial a_t}{\partial \theta_h}\bigg|_{\boldsymbol{\beta}_0} \tag{12.3.11}$$

Then a Taylor series expansion of $a_t = a_t(\boldsymbol{\beta})$ about parameter values $\boldsymbol{\beta} = \boldsymbol{\beta}_0$ can be rearranged in the form

$$\begin{aligned} a_{t,0} \simeq & \sum_{i=1}^{r} (\delta_i - \delta_{i,0}) d_{i,t}^{(\delta)} + \sum_{j=0}^{s} (\omega_j - \omega_{j,0}) d_{j,t}^{(\omega)} \\ & + \sum_{g=1}^{p} (\phi_g - \phi_{g,0}) d_{g,t}^{(\phi)} + \sum_{h=1}^{q} (\theta_h - \theta_{h,0}) d_{h,t}^{(\theta)} + a_t \end{aligned} \tag{12.3.12}$$

We proceed as in Section 7.2 to obtain adjustments $\delta_i - \delta_{i,0}, \omega_j - \omega_{j,0}$, and so on, by fitting this linearized equation by standard linear least-squares. By adding the adjustments to the first guesses $\boldsymbol{\beta}_0$, a set of second guesses can be formed and the procedure repeated until convergence is reached.

The derivatives in (12.3.11) may be computed recursively. However, it seems simplest to work with a standard nonlinear least-squares computer program in which derivatives are determined numerically and an option is available of ''constrained iteration'' to prevent instability. It is then necessary only to program the computation of a_t itself.

The covariance matrix of the estimates may be obtained from the converged value of the matrix

$$(\mathbf{X}_{\hat{\boldsymbol{\beta}}}' \mathbf{X}_{\hat{\boldsymbol{\beta}}})^{-1} \hat{\sigma}_a^2 \simeq \hat{\text{cov}}[\hat{\boldsymbol{\beta}}]$$

as described in Section 7.2.2; in addition, the least-squares estimates $\hat{\boldsymbol{\beta}}$ have been shown to have a multivariate normal asymptotic distribution (e.g., Pierce, 1972a; Reinsel, 1979). If the delay b, which is an integer, needs to be estimated, the iteration may be run to convergence for a series of values of b and the value of b giving the minimum sum of squares selected. One special feature (see, for example, Pierce, 1972a) of the covariance matrix of the least-squares estimates $\hat{\boldsymbol{\beta}}$ is that it will be approximately a block diagonal matrix whose two blocks on the diagonal consist of the covariance matrices of the

parameters $(\hat{\boldsymbol{\delta}}', \hat{\boldsymbol{\omega}}') = (\hat{\delta}_1, \ldots, \hat{\delta}_r, \hat{\omega}_0, \ldots, \hat{\omega}_s)$ and $(\hat{\boldsymbol{\phi}}', \hat{\boldsymbol{\theta}}') = (\hat{\phi}_1, \ldots, \hat{\phi}_p, \hat{\theta}_1, \ldots, \hat{\theta}_q)$, respectively. Thus, the parameter estimates of the transfer function part of the model are approximately uncorrelated with the estimates of the noise part of the model, which results from the assumed independence between the input X_t and the white noise a_t in the model.

More exact sum-of-squares and exact likelihood function methods could also be employed in the estimation of the transfer function–noise models, as in the case of the ARMA models discussed in Chapter 7 (see, e.g. Newbold, 1973). The state-space model Kalman filtering and innovations algorithm approach to the exact likelihood evaluation discussed in Section 7.4 could also be used. However, for moderate and large n and nonseasonal data, there will generally be little difference between the conditional and exact methods.

Remark. Commercially available software packages such as SAS and SCA include algorithms for estimating the parameters in transfer function–noise models. The software package R can also be used for model fitting. In particular, the newly released package MTS for multivariate time series analysis that we will use in Chapter 14 has a function tfm1() that fits a transfer function–noise model to a dataset with a single input variable X. A demonstration of this package is given in Section 12.4.1. A second function tfm2() fits a model with two input variables to the data.

12.3.3 Use of Residuals for Diagnostic Checking

Serious model inadequacy can usually be detected by examining

1. The autocorrelation function $r_{\hat{a}\hat{a}}(k)$ of the residuals $\hat{a}_t = a_t(\hat{b}, \hat{\boldsymbol{\delta}}, \hat{\boldsymbol{\omega}}, \hat{\boldsymbol{\phi}}, \hat{\boldsymbol{\theta}})$ from the fitted model.
2. Certain cross-correlation functions involving input and residuals: in particular, the cross-correlation function $r_{\alpha\hat{a}}(k)$ between prewhitened input α_t and the residuals $\hat{a}_t$.

Suppose, if necessary after suitable differencing, that the model can be written as

$$\begin{aligned} y_t &= \delta^{-1}(B)\omega(B)x_{t-b} + \phi^{-1}(B)\theta(B)a_t \\ &= \upsilon(B)x_t + \psi(B)a_t \end{aligned} \tag{12.3.13}$$

Now, suppose that we select an incorrect model leading to residuals a_{0t}, where

$$y_t = \upsilon_0(B)x_t + \psi_0(B)a_{0,t}$$

Then

$$a_{0t} = \psi_0^{-1}(B)[\upsilon(B) - \upsilon_0(B)]x_t + \psi_0^{-1}(B)\psi(B)a_t \tag{12.3.14}$$

Thus, it is apparent in general that if a wrong model is selected, the a_{0t}'s will be autocorrelated and the a_{0t}'s will be cross-correlated with the x_t's and hence with the α_t's, which generate the x_t's.

Now consider what happens in two special cases: (1) when the transfer function model is correct but the noise model is incorrect, and (2) when the transfer function model is incorrect.

Transfer Function Model Correct, Noise Model Incorrect. If $v_0(B) = v(B)$ but $\psi_0(B) \neq \psi(B)$, then (12.3.14) becomes

$$a_{0t} = \psi_0^{-1}(B)\psi(B)a_t \tag{12.3.15}$$

Therefore, the a_{0t}'s would *not* be cross-correlated with x_t's or with α_t's. However, the a_{0t} process would be autocorrelated, and the form of the autocorrelation function could indicate appropriate modification of the noise structure, as discussed for univariate ARIMA models in Section 8.3.

Transfer Function Model Incorrect. From (12.3.14) it is apparent that if the transfer function model were incorrect, not only would the a_{0t}'s be cross-correlated with the x_t's (and α_t's), but *also the a_{0t}'s would be autocorrelated*. This would be true even if the noise model were correct, for then (12.3.14) would become

$$a_{0t} = \psi^{-1}(B)[v(B) - v_0(B)]x_t + a_t \tag{12.3.16}$$

Whether or not the noise model was correct, a cross-correlation analysis could indicate the modifications needed in the transfer function model. This aspect is clarified by considering the model after prewhitening. If the output and the input are assumed to be transformed so that the input is white noise, then, as in (12.2.8), we may write the model as

$$\beta_t = v(B)\alpha_t + \varepsilon_t$$

where $\beta_t = \theta_x^{-1}(B)\phi_x(B)y_t$ and $\varepsilon_t = \theta_x^{-1}(B)\phi_x(B)n_t$. Now, consider the quantities

$$\varepsilon_{0t} = \beta_t - v_0(B)\alpha_t$$

Since $\varepsilon_{0t} = [v(B) - v_0(B)]\alpha_t + \varepsilon_t$, arguing as in Section 12.1.1, the cross-correlations between the ε_{0t}'s and the α_t's measure the discrepancy between the correct and incorrect impulse functions. Specifically, as in (12.2.11),

$$v_k - v_{0k} = \frac{\rho_{\alpha\varepsilon_0}(K)\sigma_{\varepsilon_0}}{\sigma_\alpha} \qquad k = 0, 1, 2, \ldots \tag{12.3.17}$$

12.3.4 Specific Checks Applied to the Residuals

In practice, we do not know the process parameters exactly but must apply our checks to the residuals $\hat{a}_t$ computed after least-squares fitting. Even if the functional form of the fitted model were adequate, the parameter estimates would differ somewhat from the true values and the distribution of the autocorrelations of the residuals $\hat{a}_t$'s would also differ to some extent from that of the autocorrelations of the a_t's. Therefore, some caution is necessary in using the results of the previous sections to suggest the behavior of residual correlations. The brief discussion that follows is based in part on a more detailed study by Pierce (1972b).

Autocorrelation Checks. Suppose that a transfer function–noise model having been fitted by least-squares and the residuals $\hat{a}_t$'s calculated by substituting least-squares estimates for the parameters and the estimated autocorrelation function $r_{\hat{a}\hat{a}}(k)$ of these residuals is computed. Then, as we have seen

1. If the autocorrelation function $r_{\hat{a}\hat{a}}(k)$ shows marked correlation patterns, this suggests model inadequacy.
2. If the cross-correlation checks do not indicate inadequacy of the transfer function model, the inadequacy is probably in the fitted noise model $n_t = \psi_0(B)\hat{a}_{0t}$.

In the latter case, identification of a subsidiary model

$$\hat{a}_{0t} = T(B)a_t$$

to represent the correlation of the residuals from the primary model can, in accordance with (12.3.15), indicate roughly the form

$$n_t = \psi_0(B)T(B)a_t$$

to take for the modified noise model. However, in making assessments of whether an apparent discrepancy of estimated autocorrelations from zero is, or is not, likely to point to a nonzero theoretical value, certain facts must be borne in mind analogous to those discussed in Section 8.2.1.

Suppose that after allowing for starting values, $m = n - u - p$ values of the $\hat{a}_t$'s are actually available for this computation. Then if the model was correct in functional form and the *true parameter values were substituted*, the residuals would be white noise and the estimated autocorrelations would be distributed mutually independently about zero with variance $1/m$. When estimates are substituted for the parameter values, the distributional properties of the estimated autocorrelations at low lags are affected. In particular, the variance of these estimated low-lag autocorrelations can be considerably less than $1/m$, and the values can be highly correlated. Thus, with k small, comparison of an estimated autocorrelation $r_{\hat{a}\hat{a}}(k)$ with a ''standard error'' $1/\sqrt{m}$ could greatly underestimate its significance. Also, ripples in the estimated autocorrelation function at low lags can arise simply because of the high induced correlation between these estimates. If the amplitude of such low-lag ripples is small compared with $1/\sqrt{m}$, they could have arisen by chance alone and need not be indicative of some real pattern in the theoretical autocorrelations.

A helpful overall check, which takes account of these distributional effects produced by fitting, is as follows. Consider the first K estimated autocorrelations $r_{\hat{a}\hat{a}}(1), \ldots, r_{\hat{a}\hat{a}}(K)$ and let K be taken sufficiently large so that if the model is written as $y_t = v(B)x_t + \psi(B)a_t$, the weights ψ_j can be expected to be negligible for $j > K$. Then if the functional form of the model is adequate, the quantity

$$Q = m\sum_{k=1}^{K} r_{\hat{a}\hat{a}}^2(k) \tag{12.3.18}$$

is approximately distributed as χ^2 with $K - p - q$ degrees of freedom. Note that the degrees of freedom in χ^2 depend on the number of parameters in the noise model but not on the number of parameters in the transfer function model. By referring Q to a table of percentage points of χ^2, we can obtain an approximate test of the hypothesis of model adequacy. However, in practice, the modified statistic

$$\tilde{Q} = m(m+2)\sum_{k=1}^{K}(m-k)^{-1}r_{\hat{a}\hat{a}}^2(k) \tag{12.3.18a}$$

analogous to (8.2.3) of Section 8.2.2 for the ARIMA model, would be recommended instead of (12.3.18) because $\tilde{Q}$ provides a closer approximation to the chi-squared distribution than Q under the null hypothesis of model adequacy.

Cross-Correlation Check. As we have seen in Section 12.3.3,

1. A pattern of markedly nonzero cross-correlations $r_{x\hat{a}}(k)$ suggests inadequacy of the transfer function model.
2. A somewhat different cross-correlation analysis can suggest the *type* of modification needed in the transfer function model. Specifically, if the fitted transfer function is $\hat{v}_0(B)$ and we consider the cross-correlations between the quantities $\hat{\varepsilon}_{0t} = \beta_t - \hat{v}_0(B)\alpha_t$ and α_t, rough estimates of the discrepancies $v_k - v_{0k}$ are given by

$$\frac{r_{\alpha\hat{\varepsilon}_0}(k)s_{\hat{\varepsilon}_0}}{s_\alpha}$$

Suppose that the model were of the correct functional form and *true* parameter values had been substituted. The residuals would be white noise uncorrelated with the x_t's and, using (12.1.11), the variance of the $r_{xa}(k)$ for an effective length of series m would be approximately $1/m$. However, unlike the autocorrelations $r_{aa}(k)$, these cross-correlations will not be approximately uncorrelated. In general, if the x_t's are autocorrelated, so are the cross-correlations $r_{xa}(k)$. In fact, as has been seen in (12.1.12), on the assumption that the x_t's and the a_t's have no cross-correlation, the correlation coefficient between $r_{xa}(k)$ and $r_{xa}(k+l)$ is

$$\rho[r_{xa}(k), r_{xa}(k+l)] \simeq \rho_{xx}(l) \tag{12.3.19}$$

That is, approximately, the cross-correlations have the *same* autocorrelation function as does the original input series x_t. Thus, when the x_t's are autocorrelated, a perfectly adequate transfer function model will give rise to estimated cross-correlations $r_{x\hat{a}}(k)$, which, although small in magnitude, may show *pronounced patterns*. This effect is eliminated if the check is made by computing cross-correlations $r_{\alpha\hat{a}}(k)$ with the *prewhitened* input α_t.

As with the autocorrelations, when estimates are substituted for parameter values, the distributional properties of the estimated cross-correlations are affected. However, a rough overall test of the hypothesis of model adequacy, similar to the autocorrelation test, can be obtained based on the magnitudes of the estimated cross-correlations. To employ the check, the cross-correlations $r_{\alpha\hat{a}}(k)$ for $k = 0, 1, 2, \ldots, K$ between the input α_t in *prewhitened* form and the residuals $\hat{a}_t$ are estimated, and K is chosen sufficiently large so that the weights v_j and ψ_j in (12.3.13) can be expected to be negligible for $j > K$. The effects resulting from the use of estimated parameters in calculating residuals are, as before, principally confined to cross-correlations of low order whose variances are considerably less than m^{-1} and that may be highly correlated even when the input is white noise.

For an overall test, Pierce (1972b) showed that

$$S = m\sum_{k=0}^{K} r^2_{\alpha\hat{a}}(k) \tag{12.3.20}$$

is approximately distributed as χ^2 with $K + 1 - (r + s + 1)$ degrees of freedom, where $(r + s + 1)$ is the number of parameters fitted in the transfer function model. Note that the number of degrees of freedom is independent of the number of parameters fitted in the noise model. Based on studies of the behavior of the Q statistic discussed in Chapter 8, the modified statistic, $\tilde{S} = m(m+2)\sum_{k=0}^{K}(m-k)^{-1}r_{\alpha\hat{a}}^2(k)$, might be suggested for use in practice because it may more accurately approximate the χ^2 distribution under the null model, although detailed investigations of its performance have not been made (however, see empirical results in Poskitt and Tremayne, 1981).

12.4 SOME EXAMPLES OF FITTING AND CHECKING TRANSFER FUNCTION MODELS

12.4.1 Fitting and Checking of the Gas Furnace Model

We now illustrate the approach described in Section 12.2 to the fitting of the model

$$Y_t = \frac{\omega_0 - \omega_1 B - \omega_2 B^2}{1 - \delta_1 B - \delta_2 B^2} X_{t-3} + \frac{1}{1 - \phi_1 B - \phi_2 B^2} a_t$$

which was identified for the gas furnace data in Sections 12.2.2 and 12.2.3.

Nonlinear Estimation. Using the initial estimates $\hat{\omega}_0 = -0.53, \hat{\omega}_1 = 0.33, \hat{\omega}_2 = 0.51, \hat{\delta}_1 = 0.57, \hat{\delta}_2 = 0.02, \hat{\phi}_1 = 1.54$, and $\hat{\phi}_2 = -0.64$ derived in Sections 12.2.2 and 12.2.3 with the conditional least-squares algorithm described in Section 12.3.2, least-squares values, to two decimals, were achieved in four iterations. However, to test whether the results would converge in much less favorable circumstances, Table 12.3 shows the iterations produced with all starting values taken to be either $+0.1$ or -0.1. The fact that, even then, convergence was achieved in 10 iterations with as many as seven parameters in the model is encouraging.

The last line in Table 12.3 shows the rough preliminary estimates obtained at the identification stage in Sections 12.2.2 and 12.2.3. It is seen that for this example, they are in close agreement with the least-squares estimates given on the previous line. Thus, the final fitted transfer function model is

$$\begin{array}{rcl} (1 - 0.57B - 0.01B^2)Y_t & = & -(0.53 + 0.37B + 0.51B^2)X_{t-3} \\ (\pm 0.21)(\pm 0.14) & & (\pm 0.08)(\pm 0.15)(\pm 0.16) \end{array} \qquad (12.4.1)$$

and the fitted noise model is

$$\begin{array}{c} (1 - 1.53B + 0.63B^2)N_t = a_t \\ (\pm 0.05)(\pm 0.05) \end{array} \qquad (12.4.2)$$

with $\hat{\sigma}_a^2 = 0.0561$, where the limits in parentheses are the ± 1 standard error limits obtained from the nonlinear least-squares estimation procedure.

Diagnostic Checking. Before accepting the model above as an adequate representation of the system, autocorrelation and cross-correlation checks should be applied, as described in Section 12.3.4. The first 36 lags of the residual autocorrelations are given in Table 12.4(a) and plotted in Figure 12.6(a), together with their approximate two standard error limits

TABLE 12.3 Convergence of Nonlinear Least-Squares Fit of Gas Furnace Data

Iteration	ω_0	ω_1	ω_2	δ_1	δ_2	ϕ_1	ϕ_2	Sum of Squares
0	0.10	−0.10	−0.10	0.10	0.10	0.10	0.10	13,601.00
1	−0.46	0.63	0.60	0.14	0.27	1.33	−0.27	273.10
2	−0.52	0.45	0.31	0.40	0.52	1.37	−0.43	92.50
3	−0.63	0.60	0.01	0.12	0.73	1.70	−0.76	31.80
4	−0.54	0.50	0.29	0.24	0.42	1.70	−0.81	19.70
5	−0.50	0.31	0.51	0.63	0.09	1.56	−0.68	16.84
6	−0.53	0.38	0.53	0.54	0.01	1.54	−0.64	16.60
7	−0.53	0.37	0.51	0.56	0.01	1.53	−0.63	16.60
8	−0.53	0.37	0.51	0.56	0.01	1.53	−0.63	16.60
9	−0.53	0.37	0.51	0.57	0.01	1.53	−0.63	16.60
Preliminary estimates	−0.53	0.33	0.51	0.57	0.02	1.54	−0.64	

$\pm 2/\sqrt{m} \simeq 0.12$ ($m = 289$) under the assumption that the model is adequate. There seems to be no evidence of model inadequacy from the behavior of individual autocorrelations. This is confirmed by calculating the $\tilde{Q}$ criterion in (12.3.18a), which is

$$\tilde{Q} = (289)(291)\sum_{k=1}^{36}(289-k)^{-1}r_{\hat{a}\hat{a}}^2(k) = 43.8$$

Comparison of $\tilde{Q}$ with the χ^2 table for $K - p - q = 36 - 2 - 0 = 34$ degrees of freedom provides no grounds for questioning model adequacy.

The first 36 lags of the cross-correlation function $r_{x\hat{a}}(k)$ between the input X_t and the residuals $\hat{a}_t$ are given Table 12.4(b) and shown in Figure 12.6(b), together with their approximate two standard error limits $\pm 2/\sqrt{m}$. It is seen that although the cross-correlations $r_{x\tilde{a}}(k)$ do not exceed their two standard error limits, they are themselves highly autocorrelated. This is to be expected because as indicated by (12.3.19), the estimated cross-correlations follow the same stochastic process as does the input X_t, and as we have already seen, for this example the input was highly autocorrelated.

The corresponding cross-correlations between the prewhitened input α_t and the residuals $\hat{a}_t$ are given in Table 12.4(c) and shown in Figure 12.6(c). The $\tilde{S}$ criterion yields

$$\tilde{S} = (289)(291)\sum_{k=0}^{35}(289-k)^{-1}r_{a\hat{a}}^2(k) = 32.1$$

Comparison of $\tilde{S}$ with the X^2 table for $K + 1 - (r + s + 1) = 36 - 5 = 31$ degrees of freedom again provides no evidence that the model is inadequate.

Parameter Estimation Using R. We will now use the R software to fit the model employed in (12.4.1) and (12.4.2) to the gas furnace data. The parameter estimation can be performed using the function tfm1() in the MTS package developed for multivariate time series analysis. The arguments of this function are tfm1(Y, X,orderX=c(r,s,b),orderN=c(p,d,q)). The function call and the resulting output are shown below:

TABLE 12.4 Estimated Autocorrelation and Cross-Correlation Functions of Residuals from Fitted Gas Furnace Model

Lag k					(a) Autocorrelation $r_{\hat{a}\hat{a}}(k)$								Upper Bound to Standard Error
1–12	0.02	0.06	−0.07	−0.05	−0.05	0.12	0.03	0.03	−0.08	0.05	0.02	0.10	±0.06
13–24	−0.04	0.05	−0.09	−0.01	−0.08	0.00	−0.12	0.00	−0.01	0.08	0.02	−0.01	±0.06
25–36	0.04	−0.02	0.02	0.09	−0.12	0.06	−0.03	−0.06	0.11	0.02	0.03	0.06	±0.06
					(b) $r_{x\hat{a}}(k)$ between the input and the output residuals								
0–11	0.00	0.00	0.00	0.00	0.00	0.00	−0.01	−0.02	−0.03	−0.05	−0.06	−0.05	±0.06
12–23	−0.03	−0.03	−0.03	−0.07	−0.10	−0.12	−0.12	−0.10	−0.04	−0.01	−0.01	−0.02	±0.06
24–35	−0.03	−0.04	−0.04	−0.02	−0.01	0.02	0.04	0.05	0.06	0.07	0.07	0.06	±0.06
					(c) $r_{u\hat{a}}(k)$ between the prewhitened input and the output residuals								
0–11	−0.06	0.03	−0.01	0.00	0.01	0.01	0.01	−0.04	0.02	0.07	−0.03	−0.02	±0.06
12–23	−0.03	−0.11	0.02	0.04	0.04	0.01	0.01	−0.15	−0.03	−0.07	−0.08	0.02	±0.06
24–35	−0.01	0.02	0.05	−0.07	0.00	0.04	−0.15	0.04	0.03	−0.02	0.00	−0.03	±0.06

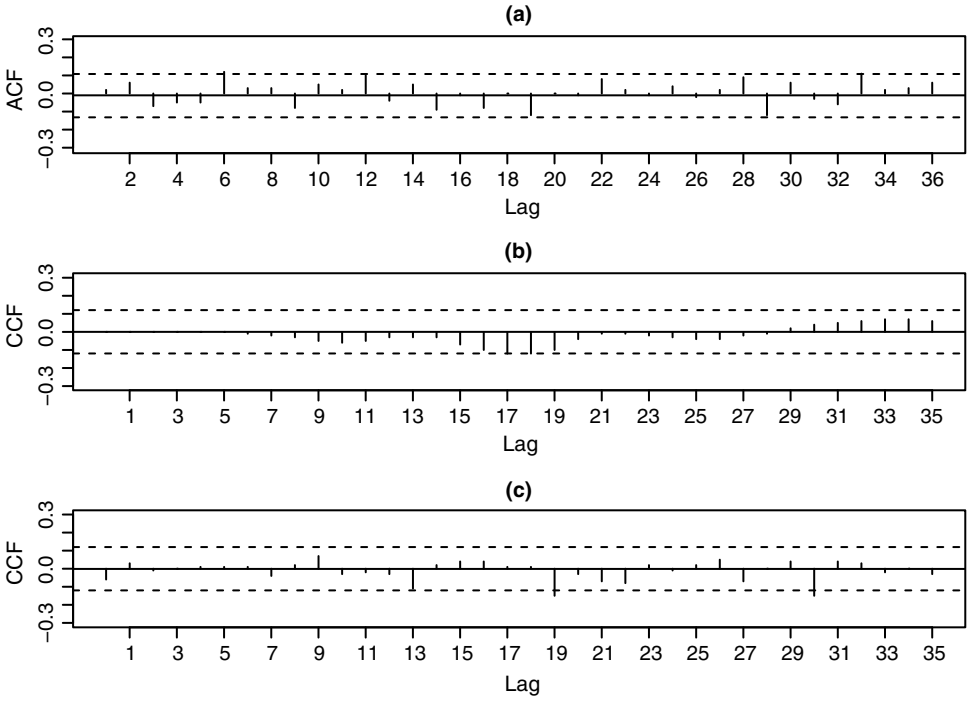

FIGURE 12.6 (a) Estimated autocorrelations of the residuals $r_{\hat{a}\hat{a}}(k)$ from the fitted gas furnace model, (b) estimated cross-correlations $r_{x\hat{a}}(k)$ between the input and the output residuals $r_{x\hat{a}}(k)$, and (c) estimated cross-correlations $r_{\alpha\hat{a}}(k)$ between the prewhitened input and the output residuals.

```
>  library(MTS)
>  m1=tfm1(Y,X,orderX=c(2,2,3),orderN=c(2,0,0))
   Model Output:
     Delay:  3
     Transfer function coefficients & s.e.:
     in the order: constant, omega, and delta: 1 3 2
         [,1]    [,2]   [,3]   [,4]  [,5]    [,6]
  v    53.371 -0.5302 -0.371 -0.511 0.565 -0.0119
  se.v  0.142  0.0745  0.146  0.149 0.200  0.1415
  ARMA order: [1] 2 0 0
  ARMA coefficients & s.e.:
              [,1]    [,2]
  coef.arma 1.5315 -0.6321
  se.arma   0.0472  0.0502

>  names(m1)    % check contents of output
     [1] "estimate"  "sigma2"  "residuals" "varcoef" "Nt"
>  m1$sigma2
     [1] 0.0576   % residual variance
>  acf(m1$residuals)       % acf of the residuals
>  ccf(m1$residuals,X)     % cross-correlation
```

```
            between input series and residuals
>  ccf(m1$residuals,xprev) % cross-correlation
            between prewhitened input and residuals
```

Using the output from R and allowing for sign differences in the definition of $\omega(B)$, the estimated transfer function–noise model is

$$Y_t = \frac{-(0.53 + 0.37B + 0.51B^2)}{1 - 0.57B + 0.01B^2}X_{t-3} + \frac{1}{1 - 1.53B + 0.63B^2}a_t$$

We see that the parameter estimates for the transfer function and noise models are nearly identical to those shown in (12.4.1) and (12.4.2). The estimate of the residual variance is 0.0576, which is also close to the value 0.0561 quoted in the text. In addition, the residual autocorrelations, the cross-correlations between the input X_t and the residuals, and the cross-correlations between the prewhitened input and the residuals (not shown) were small and close to those displayed in Figure 12.6 although some minor differences were seen in the patterns.

Step and Impulse Responses. The estimate $\hat{\delta}_2 = 0.01$ in (12.4.1) is very small compared with its standard error ± 0.14, and the parameter δ_2 can in fact be omitted from the model without affecting the estimates of the remaining parameters to the accuracy considered. The final form of the combined transfer function–noise model for the gas furnace data is

$$Y_t = \frac{-(0.53 + 0.37B + 0.51B^2)}{1 - 0.57B}X_{t-3} + \frac{1}{1 - 1.53B + 0.63B^2}a_t$$

The step and impulse response functions corresponding to the transfer function model

$$(1 - 0.57B)Y_t = -(0.53 + 0.37B + 0.51B^2)X_{t-3}$$

are given in Figure 12.7. Using (11.2.5), the steady-state gain of the coded data is

$$g = \frac{-(0.53 + 0.37 + 0.51)}{1 - 0.57} = -3.3$$

The results agree very closely with those obtained by cross-spectral analysis (Jenkins and Watts, 1968).

Choice of Sampling Interval. When a choice is available, the sampling interval should be taken as fairly short compared with the time constants expected for the system. When in doubt, the analysis can be repeated with several trial sampling intervals. In the choice of sampling interval, it is the noise at the output that is important, and its variance should approach a minimum value as the interval is shortened. Thus, in the gas furnace example that we have used for illustration, a pen recorder was used to provide a continuous record of input and output. The discrete data that we have actually analyzed were obtained by reading off values from this continuous record at points separated by 9-second intervals. This interval was chosen because inspection of the traces shown in Figure 12.1 suggested that it ought to be adequate to allow all the variation (apart from slight pen chatter) that occurred in input and output to be taken account of. The use of this kind of common sense is usually a reliable guide in choosing the interval. The estimated mean square error for the gas furnace data, obtained by dividing $\sum_t (Y_t - \hat{Y}_t)^2$ by the appropriate number of

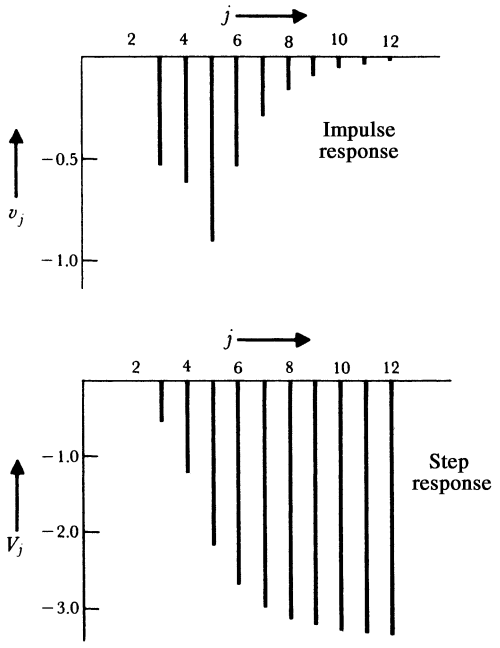

FIGURE 12.7 Impulse and step responses for transfer function model $(1 - 0.57B)Y_t = -(0.53 + 0.37B + 0.51B^2)X_{t-3}$ fitted to coded gas furnace data.

TABLE 12.5 Mean Square Error at the Output for Various Choices of the Sampling Interval for Gas Furnace Data

	Interval (Seconds)						
	9	18	27	36	45	54	72
Number of data points N	296	148	98	74	59	49	37
MS error	0.71	0.78	0.74	0.95	0.97	1.56	7.11

degrees of freedom, is shown for various time intervals in Table 12.5. These values are also plotted in Figure 12.8. Little change in mean square error occurs until the interval is almost 40 seconds, when a very rapid rise occurs. There is little difference in the mean square error, or indeed the plotted step response, for the 9-, 18-, and 27-second intervals, but a considerable change occurs when the 36-second interval is used. It will be seen that the 9-second interval we have used in this example is, in fact, conservative.

12.4.2 Simulated Example with Two Inputs

The fitting of models involving more than one input series involves no difficulty in principle, except for the increase in the number of parameters that has to be handled. For example, for two inputs we can write the model as

$$y_t = \delta_1^{-1}(B)\omega_1(B)x_{1,t-b_1} + \delta_2^{-1}(B)\omega_2(B)x_{2,t-b_2} + n_t$$

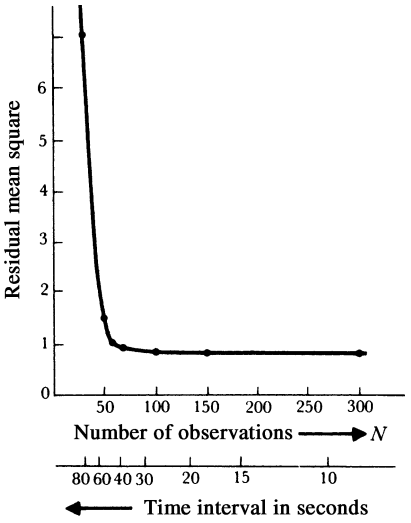

FIGURE 12.8 Mean square error at the output for various choices of sampling interval.

with

$$n_t = \phi^{-1}(B)\theta(B)a_t$$

where $y_t = \nabla^d Y_t$, $x_{1,t} = \nabla^d X_{1,t}$, $x_{2,t} = \nabla^d X_{2,t}$, and $n_t = \nabla^d N_t$ are stationary processes. To compute the a_t's, we first calculate for specific values of the parameters $b_1, \boldsymbol{\delta}_1, \boldsymbol{\omega}_1$,

$$y_{1,t} = \delta_1^{-1}(B)\omega_1(B)x_{1,t-b_1} \tag{12.4.3}$$

and for specific values of $b_2, \boldsymbol{\delta}_2, \boldsymbol{\omega}_2$,

$$y_{2,t} = \delta_2^{-1}(B)\omega_2(B)x_{2,t-b_2} \tag{12.4.4}$$

Then the noise n_t can be calculated from

$$n_t = y_t - y_{1,t} - y_{2,t} \tag{12.4.5}$$

and finally, a_t from

$$a_t = \theta^{-1}(B)\phi(B)n_t \tag{12.4.6}$$

Simulated Example. It is clear that even simple situations can lead to the estimation of a large number of parameters. The example below, with two input variables and delayed first-order models, has eight unknown parameters. To illustrate the behavior of the iterative nonlinear least-squares procedure described in Section 12.3.2 when used to obtain estimates of the parameters in such models, an experiment was performed using manufactured data, details of which are given in Box et al. (1967b). The data were generated from the model written in ∇ form as

$$Y_t = \beta + g_1 \frac{1 + \eta_1 \nabla}{1 + \xi_1 \nabla} X_{1,t-1} + g_2 \frac{1 + \eta_2 \nabla}{1 + \xi_2 \nabla} X_{2,t-1} + \frac{1}{1 - \phi_1 B} a_t \tag{12.4.7}$$

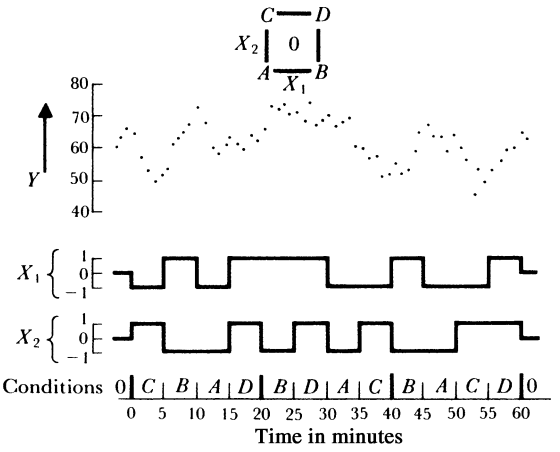

FIGURE 12.9 Data for simulated two-input example (Series K).

with $\beta = 60, g_1 = 13.0, \eta_1 = -0.6, \xi_1 = 4.0, g_2 = -5.5, \eta_2 = -0.6, \xi_2 = 4.0, \phi_1 = 0.5$, and $\sigma_a^2 = 9.0$. The input variables X_1 and X_2 were changed according to a randomized 2^2 factorial design replicated three times. Each input condition was supposed to be held fixed for 5 minutes and output observations taken every minute. The data are plotted in Figure 12.9 and appear as Series K in the Collection of Time Series section in Part Five.

The constrained iterative nonlinear least-squares program, described in Chapter 7, was used to obtain the least-squares estimates, so that it was only necessary to set up the calculation of the a_t's. Thus, for specified values of the parameters $g_1, g_2, \xi_1, \xi_2, \eta_1$, and η_2, the values $y_{1,t}$ and $y_{2,t}$ can be obtained from

$$(1 + \xi_1 \nabla) y_{1,t} = g_1 (1 + \eta_1 \nabla) X_{1,t-1}$$
$$(1 + \xi_2 \nabla) y_{2,t} = g_2 (1 + \eta_2 \nabla) X_{2,t-1}$$

and can be used to calculate

$$N_t = Y_t - y_{1,t} - y_{2,t}$$

Finally, for a specified value of ϕ_1, a_t can be calculated from

$$a_t = N_t - \phi_1 N_{t-1}$$

It was assumed that the process inputs had been maintained at their center conditions for some time before the start of the experiment, so that $y_{1,t}, y_{2,t}$, and N_t may be computed from $t = 0$ onward and a_t from $t = 1$.

Two runs were made of the nonlinear least-squares procedure using two different sets of initial values. In the first, the parameters were chosen as representing what a person reasonably familiar with the process might guess for initial values. In the second, the starting value for β was chosen to be the sample mean $\overline{Y}$ of all observations and all other starting values were set equal to 0.1. Thus, the second run represents a much more extreme situation than would normally arise in practice. Convergence with the first set of initial values occurred after five iterations, while convergence with the second set occurred

after nine iterations. These results suggest that in realistic circumstances, multiple inputs can be handled without serious estimation difficulties.

12.5 FORECASTING WITH TRANSFER FUNCTION MODELS USING LEADING INDICATORS

Frequently, forecasts of a time series $Y_t, Y_{t-1}, \ldots$ may be considerably improved by using information coming from some associated series $X_t, X_{t-1}, \ldots$. This is particularly true if changes in Y tend to be *anticipated* by changes in X, in which case economists call X a ''leading indicator'' for Y.

To obtain an optimal forecast using information from both series Y_t and X_t, we first build a transfer function–noise model connecting the series Y_t and X_t in the manner already outlined. Suppose, using previous notations, that an adequate model is

$$Y_t = \delta^{-1}(B)\omega(B)X_{t-b} + \varphi^{-1}(B)\theta(B)a_t \quad b \geq 0 \tag{12.5.1}$$

In general, the noise component of this model, which is assumed statistically independent of the input X_t, is nonstationary with $\varphi(B) = \phi(B)\nabla^d$, so that if $y_t = \nabla^d Y_t$ and $x_t = \nabla^d X_t$,

$$y_t = \delta^{-1}(B)\omega(B)X_{t-b} + \phi^{-1}(B)\theta(B)a_t$$

Also, we will assume that an adequate stochastic model for the input or leading series X_t is

$$X_t = \varphi_x^{-1}(B)\theta_x(B)\alpha_t \tag{12.5.2}$$

so that with $\varphi_x(B) = \phi_x(B)\nabla^d$,

$$x_t = \phi_x^{-1}(B)\theta_x(B)\alpha_t$$

12.5.1 Minimum Mean Square Error Forecast

Now (12.5.1) may be written as

$$Y_t = \upsilon(B)\alpha_t + \psi(B)a_t \tag{12.5.3}$$

with the a_t's and the α_t's statistically independent white noise, and

$$\upsilon(B) = \delta^{-1}(B)\omega(B)B^b\varphi_x^{-1}(B)\theta_x(B)$$

Arguing as in Section 5.1.1, suppose that the forecast $\hat{Y}_t(l)$ of Y_{t+l} made at origin t is of the form

$$\hat{Y}_t(l) = \sum_{j=0}^{\infty} \nu_{l+j}^0 \alpha_{t-j} + \sum_{j=0}^{\infty} \psi_{l+j}^0 a_{t-j}$$

Then

$$Y_{t+l} - \hat{Y}_t(l) = \sum_{i=0}^{l-1}(\nu_i \alpha_{t+l-i} + \psi_i a_{t+l-i}) + \sum_{j=0}^{\infty}[(\nu_{l+j} - \nu_{l+j}^0)\alpha_{t-j} + (\psi_{l+j} - \psi_{l+j}^0)a_{t-j}]$$

and

$$E[(Y_{t+l} - \hat{Y}_t(l))^2] = (\nu_0^2 + \nu_1^2 + \cdots + \nu_{l-1}^2)\sigma_\alpha^2 + (1 + \psi_1^2 + \cdots + \psi_{l-1}^2)\sigma_a^2 + \sum_{j=0}^{\infty}[(\nu_{l+j} - \nu_{l+j}^0)^2\sigma_\alpha^2 + (\psi_{l+j} - \psi_{l+j}^0)^2\sigma_a^2]$$

which is minimized only if $\upsilon_{l+j}^0 = \upsilon_{l+j}$ and $\psi_{l+j}^0 = \psi_{l+j}$ for $j = 0, 1, 2 \ldots$. Thus, the minimum mean square error forecast $\hat{Y}_t(l)$ of Y_{t+l} at origin t is given by the conditional expectation of Y_{t+l} at time t, based on the past history of information on *both* series Y_t and X_t through time t. Theoretically, this expectation is conditional on knowledge of the series from the infinite past up to the present origin t. As in Chapter 5, such results are of practical use because, usually, the forecasts depend appreciably only on *recent* past values of the series X_t and Y_t.

Computation of the Forecast. Now (12.5.1) may be written as

$$\varphi(B)\delta(B)Y_t = \varphi(B)\omega(B)X_{t-b} + \delta(B)\theta(B)a_t$$

which we will write as

$$\delta^*(B)Y_t = \omega^*(B)X_{t-b} + \theta^*(B)a_t$$

Then, using square brackets to denote conditional expectations at time t, and writing $p^* = p + d$, we have for the lead l forecast

$$\begin{aligned}\hat{Y}_t(l) = [Y_{t+l}] = {} & \delta_1^*[Y_{t+l-1}] + \cdots + \delta_{p^*+r}^*[Y_{t+l-p^*-r}] + \omega_0^*[X_{t+l-b}] \\ & - \cdots - \omega_{p^*+s}^*[X_{t+l-b-p^*-s}] + [a_{t+l}] - \theta_1^*[a_{t+l-1}] \\ & - \cdots - \theta_{q+r}^*[a_{t+l-q-r}]\end{aligned} \tag{12.5.4}$$

where

$$[Y_{t+j}] = \begin{cases} Y_{t+j} & j \le 0 \\ \hat{Y}_t(j) & j > 0 \end{cases}$$

$$[X_{t+j}] = \begin{cases} X_{t+j} & j \le 0 \\ \hat{X}_t(j) & j > 0 \end{cases} \tag{12.5.5}$$

$$[a_{t+j}] = \begin{cases} a_{t+j} & j \le 0 \\ 0 & j > 0 \end{cases}$$

and a_t is calculated from (12.5.1), which if $b \geq 1$ is equivalent to

$$a_t = Y_t - \hat{Y}_{t-1}(1)$$

Thus, by appropriate substitutions, the minimum mean square error forecast is readily computed directly using (12.5.4) and (12.5.5). The forecasts $\hat{X}_t(j)$ are obtained in the usual way (see Section 5.2) utilizing the univariate ARIMA model (12.5.2) for the input series X_t.

It is important to note that the conditional expectations in (12.5.4) and (12.5.5) are taken with respect to values in *both* series Y_t and X_t through time t, but because of the assumed independence between input X_t and noise N_t in (12.5.1), it follows in particular that we will have

$$\hat{X}_t(j) = E[X_{t+j}|X_t, X_{t-1}, \ldots, Y_t, Y_{t-1}, \ldots] = E[X_{t+j}|X_t, X_{t-1}, \ldots]$$

That is, given the past values of the input series X_t, the optimal forecasts of its future values depend only on the past X's and cannot be improved by the additional knowledge of the past Y's; hence, the optimal values $\hat{X}_t(j)$ can be obtained directly from the univariate model (12.5.2).

Variance of the Forecast Error. The v_j weights and the ψ_j weights of (12.5.3) may be obtained explicitly by equating coefficients in

$$\delta(B)\varphi_x(B)v(B) = \omega(B)\theta_x(B)B^b$$

and in

$$\varphi(B)\psi(B) = \theta(B)$$

The variance of the lead l forecast error is then given by

$$V(l) = E[(Y_{t+l} - \hat{Y}_t(l))^2] = \sigma_\alpha^2 \sum_{j=b}^{l-1} v_j^2 + \sigma_a^2 \sum_{j=0}^{l-1} \psi_j^2 \tag{12.5.6}$$

Forecasts as a Weighted Aggregate of Previous Observations. For any given example, it is instructive to consider precisely how the forecasts of future values of the series Y_t utilize the previous values of the X_t and Y_t series. We have seen in Section 5.3.3 how the forecasts may be written as linear aggregates of previous values of the series. Thus, for forecasts of the input or leading indicator, we could write

$$\hat{X}_t(l) = \sum_{j=1}^{\infty} \pi_j^{(l)} X_{t+1-j} \tag{12.5.7}$$

The weights $\pi_j^{(1)} = \pi_j$ arise when the model (12.5.2) is written in the infinite autoregressive form

$$\alpha_t = \theta_x^{-1}(B)\varphi_x(B)X_t = X_t - \pi_1 X_{t-1} - \pi_2 X_{t-2} - \cdots$$

and may thus be obtained by explicitly equating coefficients in

$$\varphi_x(B) = (1 - \pi_1 B - \pi_2 B^2 - \cdots)\theta_x(B)$$

Also, using (5.3.9),

$$\pi_j^{(l)} = \pi_{j+l-1} + \sum_{h=1}^{l-1} \pi_h \pi_j^{(l-h)} \tag{12.5.8}$$

In a similar way, we can write the transfer function model (12.5.1) in the form

$$a_t = Y_t - \sum_{j=1}^{\infty} P_j Y_{t-j} - \sum_{j=0}^{\infty} Q_j X_{t-j} \tag{12.5.9}$$

It should be noted that if the transfer function between the input or leading indicator series X_t and the output Y_t is such that $b > 0$, then $\nu_j = 0$ for $j < b$, and so $Q_0, Q_1, \ldots, Q_{b-1}$ in (12.5.9) will also be zero.

Now (12.5.9) may be written as

$$a_t = \left(1 - \sum_{j=1}^{\infty} P_j B^j\right) Y_t - \left(\sum_{j=0}^{\infty} Q_j B^j\right) X_t$$

Comparison with (12.5.1) shows that the P_j and Q_j weights may be obtained by equating coefficients in the expressions

$$\theta(B)\left(1 - \sum_{j=1}^{\infty} P_j B^j\right) = \varphi(B)$$

$$\theta(B)\delta(B)\left(\sum_{j=0}^{\infty} Q_j B^j\right) = \varphi(B)\omega(B)B^b$$

On substituting $t + l$ for t in (12.5.9), and taking conditional expectations at origin t, we have the lead l forecast in the form

$$\hat{Y}_t(l) = \sum_{j=1}^{\infty} P_j[Y_{t+l-j}] + \sum_{j=0}^{\infty} Q_j[X_{t+l-j}] \tag{12.5.10}$$

Now the lead 1 forecast is $\hat{Y}_t(1) = \Sigma_{j=1}^{\infty} P_j Y_{t+1-j} + Q_0[X_{t+1}] + \Sigma_{j=1}^{\infty} Q_j X_{t+1-j}$, which for $b > 0$ becomes

$$\hat{Y}_t(1) = \sum_{j=1}^{\infty} P_j Y_{t+1-j} + \sum_{j=1}^{\infty} Q_j X_{t+1-j}$$

Also, the quantities in square brackets in (12.5.10) are either known values of the X_t and Y_t series or forecasts that are linear functions of these known values.

Thus, we can write the lead l forecast in terms of the values of the series that have already occurred at time t in the form

$$\hat{Y}_t(l) = \sum_{j=1}^{\infty} P_j^{(l)} Y_{t+1-j} + \sum_{j=1}^{\infty} Q_j^{(l)} X_{t+1-j} \tag{12.5.11}$$

where, for $b > 0$, the coefficients $P_j^{(l)}$ and $Q_j^{(l)}$ may be computed recursively as follows:

$$\begin{aligned} P_j^{(1)} &= P_j \qquad Q_j^{(1)} = Q_j \\ P_j^{(l)} &= P_{j+l-1} + \sum_{h=1}^{l-1} P_h P_j^{(l-h)} \\ Q_j^{(l)} &= Q_{j+l-1} + \sum_{h=1}^{l-1} \left\{ P_h Q_j^{(l-h)} + Q_h \pi_j^{(l-h)} \right\} \end{aligned} \tag{12.5.12}$$

12.5.2 Forecast of CO_2 Output from Gas Furnace

For illustration, consider the gas furnace data shown in Figure 12.1. For this example, the fitted model (see Section 12.4.1) was

$$Y_t = \frac{-(0.53 + 0.37B + 0.51B^2}{1 - 0.57B} X_{t-3} + \frac{1}{1 - 1.53B + 0.63B^2} a_t$$

and $(1 - 1.97B + 1.37B^2 - 0.34B^3)X_t = \alpha_t$. The forecast function, written in the form (12.5.4), is thus

$$\begin{aligned} \hat{Y}_t(l) = [Y_{t+l}] = {} & 2.1[Y_{t+l-1}] - 1.5021[Y_{t+l-2}] + 0.3591[Y_{t+l-3}] \\ & - 0.53[X_{t+l-3}] + 0.4409[X_{t+l-4}] - 0.2778[X_{t+l-5}] \\ & + 0.5472[X_{t+l-6}] - 0.3213[X_{t+l-7}] \\ & + [a_{t+l}] - 0.57[a_{t+l-1}] \end{aligned}$$

Figure 12.10 shows the forecasts for lead times $l = 1, 2, \ldots, 12$ made at origin $t = 206$. The π_j, P_j, and Q_j weights for the model are given in Table 12.6.

Figure 12.10 shows the weights $P_j^{(5)}$ and $Q_j^{(5)}$ appropriate to the lead 5 forecast. The weights ν_i and ψ_i of (12.5.3) are listed in Table 12.7. Using estimates $\hat{\sigma}_\alpha^2 = 0.0353$ and $\hat{\sigma}_a^2 = 0.0561$, obtained in Sections 12.2.2 and 12.4.1, respectively, (12.5.6) may be employed to obtain variances of the forecast errors and the 50 and 95% probability limits shown in Figure 12.10.

To illustrate the advantages of using an input or leading indicator series X_t in forecasting, assume that only the Y_t series is available. The usual identification and fitting procedure

TABLE 12.6 π_j, P_j, and Q_j Weights for Gas Furnace Model

j	π_j	P_j	Q_j	j	π_j	P_j	Q_j
1	1.97	1.53	0	7	0	0	−0.07
2	−1.37	−0.63	0	8	0	0	−0.04
3	0.34	0	−0.53	9	0	0	−0.02
4	0	0	0.14	10	0	0	−0.01
5	0	0	−0.20	11	0	0	−0.01
6	0	0	0.43				

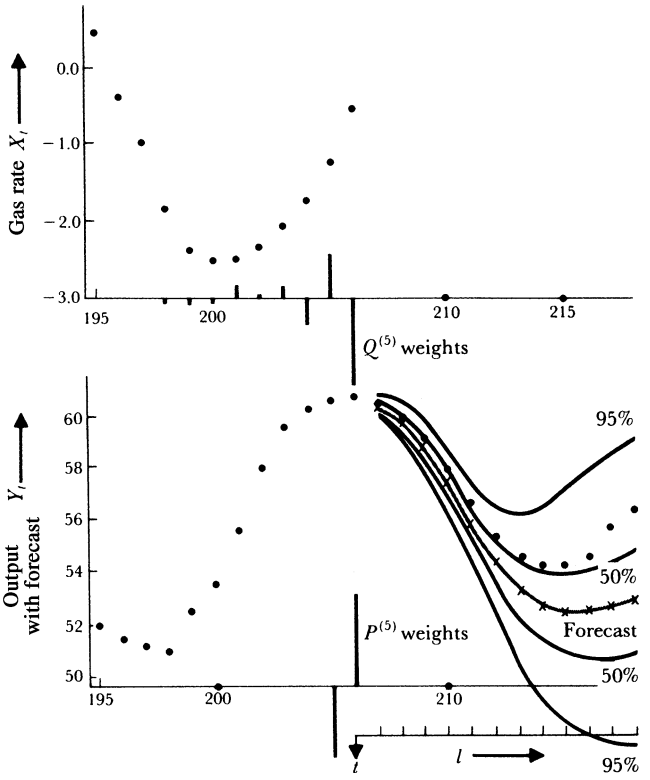

FIGURE 12.10 Forecast of CO_2 output from a gas furnace using input and output series.

TABLE 12.7 ν_i and ψ_i Weights for Gas Furnace Model

i	ν_i	ψ_i	i	ν_i	ψ_i
0	0	1	6	−5.33	0.89
1	0	1.53	7	−6.51	0.62
2	0	1.71	8	−6.89	0.39
3	−0.53	1.65	9	−6.57	0.20
4	−1.72	1.45	10	−5.77	0.06
5	−3.55	1.18	11	−4.73	−0.03

applied to this series indicated that it is well described by an ARMA(4, 2) process,

$$(1 - 2.42B + 2.388B^2 - 1.168B^3 + 0.23B^4)Y_t = (1 - 0.31B + 0.47B^2)\varepsilon_t$$

with $\sigma_\varepsilon^2 = 0.1081$. Table 12.8 shows estimated standard deviations of forecast errors made with and without the leading indicator series X_t. As might be expected, for short lead times use of the leading indicator can produce forecasts of considerably greater accuracy.

Univariate Modeling Check. To further confirm the univariate modeling results for the series Y_t, we can use results from Appendix A4.3 to obtain the nature of the univariate

TABLE 12.8 Estimated Standard Deviations of Forecast Errors Made With and Without the Leading Indicator for Gas Furnace Data

l	With Leading Indicator	Without Leading Indicator	l	With Leading Indicator	Without Leading Indicator
1	0.23	0.33	7	1.52	2.74
2	0.43	0.77	8	1.96	2.86
3	0.59	1.30	9	2.35	2.95
4	0.72	1.82	10	2.65	3.01
5	0.86	2.24	11	2.87	3.05
6	1.12	2.54	12	3.00	3.08

ARIMA model for Y_t that is implied by the transfer function–noise model between Y_t and X_t and the univariate AR(3) model for X_t. These models imply that

$$\begin{aligned}&(1-0.57B)(1-1.53B+0.63B^2)Y_t\\&=-(0.53+0.37B+0.51B^2)(1-1.53B+0.63B^2)X_{t-3}\\&\quad+(1-0.57B)a_t\end{aligned}\tag{12.5.13}$$

But since

$$\varphi_x(B)=1-1.97B+1.37B^2-0.34B^3\simeq(1-1.46B+0.60B^2)(1-0.52B)$$

in the AR(3) model for X_t, the right-hand side of (12.5.13) reduces approximately to $-(0.53+0.37B+0.51B^2)(1-0.52B)^{-1}\alpha_{t-3}+(1-0.57B)a_t$, and hence we obtain

$$\begin{aligned}&(1-0.52B)(1-0.57B)(1-1.53B+0.63B^2)Y_t\\&\quad=-(0.53+0.37B+0.51B^2)\alpha_{t-3}+(1-0.52B)(1-0.57B)a_t\end{aligned}$$

The results of Appendix A4.3 imply that the right-hand side of this last equation has an MA(2) model representation as $(1-\theta_1B-\theta_2B^2)\epsilon_t$, and the nonzero autocovariances of the MA(2) are determined from the right-hand side expression above to be

$$\lambda_0=0.1516\qquad\lambda_1=-0.0657\qquad\lambda_2=0.0262$$

Hence, the implied univariate model for Y_t would be ARMA(4, 2), with approximate AR operator equal to $(1-2.62B+2.59B^2-1.14B^3+0.19B^4)$, and from methods of Appendix A6.2, the MA(2) operator would be $(1-0.44B+0.21B^2)$, with $\sigma_\epsilon^2=0.1220$; that is, the univariate model for Y_t would be

$$(1-2.62B+2.59B^2-1.14B^3+0.19B^4)Y_t=(1-0.44B+0.21B^2)\epsilon_t$$

This model result is in good agreement with the univariate model actually identified and fitted to the series Y_t, which gives an additional check and provides further support to the transfer function–noise model that has been specified for the gas furnace data.

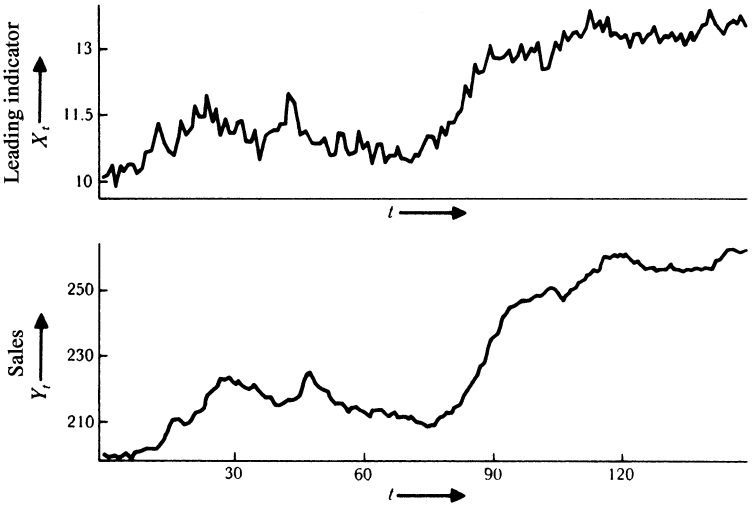

FIGURE 12.11 Sales data with leading indicator.

12.5.3 Forecast of Nonstationary Sales Data Using a Leading Indicator

As a second illustration, consider the data on sales Y_t in relation to a leading indicator X_t, plotted in Figure 12.11 and listed as Series M in the Collection of Time Series section in Part Five. The data are typical of that arising in business forecasting and are well fitted by the nonstationary model[3]

$$y_t = 0.035 + \frac{4.82}{1 - 0.72B} x_{t-3} + (1 - 0.54B)a_t$$
$$x_t = (1 - 0.32B)\alpha_t$$

with y_t and x_t first differences of the series. The forecast function, in the form (12.54), is then

$$\begin{aligned}\hat{Y}_t(l) = [Y_{t+l}] = 1.72[Y_{t+l-1}] - 0.72[Y_{t+l-2}] + 0.0098 + 4.82[X_{t+l-3}] \\ - 4.82[X_{t+l-4}] + [a_{t+l}] - 1.26[a_{t+l-1}] \\ + 0.3888[a_{t+l-2}]\end{aligned}$$

Figure 12.12 shows the forecasts for lead times $l = 1, 2, \ldots, 12$ made at origin $t = 89$. The weights ν_j and ψ_j are given in Table 12.9.

Using the estimates $\hat{\sigma}_\alpha^2 = 0.0676$ and $\hat{\sigma}_a^2 = 0.0484$, obtained in fitting the above model, the variance of the forecast error may be found from (12.5.6). In particular, $V(l) = \sigma_a^2 \Sigma_{j=0}^{l-1} \psi_j^2$ for $l = 1, 2$, and 3 in this specific case (note the delay of $b = 3$ in the transfer function model). The 50 and 95% probability limits are shown in Figure 12.12. It will be seen that in this particular example, the use of the leading indicator allows very accurate forecasts to be obtained for lead times $l = 1, 2$, and 3.

The π_j, P_j, and Q_j weights for this model are given in Table 12.10. The weights $p_j^{(5)}$ and $Q_j^{(5)}$ appropriate to the lead 5 forecast are shown in Figure 12.12.

[3]Using data the latter part of which is listed as Series M.

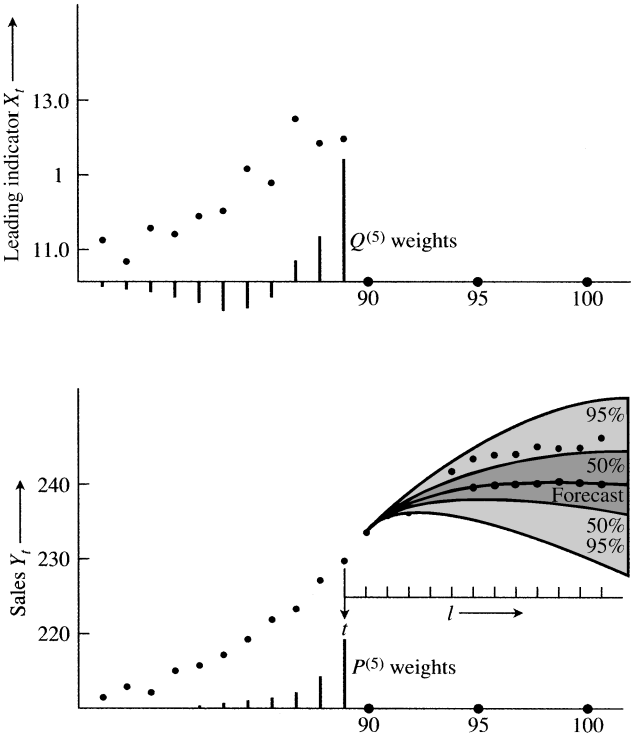

FIGURE 12.12 Forecast of sales at origin $t = 89$ with P and Q weights for lead 5 forecast.

TABLE 12.9 v_j and ψ_j Weights for Nonstationary Model for Sales Data

j	v_j	ψ_j	j	v_j	ψ_j
0	0	1	6	9.14	0.46
1	0	0.46	7	9.86	0.46
2	0	0.46	8	10.37	0.46
3	4.82	0.46	9	10.75	0.46
4	6.75	0.46	10	11.02	0.46
5	8.14	0.46	11	11.21	0.46

12.6 SOME ASPECTS OF THE DESIGN OF EXPERIMENTS TO ESTIMATE TRANSFER FUNCTIONS

In some engineering applications, the form of the input X_t can be deliberately chosen so as to obtain good estimates of the parameters in the transfer function–noise model:

$$Y_t = \delta^{-1}(B)\omega(B)X_{t-b} + N_t$$

The estimation of the transfer function is equivalent to estimation of a dynamic ''regression'' model, and the methods that can be used are very similar to those used in ordinary

TABLE 12.10 π_j, P_j, and Q_j Weights for Nonstationary Model for Sales Data

j	π_j	P_j	Q_j	j	π_j	P_j	Q_j
1	0.68	0.46	0	9	0.00	0.00	−0.74
2	0.22	0.25	0	10	0.00	0.00	−0.59
3	0.07	0.13	4.82	11	0.00	0.00	−0.29
4	0.02	0.07	1.25	12	0.00	0.00	−0.13
5	0.01	0.04	−0.29	13	0.00	0.00	−0.06
6	0.00	0.02	−0.86	14	0.00	0.00	−0.02
7	0.00	0.01	−0.97	15	0.00	0.00	0.00
8	0.00	0.01	−0.89				

nondynamic regression. As might be expected, the same problems (see e.g. Box, 1966) face us.

As with static regression, it is very important to be clear on the objective of the investigation. In some situations, we want to answer the question: If the input X is merely observed (but not interfered with), what can this tell us of the present and future behavior of the output Y under *normal* conditions of process operation? In other situations, the appropriate question is: If the input X is *changed* in some specific way, what *change* will be induced in the present and future behavior of the output Y? The types of data we need to answer these two questions are different.

To answer the first question unambiguously, we must use data obtained by observing, *but not interfering with*, the normal operation of the system. In contrast, the second question can only be answered unambiguously from data in which *deliberate* changes have been induced into the input of the system; that is, the data must be specially generated by *a designed experiment*.

Clearly, if X is to be used as a control variable, that is, a variable that may be used to manipulate the output, we need to answer the second question. To understand how we can design experiments to obtain valid estimates of the parameters of a cause-and-effect relationship, it is necessary to examine the assumptions of the analysis.

A critical assumption is that the X_t's are distributed independently of the N_t's. When this assumption is violated, the following issues arise:

1. The estimates we obtain are, in general, not even consistent. Specifically, as the sample size is made large, the estimates converge not on the true values but on other values differing from the true values by an unknown amount.
2. The violation of this assumption is not detectable by examining the data. Therefore, the possibility that in any particular situation the independence assumption may not be true is a particularly disturbing one. The only way it is possible to guarantee its truth is by deliberately *designing* the experiment rather than using data that have simply ''happened.'' Specifically, we must deliberately generate and feed into the process an input X_t, which we know to be uncorrelated with N_t because we have generated it by some external random process.

The input X_t can, of course, be autocorrelated; it is necessary only that it should not be cross-correlated with N_t. To satisfy this requirement, we could, for example, draw a set of random variates α_t and use them to generate any desired input process $X_t = \psi_X(B)\alpha_t$.

Alternatively, we can choose a fixed ''design,'' for example, the factorial design used in Section 12.4.2, and randomize the order in which the runs are made. Appendix A12.2 contains a preliminary discussion of some elementary design problems, and it is sufficient to expose some of the difficulties in the practical selection of the ''optimal'' stochastic input. In particular, as is true in a wider context: (1) it is difficult to decide what is a sensible criterion for optimality, and (2) the choice of ''optimal'' input depends on the values of the unknown parameters that are to be optimally estimated. In general, a white noise input has distinct advantages in simplifying identification, and if nothing very definite were known about the system under study, it would provide a sensible initial choice of input.

APPENDIX A12.1 USE OF CROSS-SPECTRAL ANALYSIS FOR TRANSFER FUNCTION MODEL IDENTIFICATION

In this appendix, we show that an alternative method for identifying transfer function models, which does not require prewhitening of the input, can be based on spectral analysis. Furthermore, it is easily generalized to multiple inputs.

A12.1.1 Identification of Single-Input Transfer Function Models

Suppose that the transfer function $v(B)$ is *defined* so as to allow the possibility of nonzero impulse response weights v_j for j a negative integer, so that

$$v(B) = \sum_{k=-\infty}^{\infty} v_k B^k$$

Then if, corresponding to (12.2.3), the transfer function–noise model is

$$y_t = v(B)x_t + n_t$$

equations (12.2.5) become

$$\gamma_{xy}(k) = \sum_{j=-\infty}^{\infty} v_j \gamma_{xx}(k-j) \qquad k = 0, \pm 1, \pm 2, \ldots \tag{A12.1.1}$$

We now define a *cross-covariance generating function*

$$\gamma^{xy}(B) = \sum_{k=-\infty}^{\infty} \gamma_{xy}(k) B^k \tag{A12.1.2}$$

which is analogous to the autocovariance generating function (3.1.10). On multiplying throughout in (A12.1.1) by B^k and summing, we obtain

$$\gamma^{xy}(B) = v(B)\gamma^{xx}(B) \tag{A12.1.3}$$

If we now substitute $B = e^{-i2\pi f}$ in (A12.1.2), we obtain the cross-spectrum $p_{xy}(f)$ between input x_t and output y_t. Making the same substitution in (A12.1.3) yields

$$v(e^{-i2\pi f}) = \frac{p_{xy(f)}}{p_{xx}(f)} \qquad -\frac{1}{2} \le f < \frac{1}{2} \tag{A12.1.4}$$

where

$$v(e^{-i2\pi f}) = G(f)e^{i2\pi\phi(f)} = \sum_{k=-\infty}^{\infty} v_k e^{-i2\pi fk} \tag{A12.1.5}$$

is called the *frequency response function* of the system transfer function relationship and is the Fourier transform of the impulse response function. Since $v(e^{-i2\pi f})$ is complex valued, we write it as a product involving a *gain function* $G(f) =\mid v(e^{i2\pi f}) \mid$ and a *phase function* $\phi(f)$. Equation (A12.1.4) shows that the frequency response function is the ratio of the cross-spectrum to the input spectrum. Methods for estimating the frequency response function $v(e^{-i2\pi f})$ are described by Jenkins and Watts (1968). Knowing $v(e^{-i2\pi f})$, the impulse response function v_k can then be obtained from

$$v_k = \int_{-1/2}^{1/2} v(e^{-i2\pi f})e^{i2\pi fk}df \tag{A12.1.6}$$

Using a similar approach, the autocovariance generating function of the noise n_t is

$$\gamma^{nn}(B) = \gamma^{yy}(B) - \frac{\gamma^{xy}(B)\gamma^{xy}(F)}{\gamma^{xx}(B)} \tag{A12.1.7}$$

On substituting $B = e^{-i2\pi f}$ in (A12.1.7), we obtain the expression

$$p_{nn}(f) = p_{yy}(f)[1 - k_{xy}^2(f)] \tag{A12.1.8}$$

for the spectrum of the noise process, where

$$k_{xy}^2(f) = \frac{\mid p_{xy}(f) \mid^2}{p_{xx}(f)p_{yy}(f)}$$

and $k_{xy}(f)$ is the *coherency spectrum* between the series x_t and y_t. The coherency spectrum $k_{xy}(f)$ at each frequency f behaves like a correlation coefficient between the random components at frequency f in the spectral representations of x_t and y_t. Knowing the noise spectrum, the noise autocovariance function $\gamma_{nn}(k)$ may then be obtained from

$$\gamma_{nn}(k) = 2\int_0^{1/2} p_{nn}(f)\cos(2\pi fk)df$$

By substituting estimates of the spectra such as those described in Jenkins and Watts (1968), estimates of the impulse response weights v_k and noise autocorrelation function are obtained. These can be used to identify the transfer function model and noise model as described in Sections 12.2.1 and 6.2.1.

A12.1.2 Identification of Multiple-Input Transfer Function Models

We now generalize the model

$$\begin{aligned} Y_t &= v(B)X_t + N_t \\ &= \delta^{-1}(B)\omega(B)X_{t-b} + N_t \end{aligned}$$